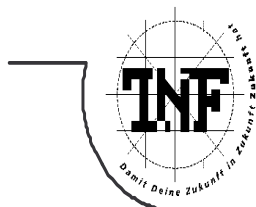JOHANNES KEPLER
UNIVERSITÄT LINZ
Netzwerk für Forschung, Lehre und Praxis

Magnetic Resonance Studies on Conjugated Polymers and Conjugated Polymer Fullerene Mixtures

DISSERTATION

zur Erlangung des akademischen Grades

DOKTOR DER TECHNISCHEN WISSENSCHAFTEN

Angefertigt am *Institut für Chemie, Abteilung für Physikalische Chemie*

Betreuung   *o.Univ.-Prof. Mag. Dr. Niyazi Serdar Sariciftci*
Gutachter: *o.Univ.-Prof. Mag. Dr. Niyazi Serdar Sariciftci*
                ao.Univ.-Prof. Dipl.Ing. Dr. Helmut Sitter

Eingereicht von: *Dipl.Ing. Markus Clark Scharber*

Linz, Oktober 2002

Table of Content

5. Summary and Conclusion   90

Appendix

1. Introduction

Conjugated polymers have attracted wide-spread interest in the scientific community because of their outstanding properties: They combine the opto-electronic properties of semiconductors with the processing advantages and mechanical plasticity of conventional polymers.[1-4] The importance of the new and promising material class as well as the scientific progress in the field of conjugated polymers were recognized by the nobel-committee awarding the nobel-prize of chemistry 2000 to A. J. Heeger, A. G. McDiarmid, and H. Shirakawa for their initial discovery of conduction polymers in 1977.[5]

Conjugated polymers can become highly conducting in the doped state.[2,3] In this form, they may find applications in e.g. batteries, electromagnetic shields, antistatic coatings or sensors. In the semiconducting form, conjugated polymers are used as active materials in light emitting diodes and field-effect transistors.[1] Although displays for mobile phones or similar applications and simple integrated circuit based on conjugated polymers will be commercially available very soon, the nature of the primary photoexcitation in conjugated polymers is still controversial.[6] The question is: Is it a neutral excited state (singlet exciton), or mobile charge carriers? An equivalent formulation of the question is: Is the electronic structure of a conjugated polymer that of a molecular crystal or a one-dimensional semiconductor?[6] Recent experiments in the femto-second time domain demonstrated the formation of charges with a yield of 10 % within the time resolution of the experiments (~100 fs).[7-9] Results were interpreted as evidence for direct generation of charges by photoexcitation[7] but also ultra-fast dissociation of singlet excitons[8,9] leaving the question unresolved.

Besides the application in light emitting displays and integrated electronic circuits photodetectors and photovoltaic devices are among the most promising applications of conjugated polymers. Here conjugated polymers are mixed with electron acceptor molecules like C_{60} to form a solid state composite of donors and acceptors. In these systems very remarkable photo-physical processes have been observed.[10] Upon photoexcitation of the conjugated polymer an electron is transfer onto the fullerene. Also photoexcitation of the fullerene can lead to a charge-separated state via a hole

transfer. In a mixture of poly(2-methoxy-5-(3',7'-dimethyloctyloxy)-1,4-phenylenevinylene) (MDMO-PPV), a typical conjugated polymer, and [6,6]-phenyl C_{61}butyric acid methyl ester (PCBM), a fullerene derivative a charge transfer time of 45 fs was measured.[11] This is one of the fastest charge transfer processes observed in donor acceptor systems. The first unambiguous proof for a charge-separated state was found in light induced electron spin resonance experiments where two light induced features could be identified as positive radical (cation) on the conjugated polymer (polaron) and negative radical (anion) on the fullerene.[12-14] In addition several other methods have been used to study the photo-physics of these systems like photoinduced absorption, fluorescence and photocurrent spectroscopy.[10] The charge transfer is manifested in these experiments as the appearance of new photoexcited states, a quenching of the photoluminescence and an enhancement of the photoconductivity. Although the forward charge transfer is very fast the recombination of the light induced charges is found to be much slower and lifetimes in the millisecond range have been observed at liquid nitrogen temperatures.[10] The generation and recombination asymmetry of photoexcited charges makes conjugated polymer fullerene composites to almost ideal systems for photon harvesting devices. This has been demonstrated by several groups presenting photodetectors with sensitivities comparable to silicon photodiodes and photovoltaic devices with efficiencies up to 3 % under AM1.5 conditions.[15-17]

The work presented here is an experimental study. It includes the design and setup of the photoluminescence and photocurrent detected magnetic resonance experiment as well as the development data-acquisition programs for several experiments (using CEC2000 Testpoint interface). The study is dedicated to the investigation of the nature of photoexcited states and their recombination in conjugated polymers and conjugated polymer electron acceptor mixtures. Improving the knowledge about excited species and their recombination processes in these systems may also contribute to the understanding of the working principles and the intrinsic limitations of different applications.

Different magnetic resonance and excited state spectroscopic techniques were applied, namely light induced electron spin resonance (LESR) (to study long-lived photoinduced charges at low temperatures), photoluminescence and photocurrent detected magnetic resonance (PLDMR, PCDMR) (to investigate the role of charged

pairs) and photoinduced absorption and special modulation technique (to identify the nature of photoexcited species and to study second order processes).

The manuscript is divided into five chapters. It does not provide a general introduction to conjugated polymers or to charge transfer processes in conjugated polymer electron acceptor composites. An overview can be found in several text books, e.g. in *Semiconducting Polymers*, Editors Hadziioannou, P. F. van Hutten Wiley-VCH, Weinheim (2000), *Handbook of Organic Conductive Molecules and Polymers*, Editor H. S. Nalva, John Wiley&Sons, New York (1997), *Handbook of Conducting Polymers,* Editors T. A. Skotheim, R. L. Elsenbaumer, J. R. Reynolds, Marcel Dekker Inc., New York-Basel-Hong Kong (1998), *Electronic Processes in Organic Crystals*, Editors M. Pope, C. E. Swenberg, Oxford University Press, New York (1998), *The Nature of Photoexcitations in Conjugated Polymers,* N. S. Sariciftci, World Scientific, Singapore (1997).

After the introduction some theoretical background is presented to all experiments performed in this study. All equations used to interpret experimental results are derived or at least explained in some detail. References are given to each subsection of chapter two for further information. The third chapter is devoted to the experimental setup. Experiments are illustrated by a schematic drawing and used components are listed and described. Important steps when arranging and performing the experiments are discussed in detail. In chapter four experimental results are presented and discussed. Results are compiled either with respect to the experimental technique or the investigated samples. In the last chapter, summary and concluding remarks are given.

References

[1]G. Hadziioannou, P. F. van Hutten, *Semiconducting Polymers*, Wiley-VCH, Weinheim (2000).

[2]H. S. Nalva, *Handbook of Organic Conductive Molecules and Polymers*, Vol.1-4, John Wiley&Sons, New York (1997).

[3]T. A. Skotheim, R. L. Elsenbaumer, J. R. Reynolds, *Handbook of Conducting Polymers,* Marcel Dekker Inc., New York-Basel-Hong Kong (1998)

[4]Eds. M. Pope, C. E. Swenberg, *Electronic Processes in Organic Crystals*, Oxford University Press, New York (1998).

[5]H. Shirakawa, E. J. Louis, A. G. McDiarmaid, C. K. Chiang, A. J. Heeger, J. Chem. Soc. Chem. Commun. 578 (1977).

[6]N. S. Sariciftci, *The Nature of Photoexcitations in Conjugated Polymers,* World Scientific, Singapore (1997).

[7]P. B. Miranda, D. Moses, and A. J. Heeger, Phys. Rev. B 64, 081201R (2001).

[8]C. Silva, A. S. Dhoot, D. M. Russell, M. A. Stevens, A. C. Arias, J. D. MacKenzie, N. C. Greenham, and R. H. Friend, S. Setayesh and K. Müllen Phys. Rev. B, 64, 125211 (2001).

[9]J. G. Müller, U. Lemmer, and J. Feldmann, U. Scherf, Phys. Rev. Lett. 88 147401 (2002).

[10]N. S. Sariciftci, A. J. Heeger, in *Handbook of Organic Conductive Molecules and Polymers* (Ed. H. S. Nalva), Vol. 1. John Wiley & Sons, New York (1997).

[11]C. J. Brabec, G. Zerza, N. S. Sariciftci, G. Cerullo, S. DeSilvestri, S. Luzatti, J. C. Hummelen, Chem. Phys. Lett. 340, 232 (2001).

[12]Y. Wang, Nature (London) 356, 585 (1992).

[13]N. S. Sariciftci, L. Smilowitz, A. J. Heeger, and F. Wudl, Science 258, 1474 (1992).

[14]S. Morita, A. A. Zakhidov, and Y. Yoshino, Solid State Comm. 82, 249 (1992).

[15]G. Yu, J. Gao, C. Yang, A. J. Heeger, Proceedings of the SPIE, The-International-Society-for-Optical-Engineering. vol. 2999; 1997; p.306-14.

[16]G. Yu, J. Gao, J. C. Hummelen, F. Wudl, A. J. Heeger, Science 270, 1789 (1995).

[17]S. E. Shaheen, C. J. Brabec, N. S. Sariciftci, F. Padinger, T. Fromherz, J.C. Hummelen, Appl. Phys. Lett. 78, 841 (2001).

2. Theoretical considerations

In this chapter background information to all experiments performed in this study is provided. Models, which were used to explain experimental results, are discussed in detail.

2.1 Recombination of long-lived charge carriers at low temperature[1]

In disordered systems like amorphous silicon very long lifetimes (several hours) of light induced charge carriers have been found.[2] However not only the decay, but also the increase of the number of photoexcited charge carriers has been observed to be very slow, for sufficiently low photoexcitation intensities. These long–lived species can only be detected at low temperatures. This is consistent with a picture in which the long-lived carriers are trapped (i.e. localized) below the mobility edge with trap energies larger than their thermal energy $k_B T$. It has been suggested that a tunneling process governs the recombination kinetics of these trapped species.[3] Shklovskii and co-workers have proposed a detailed model that describes these recombination kinetics of photoexcited carriers at low temperatures.[4-7]

Neglecting thermal reexcitation of trapped species and assuming that spatially close pairs have a higher recombination rate than distant pairs, an equation for the time-dependent density of long-lived charge carriers can be derived. For a tunneling process the recombination rate can be described by

$$\nu(R) = \nu_0 \exp\left(-\frac{2R}{a}\right) \tag{2.1}$$

where $\nu(R)$ describes the recombination rate of any electron and hole that are separated by a distance R. $\nu_0 = \tau_0^{-1}$ is a recombination constant that may be interpreted as an attempt-to-recombine frequency. The parameter a describes an effective localization radius. From equation (2.1) it follows that after some time, t, spatially close carriers will have recombined, thus leaving carriers with larger distances behind. Therefore, by recombination of the closest pairs, the nearest neighbour distance, $R(t)$, increases and can be written as:

$$R(t) = \frac{a}{2} \cdot \ln(\frac{t}{\tau_0}) \tag{2.2}$$

Now, assuming that the photoexcitation is turned off at some time t_0 at a charge carrier concentration n_0 and taking into account a time period t_1-t_0, in which geminate recombination is present, it can be shown[2] that for times larger than t_1 the remaining concentration of charge carriers *n(t)*, after cessation of the photoexcitation could be written as:

$$n(R) = \frac{n_1}{1 + \frac{4\pi}{3} n_1 (R^3 - R_1^3)} \tag{2.3}$$

for 3-dimensional recombination, where the time dependence is contained in R = R(t) given by equation (2.2) with $t > t_1$. R(t) describes the increase of the distance among the remaining electron hole pairs, which have not recombined until the time t after photoexcitation. $R_1 = R(t_1)$ describes the nearest neighbor distance between electrons and holes at time t_1 after which solely non-geminate recombination is assumed. n_1 is the charge carrier concentration at time t_1. Inserting equation (2.2) into equation (2.3) one obtains

$$\frac{n(t)}{n_0} = \frac{\dfrac{n_1}{n_0}}{1 + \left(\dfrac{n_1}{n_0}\right)\dfrac{\pi}{6} n_0 a^3 \left[\ln^3\left(\dfrac{t}{\tau_0}\right) - \ln^3\left(\dfrac{t_1}{\tau_0}\right) \right]} \tag{2.4}$$

for the normalized spin density. The normalization factor n_0 is the spin density observed at the highest photoexcitation intensity. This model can be applied to explain light induced ESR experiments on conjugated polymers and conjugated polymer electron acceptor mixtures - as will be demonstrated below as - well as on inorganic amorphous semiconductors. The applicability of the model to very different systems suggests that recombination by tunneling is a common process in disordered systems at temperatures $k_B T \ll E_{trap}$.

2.2 Photoinduced absorption (PIA)[8]

PIA is a pump and probe photomodulation measurement. In cw-PIA absorption the pump which photoexcites the sample is a cw-laser beam modulated by a mechanical

chopper. The photoinduced variation in transmission ΔT is a modulated signal, which can be detected with a lock-in amplifier. In time-resolved photoinduced absorption experiments a short laser pulse is exciting the sample and the time-decay of the photoinduced absorption ΔT is measured. For thin films neglecting the sample reflectivity, the relative change in transmission is given by ΔT/T=-dΔα, where d is the sample thickness, Δα is the photoinduced absorption and T the optical transmission. The modulated signal ΔT follows the density of photoexcited states n(t). The response of the system on the pump intensity G(t) can be obtained by solving the rate equation[9-12]

$$\frac{dn}{dt} = g\ G(t) - \beta\ n(t) - \gamma\ n^2(t)\,.\tag{2.5}$$

g is the generation constant proportional to the absorption coefficient. β and γ are the monomolecular and bimolecular recombination constants. Analytical solutions of equation (2.5) can be obtained for a few special cases.[9,10] E.g. for a sinusoidal modulation of the pump intensity and monomolecular recombination only it is found that

$$\Delta T \propto \frac{1}{\sqrt{1 + (\omega\tau)^2}}\,.\tag{2.6}$$

ω is the modulation frequency of the pump and τ, which is the lifetime of the species, is given by 1/β. For more general cases only numerical simulations can help to analyze the frequency dependence of the photoinduced absorption. Another complication can arise if the investigated species has more than one lifetime. This behavior is called 'dispersive relaxation' and a model described by E. Ehrenfreund et al.[13] can help to analyze the distribution of lifetimes.

2.3 Triplet –Triplet annihilation (TTA) in conjugated polymers

The annihilation of two triplet excitons has been discussed as a possible source of delayed fluorescence in conjugated polymers.[14-16] In this process two triplet states collide and form a new intermediate state, which can be singlet (probability 1/9), triplet (probability 1/3) or quintuplet (probability 5/9).[17,18] The formation probability

is determined by the initial spin of the two triplet states colliding. In a schematic sketch, TTA can be illustrated as follows

$$T_1+T_1 \leftrightarrow {}^{1,3,5}(T_1\ldots\ldots T_1) \leftrightarrow \begin{matrix} (S_1+S_0) \\ \\ (T_1+S_0) \end{matrix} \quad .$$
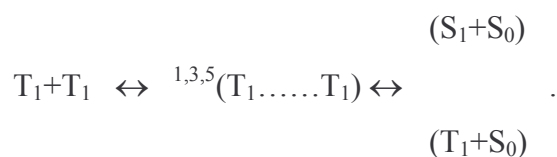
From the intermediate state only excited singlet or triplet states are produced. Excited singlet states coming from TTA are responsible for luminescence, which looks like photoluminescence but is emitted at times much later than the singlet exciton lifetime. TTA could be an important process in polymeric light emitting diodes (PLEDs). According to simple spin statistics, uncorrelated free charge carrier recombination should yield 25 % singlet and 75 % triplet excitons in a PLED.[19] Therefore the concentration of triplet excitons should be very high in these devices. Without TTA triplet excitons cannot contribute to the electro-luminescence of a PLED and thus form an intrinsically large inefficiency for these devices consisting of carbon, hydrogen and oxygen containing molecules with a small spin orbit coupling. Recent experiments and calculations suggest that the recombination of free charge carriers in conjugated polymers does not produce singlet and triplet excitons in a ratio 1:3.[19-23] It is found, that the probability to form a singlet exciton can be as high as 0.6 instead of 0.25.[21] TTA in conjugated polymers has been predicted by Dyakonov et al. based on magnetic resonance experiment.[14,24] The idea of triplet-triplet annihilation and delayed photoluminescence in conjugated polymers is supported by pulsed radiolysis studies.[25] In these experiments very high triplet concentrations on single poly(2-methoxy-5-(2'-ethyl-hexyloxy)-p-phenylenevinylene) chains dissolved in benzene were generated with a pulsed electron beam. The decay of these triplets was accompanied by delayed fluorescence resulting from TTA.

It is difficult to create a high density of triplet excitons in solutions of a conjugated polymer by optical excitation. The quantum yield of intersystem crossing is thought to be small for most of the commonly used materials. The situation could be different in the solid state. There, recombination of polarons could increase the yield of triplet formation. Further only a small fraction of triplet excitons annihilate creating singlet excitons. Therefore the direct observation of TTA by a photoluminescence decay

measurement is very difficult. Another complication occurs due to delayed singlet emission of optically excited geminate charged pairs as demonstrated by Romanovski et al..[26] Frankevich et al. suggested an indirect method to demonstrate TTA in optically excited conjugated polymers.[27] Their quasi cw-modulation method is based on the following model. The triplet exciton population n_T is governed by the rate equation

$$\frac{dn_T}{dt} = G(t)\beta_T - \frac{n_T}{\tau_T} - \gamma n_T^2 \tag{2.7}$$

where $G(t)=G_0(1+a\cdot\sin(\omega t))$, β_T is the yield of triplet exciton formation, τ_T is their monomolecular decay rate and γn_T^2 determines the triplet-triplet annihilation process. At low excitation intensities γn_T^2 can be neglected and a solution of equation (2.7) can be found of the following form

$$n_T(t) = G_0\beta_T\tau_T\left(1 + \frac{a}{\sqrt{1+\omega^2\tau_T^2}}\sin(\omega\,t+\varphi)\right). \tag{2.8}$$

The phase shift φ is given by arctan($-\omega\tau_T$).
The intensity of the delayed fluorescence (caused by TTA) is given by

$$I_{DF} = \beta_s\frac{1}{9}\gamma n_T^2 \tag{2.9}$$

where β_s is the prompt fluorescence yield (coming for singlet excitons) and the spin-statistical factor of 1/9 is the fraction of pairs of triplets which form a singlet state by annihilation. A pair of triplets can have singlet, triplet and quintuplet spin multiplicity. Therefore only 1/9 of all created triplet pairs can be transformed into a singlet-excited state. Substituting equations (2.8) into equation (2.9) gives three components contributing to the delayed fluorescence. One component does not depend on time, the second component varies sinusoidally in time while the time dependence of the third part is given by $\sin^2(\omega t+\varphi)$. Rewriting this time dependence and adding all pre-factors one finds the component of the delayed fluorescence, which oscillates at 2ω:

$$I_{DF,2\omega} = \frac{\gamma}{9}G_0^2\tau_T^2a^2\beta_T^2\beta_s\left(\frac{1}{1+\omega^2\tau_T^2}\sin(2\omega\,t+2\varphi-\frac{\pi}{2})\right). \tag{2.10}$$

Since the component of the fluorescence at ω is given by

$$I_{fl,\omega} = G_0\beta_s a\sin(\omega\,t) \tag{2.11}$$

the ratio of $I_{DF,2\omega}$ and $I_{fl,\omega}$ is given by

$$R_{PL} = \frac{1}{9} \frac{\gamma G_0 \beta_T^2 \tau_T^2}{1 + \omega^2 \tau_T^2} \qquad (2.12)$$

A measurement of R_{PL} versus ω should give τ_T. To correct for any system response and any Fourier component of the modulated laser beam at 2ω, the ratios of the amplitudes of the x (in phase) and y (out of phase) component of the laser beam signal at 2ω to the modulus at ω ($R_{las,x}$ and $R_{las,y}$) were subtracted from the similarly defined $R_{PL,x}$ and $R_{PL,y}$. The value of R_{PL}, corrected for the system response, is then given by

$$R'_{PL} = \sqrt{\left(R_{PL,x} - R_{las,x}\right)^2 + \left(R_{PL,y} - R_{las,y}\right)}. \qquad (2.13)$$

The method described before offers a very general approach to study second order processes. It can be applied to systems in which competing first and second order processes are present. It is based on a modulation technique and therefore allows the use of very sensitive lock-in detection. However, the method does not give direct information about the active species. All species recombining in a first and a second order process will show a component oscillation with the double modulation frequency.

2.4 Reaction yield detected magnetic resonance (RYDMR)[28-30]

In RYDMR not the microwave absorption of a system is detected like in conventional ESR spectroscopy, but processes like photoluminescence, absorption, photoconductivity, photoinduced absorption are probed under microwave irradiation while a static magnetic field is tuned through the Zeeman resonance. To explain experimental results, the radical pair concept has been developed.[31-33] This concept is based on spin selective processes in a pair of radicals, which are connected to the process observed in the experiment. These spin selective processes create a polarization of the radical pair spin states, allowing the detection of very small spin concentrations. In conjugated polymers these radical pairs are called polaron pairs and their importance in RYDMR experiments is generally established.[24,34-36]

The Hamiltonian for a radical pair (polaron pair) can be expressed by[37]

$$H = g_a \mu_B B_0 S_{za} + g_b \mu_B B_0 S_{zb} - J\mathbf{S}_a \cdot \mathbf{S}_b - D(3S_{za}S_{zb} - \mathbf{S}_a \cdot \mathbf{S}_b). \qquad (2.14)$$

g_a and g_b are the g-values and S_a and S_b the spin operators of the two radicals forming the pair, B_0 is the external magnetic field, μ_B is the Bohr magneton, J the exchange coupling and D the dipolar coupling constant.

Depending on the magnitude of D, J and $\Delta g=(g_a-g_b)$ different eigenstates and transition frequencies can occur. In the case $\Delta g\neq0$ and D=J=0 only two different lines are found as solutions of H. As discussed by P. W. Andersson[38] and recently by Ito et al.[39] small Δg and small exchange coupling J merge the two lines and only one resonant transition will occur. This Hamiltonian also describes a system that can separate into one singlet and three triplet state. Depending on the value of D the triplet state gives rise to one or two ESR lines.

2.4.1 Photocurrent Detected Magnetic Resonance (PCDMR)[40,41]

In brief a scheme developed for magnetic field effect (MFE) and PCDMR experiments will be discussed. It can be used to describe the sign, the amplitude and also the temperature dependence of the observed signals.[40] Figure 2.1 shows the energy level diagram and the evolution of photoexcitations according to the polaron pair model.[40] After photogeneration of a singlet exciton $^1M_1$ from the ground state $^1M_0$ an electron can be transferred to a neighboring chain, forming with its parent hole a geminate interchain polaron pair (P^+P^-). Polarons within the pair are bound by Coulomb interaction and do not contribute to the photoconductivity. This species is often called charge transfer exciton, in which the charge carriers are located on different chains or chain segments. However, the distance between them is small enough that the exchange interaction between the two polarons is important. Charge transfer excitons can be dissociated by thermal activation or a tunneling process to distant polaron pairs $(P^+.....P^-)$. In this species the inter-polaron-distance is large and the exchange interaction is negligible. They are suggested to be the precursor state for free charge carriers. According to the spin-conservation rule, photoexcitation produces singlet polaron pairs. However, the interchain polaron pair can also exist in a triplet configuration. The recombination of a triplet polaron pair leads to the formation of a triplet exciton. Hyperfine interaction and external magnetic fields can mix singlet and triplet states of polaron pairs. This process occurs if the energies of the mixing states are equal, if the lifetime of the pair is longer than the time for converting one state into another and if the spin-lattice relaxation time T_1 is long

enough to allow spin evolution. Due to their small exchange interaction, hyperfine interaction or external magnetic fields can mix different spin states of distant polaron pairs.
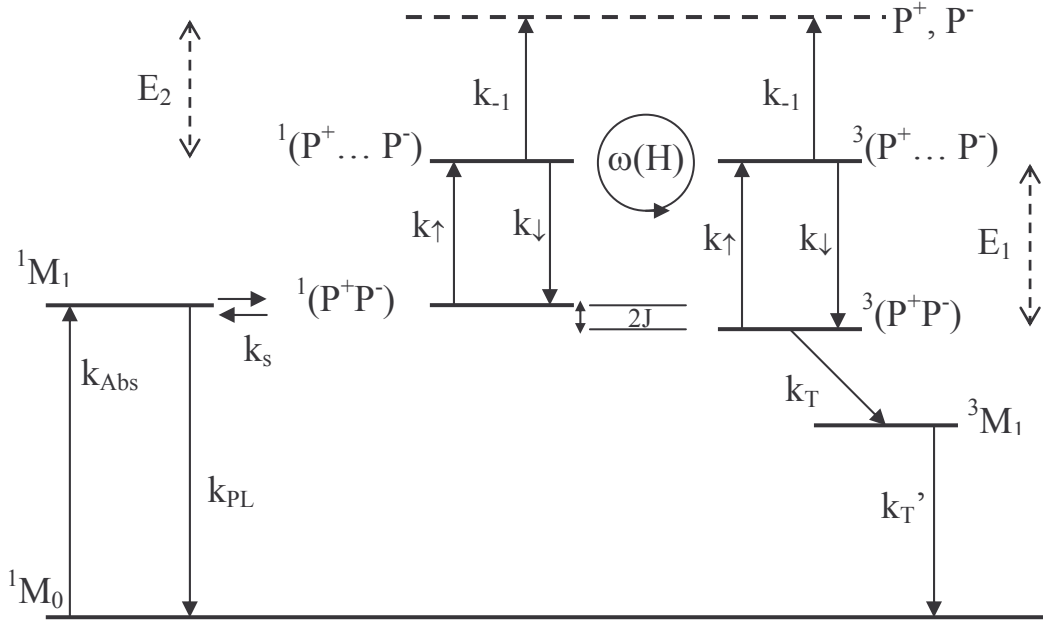
Figure 2.1: Scheme of the processes responsible for PCDMR

For times shorter than T_1 the spin system is not thermalized. Selective mixing of spin states can result in a strong polarization, which is advantageous for magnetic resonance. Due to spin polarization the detectivity of the experiment can be improved by several orders of magnitude.[42]

Using the picture described above a very comprehensive model can be derived, which explains the magnetic field effect on the photoluminescence and photoconductivity in conjugated polymers.[40,43] In these materials the g-value of positive and negative polarons is very similar and therefore hyperfine interaction is responsible for level-mixing. Two different situations have to be considered. When no external magnetic field (H) is applied, all spin states of the distant polaron pairs are mixed. In a high magnetic field (>>hyperfine interaction), only one triplet (T_0) and the singlet state are mixed.

$$^1(P^+ \dots P^-) \xrightarrow{\omega} {}^3(P^+ \dots P^-)$$

H=0

$$^1(P^+ \dots P^-) \xrightarrow{\omega} {}^3(P^+ \dots P^-)$$

H>>0

Figure 2.2: Singlet and triplet levels with a) no magnetic field applied – b) a strong magnetic field applied

Assuming that the polaron pairs are populated via the singlet channel and that the rate of free-carrier formation is proportional to the number of pairs, the yield of photocurrent for no and high external magnetic field can be calculated by solving appropriate rate equations.[40,44] The result is found to be
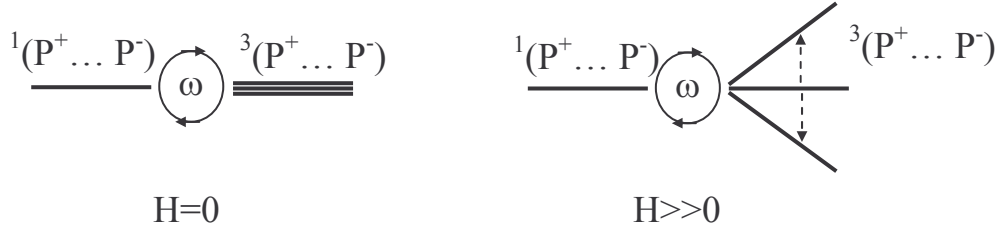
$$\frac{i(H) - i(0)}{i(0)} = \frac{1}{2}(k_T - k_s)\left[\frac{2k_s k_T}{k_\uparrow} + (k_s + k_T) + \frac{2k_{-1}(k_s + k_\uparrow)(k_T + k_\uparrow)}{k_\uparrow k_\downarrow}\right]^{-1}. \quad (2.15)$$

i(H) and i(0) represent the photocurrent with and without magnetic field applied. Rate constants are used as shown in Figure 2.1. Assuming that only the rate constant for distant polaron pair generation ($k_\uparrow$) and their dissociation into free charge carriers (k_{-1}) is thermally activated ($k_\uparrow \propto \exp(-E_1/k_B T)$, $k_{-1} \propto \exp(-E_2/k_B T)$) and assuming that k_1, $k_3 \gg k_\uparrow$ the expression can be rearranged in the following way

$$\frac{\Delta i}{i} = K\{(1 + A/k_\uparrow)(1 + Bk_{-1}) + Bk_{-1}\}^{-1} \quad (2.16)$$

where K, A and B are temperature independent parameters. This equation can be used to explain the temperature dependence of the magnetic field effect on the photocurrent in conjugated polymers and values for E_1 and E_2 can be extracted. In this model, the energy E_1+E_2 corresponds to the additional energy required to form free charge carriers from polaron pairs.

The model can also be applied to PCDMR. Magnetic resonance will change the populations in the polaron pair triplet states. At very high microwave fields, a population similar to the situation at H=0 will be established again. Therefore, if an external magnetic field increases the photocurrent, magnetic resonance will decrease the photocurrent. An equation, which describes the temperature dependence of the PCDMR amplitude, can be derived in the same way as proposed in Ref. 40 for the

magnetic field effect on the photocurrent. The expression obtained can be simplified to equation 2.16. Therefore equation 2.16 can be used to explain the magnetic field effect as well as PCDMR experiments.

2.4.2 Photoluminescence Detected Magnetic Resonance (PLDMR)

For PLDMR two different models exist which explain experimental results.[14,35,36] They all have in common that polaron pairs are the microwave resonant species and that dynamic spin polarization is created by spin selective recombination. In the so-called 'Quenching model'[35,36] the interaction between polarons and excitons is suggested to be very important. Usually the photoluminescence coming from singlet excitons and the absorption of polarons overlap. Therefore it is quite natural to believe that an energy transfer from an exciton to a polaron is a possible process, which would quench singlet excitons. The model is based on the following processes: Free polarons are created upon photoexcitation. Recombination of free polarons produces singlet and triplet polaron pairs in a certain ratio depending on the polymer.[21,22] Magnetic resonance within the polaron pair reduces the number of polarons, fewer quenching centers for singlet excitons are left and the photoluminescence increases. The model can also easily explain the reduction of the triplet exciton density by the polaron resonance as it was observed in recent experiments.[21,36] This follows directly from the model assuming that singlet polaron pairs decay faster than triplet polaron pairs. Also triplet excitons are considered as quenching sites for singlet excitons.[45] Magnetic resonant transitions within the triplet exciton levels can decrease their concentration and therefore also the PL-enhancing triplet powder pattern observed in the PLDMR spectrum can be rationalized. The 'Quenching model' is supported by a recent experiment published by the Bässler group.[46] Using a pump-probe technique they observe a very efficient quenching of singlet exciton by charges in methyl-substituted poly-(*para*-phenylene). The 'Quenching model' can easily explain all features observed in PLDMR on conjugated polymers. The main assumption of the model is that non-geminate polaron pairs are formed by photoexcitation. Therefore even at very low temperatures (4.2 K) free and mobile charges have to be created upon light excitation.

In the second model TTA is applied to explain all features observed in PLDMR.[14,24] It is based on the following processes: Photoexcitation mainly produces singlet excitons,

which can dissociate into singlet polaron pairs. Intersystem crossing mixes the singlet and one triplet polaron pair sublevels (in the presence of a static magnetic field). Magnetic resonance within the triplet manifold of the polaron pair increases the triplet polaron pair density and at the same time the triplet exciton density via recombination of triplet polaron pairs. A higher triplet exciton density leads to a higher TTA rate and therefore an increase of the photoluminescence. In addition also triplet excitons form pairs before annihilation. Resonant transitions in these pairs increase their annihilation rate and a PL enhancing signal is expected from this source. Allowed transitions in these pairs of triplet excitons appear at g=4.00 and g=2.00. Due to the fact that triplets are randomly oriented in the material, powder patterns are expected. In this way one can also explain the appearance of triplet powder patterns in the PLDMR spectrum. The model is support by the observation of delayed fluorescence in conjugated polymers.[16]

According to the TTA model magnetic resonance transition in the polaron pair should increase the triplet exciton density. However the opposite effect has been observed in photoinduced absorption detected magnetic resonance experiments.[21,22,36] Up to now no consistent explanation based on the triplet-triplet annihilation model has been suggested which could solve this problem. However, as pointed out by E. Frankevich, all triplet exciton levels are populated due to magnetic resonance transitions in the polaron pair. This causes an enhancement of the TTA process.[47] Whether or not this enhancement of TTA can compensate for the additional formation of triplet excions remains unclear.

The two models reflect the two different ways to describe the electronic structure and photoexcitations of conjugated polymers. In the quenching model the most important process is that free charge carriers are created by photoexcitation and that their non-geminate recombination populate all spin states of polarons pairs. This is also one of the main features of the band picture.

In the TTA model the dominant photoexcitations are singlet excitons like in the molecular description of conjugated polymers. Charges are mostly created in pairs, which dominantly recombine geminately.

References

[1]N. A. Schultz, M. C. Scharber, C. J. Brabec, N. S. Sariciftci, Phys. Rev. B 64 245210 (2001).

[2]B. Yan, N. Schultz, A. L. Efros, P. C. Taylor, Phys. Rev. Lett. 84, 4180 (2000).

[3]D. J. Dunstan, Physica (Amsterdam) 117B\118B, 902 (1983).

[4] B. I. Shklovskii, H. Fritzsche, S. D. Baranovskii, Phys. Rev. Lett. 62, 2989 (1989).

[5]E. I. Levin, S. Marianer, B. I. Shklovskii, Phys. Rev. B 45, 5906 (1992).

[6]S. D. Baranovskii, E. L. Ivchenko, B. I. Shklovskii, Sov. Phys. JETP 65, 1260 (1987).

[7]S. D. Baranovskii, H. Fritzsche, E. I. Levin, I. M. Ruzin, B. I. Shklovskii, Sov. Phys. JETP 69, 773 (1989).

[8]P. A. Lane, S. V. Frolov, and Z. V. Vardeny, in *Semiconducting Polymers*, (Eds. G. Hadziioannou, P. F. van Hutten) Wiley-VCH, Weinheim p. 189 (2000).

[9]C. Botta, S. Luzzati, R. Tubino, D. D. C. Bradley and R. H. Friend, Phys. Rev. B 48, 14809 (1993).

[10]G. Dellepiane, C. Cuniberti, D. Comoretto, G. F. Musso, and G. Figari, A. Piaggi ,A. Borghesi, Phys. Rev. B 48 7850 (1993).

[11]Y. Furukawa , Y.-H. Cha, T. Noguchi , T Ohnishi , M. Tasumi, J. of Mol. Struct. 521, 211 (2000).

[12]Y.-H Cha, Y. Furukawa, M. Tasumi, T. Noguchi, T. Ohnishi, Chem. Phys. Lett. 280, 464 (1997).

[13]O. Epshtein, G. Nakhmanovich, Y. Eichen, and E. Ehrenfreund, Phys. Rev. B 63, 125206 (2001).

[14]V. Dyakonov, R. Rösler, M. Schwoerer, E. L. Frankevich, Phys. Rev. B **56**, 3852 (1997).

[15]J. Partee, E. L. Frankevich, B. Uhlhorn, J. Shinar, Y. Ding, and T. J. Barton, Phys. Rev. Lett. 82, 3673 (1999).

[16]C. Rothe, R. Guentner, U. Scherf, A. P. Monkman, J. Chem. Phys. 115, 9557 (2001).

[17]U. E. Steiner, T. Ulrich, Chem. Rev. 89, 51 (1989) and references therein.

[18]P. Avakian, R. E. Merrifield, Mol. Cryst. 5, 37 (1968).

[19]R. H. Friend, R. W. Gymer, A. B. Holmes, J. H. Burroughes, R. N. Marks, C. Taliani, D. D. C. Bradley, D. A. Dos-Santos, J. L. Bredas, M. Lodglund, W. R. Salaneck, Nature 397, 121 (1999).

[20]Y. Cao, I. D. Parker, G. Yu, A. J. Heeger, Nature 397, 414 (1999).

[21]M. Wohlgenannt, K. Tandon, S. Mazumdar, S. Ramasesha, Z. V. Vardeny, Nature 409, 494 (2001).

[22]M. Wohlgenannt, X. M. Jiang, Z. V. Vardeny, R. A. J. Janssen, Phys. Rev. Lett. 88, 197401 (2002).

[23]Z. Shuai, D. Beljonne, R. J. Silbey, J. L. Bredas, Phys. Rev. Lett. 84, 131 (2000).

[24]V. Dyakonov, E. L. Frankevich, Chem. Phys. **227**, 203 (1998).

[25]A. P. Monkman, H. D. Burrows, I. Hamblett, S. Navaratnam, Chem. Phys. Lett. 2001, 467 (2001).

[26]Yu. V. Romanovskii, A. Gerhard, B. Schweitzer, U. Scherf, R. I. Personov, H. Bässler, Phys. Rev. Lett. 84 1027 (2000).

[27]J. Partee, E. L. Frankevich, B. Uhlhorn, J. Shinar, Y. Ding, T. J. Barton, Phys. Rev. Lett. 82, 3673 (1999).

[28]U. E. Steiner, T. Ulrich, Chem. Rev. 89, p. 100 (1989).

[29]E. L. Frankevich, S. I. Kubarev, in *Triplet State ODMR Spectroscopy*, Ed. R. H. Clarke, Wiley Interscience, New York (1982).

[30]A. L. Buchachenko, E. L. Frankevich, Chemical Generation and Reception of Radio- and Microwaves, VCH, New York (1994).

[31]K. M. Salikhov, Yu. N. Molin, R. Z. Sagdeev, A. L. Buchachenko, *Spin Polarization and Magnetic Field Effects in Radical Reactions*, Elsevier, Amsterdam The Netherlands (1984).

[32]U. E. Steiner, T. Ulrich, Chem. Rev. 89, p. 53 (1989).

[33]P. J. Hore in *Advanced EPR: Applications in Biology and Biochemistry*, (Ed. A. Hoff) Elsevier, Amsterdam (1989).

[34]P. A. Lane, X. Wei, Z. V. Vardeny, Phys. Rev. B 56, 4626 (1997).

[35]J. Shinar in *Handbook of organic conductive molecules and polymers*, edited by H. S. Nalwa, (John Wiley & Sons Ltd 1997), vol. 3,a p. 319.

[36] E. J. W. List, C.-H. Kim, A. K. Naik, U. Scherf, G. Leising, W. Graupner, and J. Shinar, Phys. Rev. B 64, 155204 (2001).

[37]T. Eickelkamp, S. Roth, M. Mehring, Mol. Phys. 95, 967 (1998)

[38]P. W. Anderson, J. Phys. Soc. Jpn. 9, 316 (1954)

[39]I. Hiromitsu, Y. Kaimori, M. Kitano, and T. Ito, Phys. Rev. B 59, 2151 (1999)

[40]E. L. Frankevich, A. A. Lymarev, I. Sokolik, F. E. Karasz, S. Blumstengel, R. H. Baughman, H. H. Hörhold, Phys. Rev. B **46**, 9320 (1992).

[41]V. Dyakonov, G. Roesler, M. Schwoerer, S. Blumstengl, K. Lüders, J. Appl. Phys. 79, 1556 (1996).

[42]C. D. Buckley, K. A. McLauchlan, Mol. Phys. 54, 1 (1985).

[43]E. L. Frankevich, G. E. Zoriniants, A. N. Chaban, M. M. Triebel, S. Blumstengel, V. M. Kobryanskii, Chem. Phys. Lett. **261**, 545 (1996).

[44]G. Roelser, PhD thesis, Bayreuth (1996).

[45]M. Pope and C. E. Swenberg, *Electronic Process in Organic Crystals*, Oxford University Press, New York (1998).

[46] Yu. V. Romanovskii, V. I. Arkhipov, and H. Bässler, Phys. Rev. B 64, 033104 (2001).

3. Materials and Experimental

In the first part of this chapter materials investigated in experiments discussed in Chapter 4 are presented. The chemical structures, names and abbreviations of the materials as well as references describing their syntheses and properties are given. In the second part experimental setups and procedures are described. In the schematic drawing of the experimental arrangements the distance between components and the size of components are chosen arbitrarily.

3.1 Materials

a) MDMO-PPV (poly(2-methoxy-5-(3',7'-dimethyloctyloxy)-1,4-phenylenevinylene)
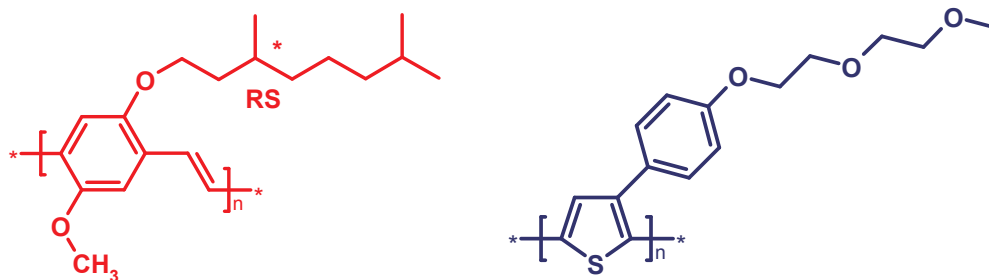

Figure 3.1: Chemical structure of the repeating units of MDMO-PPV (red) and PEOPT (blue)

This material has been obtained from Covion Inc. (Frankfurt, Germany). The synthesis of MDMO-PPV was first described by P. M. Allemand et al.[1] It is a high quality material and has been used as active material in organic light emitting diodes (OLED). UNIAX[®] has demonstrated OLEDs based on MDMO-PPV with lifetimes larger than 10000 hours.[2] The material is soluble in different organic solvents like toluene, xylene or chlorobenzene and has a high molar mass (> 100000 g/mol). Another common abbreviation for this material is OC_1C_{10} PPV.

b) PEOPT (poly(3-(4'-(1'',4'',7''-trioxaoctyl)phenyl)thiophene)

The preparation of PEOPT has been described by L. S. Roman et al.[3] The polymer belongs to a large group of phenyl-substituted polythiophenes, which exhibit very interesting structural,[4] optical[5,6] and electrical properties.[3,7] PEOPT has a high

regioregularity (88 % head to tail).[8] The photophysics of this polymer and other substituted polythiophenes have been studied by Theander et al.[5] Spin coating PEOPT from chloroform solution results in an orange film. Exposing this film to chloroform vapor or heating the film for several seconds to 80 °C gives a blue film.[5] Besides a decrease of the band-gap also a reduction of the PL yield is observed after the chloroform vapor or thermal treatment.[5] X-ray diffraction data suggest that *para*-substituted poly(phenylthiophene)s including PEOPT go into a 'metastable', poorly crystalline state after spin-casting and then achieve a thermodynamically more stable form after appropriate treatment.[4] Therefore these materials can be investigated in the ordered as well as in the disordered form.
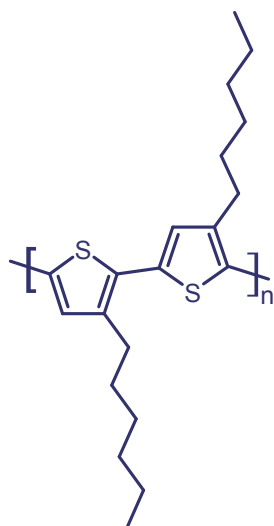
c) rr-P3HT (regio-regular poly-(3-hexyl-thiophene))

P3HT has been purchased from Aldrich. The material has shown very promising electrical properties.[9-11] In FET measurements room temperature hole mobilities as high as 10^{-2} cm^2/Vs have been observed.[10] Recently also photovoltaic devices based on P3HT/PCBM mixtures with efficiencies >3% (under AM1.5) have been demonstrated.[12]

Figure 3.2: Chemical structure of P3HT (two repeat units)

d) Polythiophene-anthraquinone (PT-AQ) double-cables

These compounds belong to the group of so-called double cable materials.[13] The electron donor (polythiophene) and the electron acceptor (anthraquinone) are linked together. After the photoinduced charge transfer the positive charge on the polythiophene (polaron) and the negative charge on the anthraquinone should be transported on one and the same chain. Therefore these materials are called double cables. Polymers were synthesized in the group of M. Catellani (CNR-Milano) in collaboration with N. Martin (UCM Madrid).

$$X\% = B/(A+B)*100$$

Cop41 25% (X=25 %)
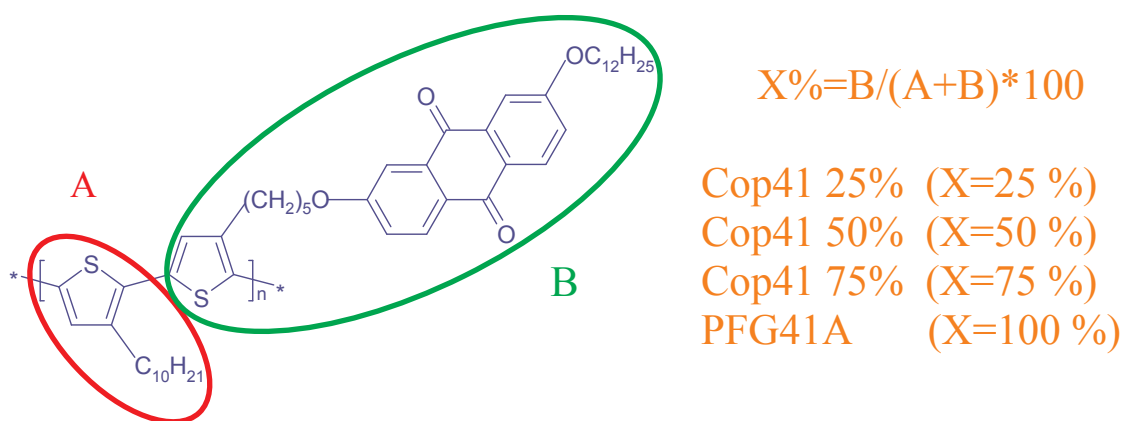Cop41 50% (X=50 %)
Cop41 75% (X=75 %)
PFG41A   (X=100 %)

Figure 3.3: Chemical structure of the polythiophene-anthraquinone double-cable material and abbreviations for materials with different composition.

Materials with different ratios of A and B (see Figure 3.3) were prepared. Originally materials were used as active layers in photovoltaic devices and the influence of the acceptor concentration on the device performance was studied. However, the solubility of these materials in common organic solvent is very different, making a detailed photovoltaic study very difficult.

e) [6,6]-phenyl C_{61} butyric acid methyl ester (PCBM)
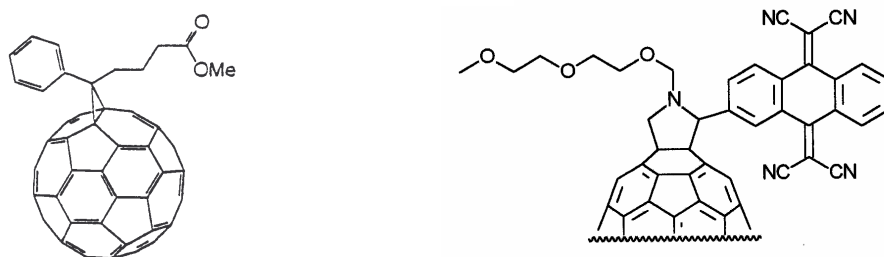
Figure 3.4: Chemical structure of PCBM (left) and UCM2 (right)

The synthesis of the highly soluble fullerene was first described by J. C. Hummelen et al.[14] Up to now, PCBM is the most promising electron acceptor in conjugated polymer/fullerene photovoltaic devices. The photophysics of MDMO-PPV/PCBM films have been discussed in several publications.[15-17]

f) UCM2

This acceptor molecule was prepared by R. G. Gomez et al.[18] The molecule was designed to replace C_{60} or PCBM as electron acceptor in the plastic solar cell. The

photophysical processes in MDMO-PPV/UCM2 mixtures were studied by G. Zerza et al.[18]

3.2 Experimental

3.2.1 Sample preparation

Materials of interest were dissolved in appropriate solvents. Special care had been taken not to form any kind of aggregates in solution. For optical experiments, thin films of material were deposited by spin-coating or doctor-blading on plastic, glass or quartz substrates. Film preparation was done in ambient atmosphere. Immediately after the coating process, samples were transferred into an argon glove-box. Samples were stored there, preferentially in the dark.

Photodiodes were prepared on a plastic substrate coated with indium-tin-oxide (ITO). Poly(3,4-ethylenedioxythiophene):poly(styrenesulfonate) (PEDOT:PSS) and the photoactive material were deposited with a thickness of ~ 100 nm consecutively by spin-coating technique on the cleaned substrate. As a last step, a 60 nm aluminum layer was evaporated as top electrode. The active area of the devices is about 6 mm^2.

3.2.2 Optical absorption, photoluminescence

Optical absorption measurements were performed on a HP 8453 absorption spectrometer. For room-temperature photoluminescence measurements a Hitachi F-4010 fluorescence spectrometer was used.

3.2.3 Current-Voltage curves

Current-Voltage (IV) curves were measured using a Keithley 2400 source-meter. Samples were illuminated by white light (80 mW/cm^2 AM1.5 except noted otherwise).

3.2.4 Light induced Electron Spin Resonance (LESR)[16,17,19]

Experiments were performed on a standard Bruker EMX X-band spectrometer. For light excitations an Ar$^+$ Laser or a lamp (CUNOW-Spotlight DC-480 000 R) attached to a monochromator (GM 252) were used. Powders, or films prepared by drop-cast,

spin-coating or doctor-blading technique were put into an ESR grade quartz tube and sealed in helium atmosphere. Samples were placed in a rectangular TE_{102} cavity with two windows for optical access. The spectrometer is equipped with Oxford 900 Continuous Flow Cryostat liquid He or a Bruker liquid N_2 Cryostat for low temperature measurements.

ESR spectra were recorded in the following way: After cooling down the sample in the dark, an ESR spectrum was recorded (dark spectrum). A so-called 'light on' spectrum was recorded while continuously illuminating the sample by light. A 'light off' spectrum was acquired after switching off the light excitation. Light induced spins can have very long lifetimes at low temperatures. These species cause the 'persistent' signal[16] in conjugated polymers. Therefore the 'light off' spectrum can differ significantly from the initial dark spectrum. The ESR spectrum of the long-lived species disappears after warming up the samples to room temperature.[16]

The decay kinetics of light induced species were studied in the following way:[19]

Samples were cooled down to temperatures ≤ 40 K in the dark. The magnetic field was set to a resonance peak of the LESR signal. After a few minutes recording the dark spin density, the photoexcitation was switched on and the accumulation of photoexcited species was monitored. After some time of continuous illumination (this can be hours for low light excitation intensities) the signal saturated. Then light excitation was switched off and the decay of photoexcited spins in the dark was monitored. To achieve reasonable signal to noise ratios the time constant of the lock-in amplifier detecting the ESR signal had to be set to values > 100 ms. Therefore the experiment was suitable for the study of lifetimes > 1 sec.

3.2.5 Photoinduced Absorption Experiment (cw) and Delayed Fluorescence Experiment
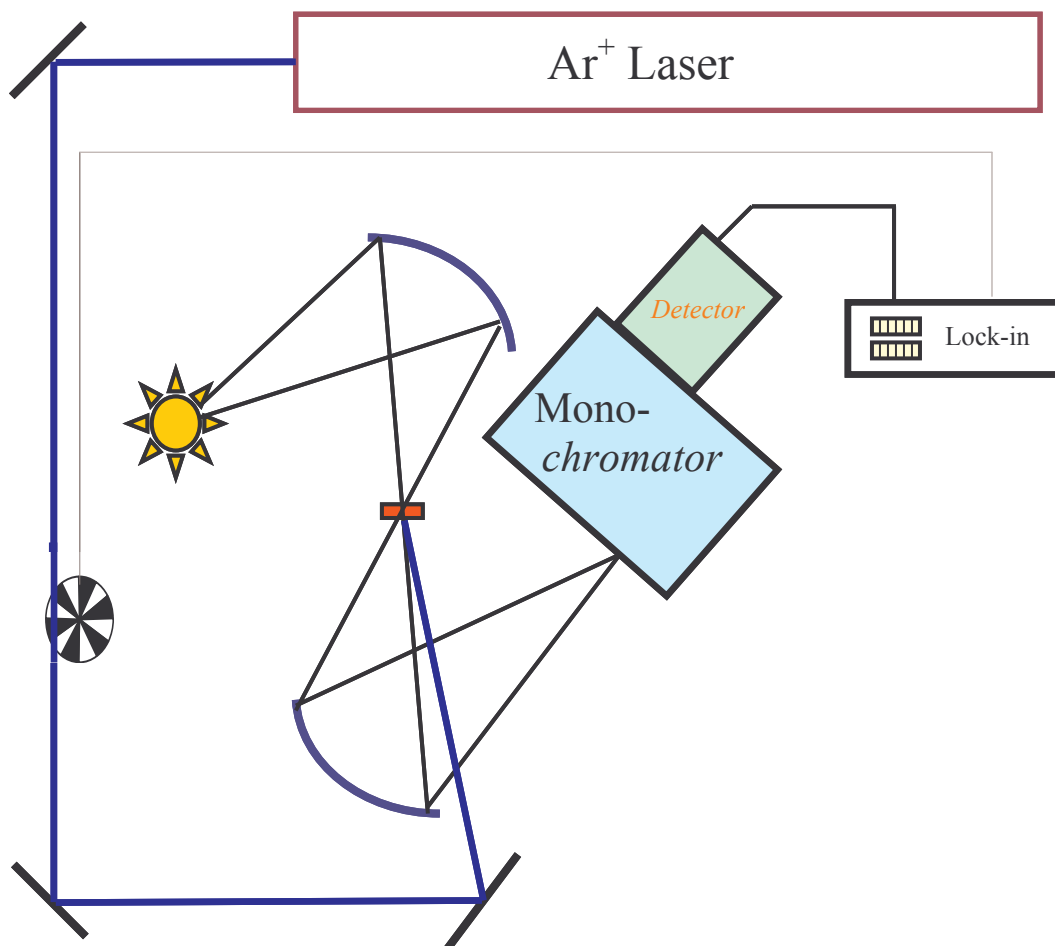
Figure 3.5: Schematic experimental setup of the photoinduced absorption experiment

Components

Coherent Innova 400 Ar$^+$ Laser
SRS 830 Lock-in Amplifier
SRS540 Chopper wheel (mechanical)
ISOMET acousto-optical modualtor Model 1206C-778 plus Driver 230
SRS DS345 Synthesized Function Generator
Acton SpetraPro 300i Monochromator
Si-GaAsInSb Two-Color Detector (cooled) Polytec
Tungsten Lamp (Polytec)
Hammamatsu R630-10 photomultiplier tube
Femto DLPCA-200 Low-noise current preamplifier
Home-built liquid N$_2$ bath cryostat or Oxford CF204 continuous flow cryostat (He)

3.2.5.1 Photoinduced Absorption (PIA)[20-22]

The experimental setup of the photoinduced absorption experiment is shown in Figure 3.5. Three aluminum mirrors guide the excitation light from the Ar$^+$-Laser onto the sample. A mechanical chopper modulates the intensity of the laser light. When very high modulation frequencies (> 3000 Hz) or a special modulation shapes are required, an acousto-optical modulator can be used. White light probing the transmission of the sample is coming from a tungsten lamp. A spherical mirror creates an image of the lamp on the sample. Another spherical mirror collects the transmitted light and creates an image of the sample on the slit of the monochromator. A two-color detector is used to measure the spectrally dispersed light. The signal from the detector is fed into a lock-in amplifier to detect the synchronous changes of the transmission due to additional laser excitation. Experiments can be carried out between room temperature and 16 K.

Measurements were performed in three steps. First the photoluminescence of the sample was recorded. The modulated laser light excited the sample and the luminescence was measured. The internal phase of the lock-in was adjusted to be in-phase to the reference signal coming form the chopper. In the second step, the white light source was switched on. Again the excitation light was chopped, the internal phase of the lock-in was in-phase to the reference signal and the photoinduced transmission changes were acquired. As a last step the transmission of the sample was measured. The white light was chopped and the excitation light was switched off. Subtracting the photoluminescence spectrum from the PIA spectrum and dividing the result by the transmission spectrum gave the corrected spectrum.

One can estimate the lifetime of a species observed in the PIA spectrum by measuring the modulation frequency dependence of this signal.[23-26] The shape of the frequency dependence depends on the shape of the excitation light modulation. Analytical formulas can be derived for rectangular and sinusoidal modulation.[23] Using a mechanical chopper the profile of the intensity modulation can be quite tricky. If the diameter of the laser beam is much smaller than the slit width of the mechanical chopper, rectangular light modulation is achieved. However, if the laser spot diameter and the slit width are comparable, the situation is different. Figure 3.6a shows the calculated variation of the laser intensity assuming a Gaussian laser profile and a slit width as shown in Figure 3.6 b).
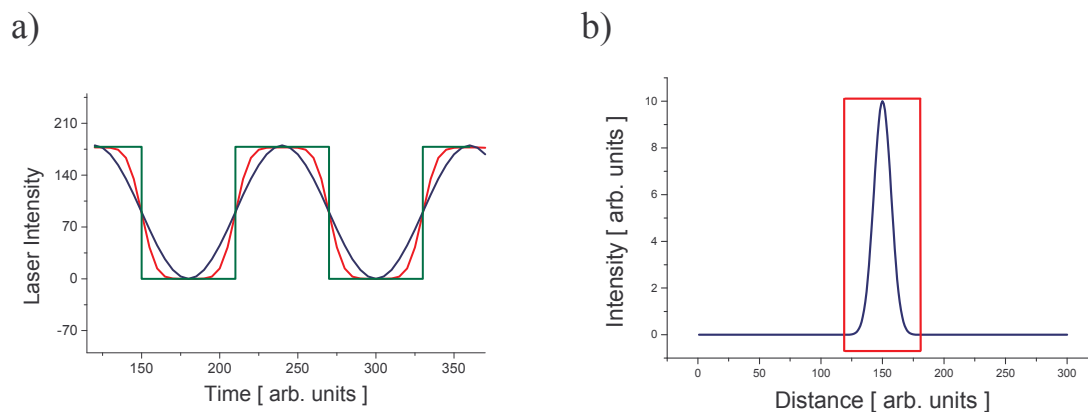
a)

b)

Figure 3.6: a) Calculated dependence of the light excitation intensity for a laser beam with gaussian intensity distribution when modulated with a mechanical chopper (red line). For comparison an ideal rectangular (green line) and sinusoidal (blue line) modulation is also shown. b) Illustration of the spot diameter and the slit width of the chopper wheel used for the calculation.

In this case neither the formula derived for rectangular nor the formula derived for sinusoidal modulation can be applied. For a detailed fitting, numerical methods have to be applied.[25,26] If the investigated species has a distribution of lifetimes a model derived by Ehrenfreund et al.[27] can be applied which gives information about the lifetime distribution of photoexcited species.

3.2.5.2 Delayed Fluorescence[28]

This experiment requires a sinusoidal modulation of the laser intensity, which can be achieved by operating an acousto-optical modulator in the so-called linear regime.[28]
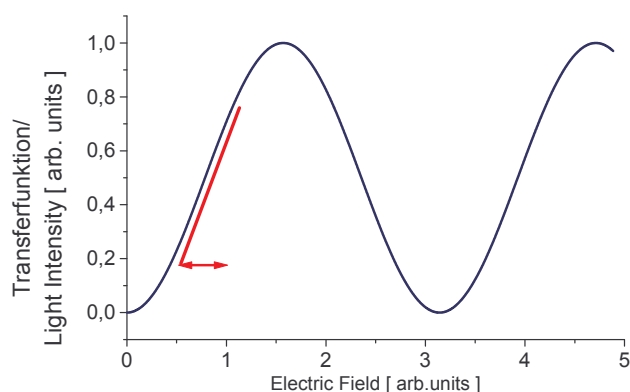

Figure 3.7 Transfer function of an acousto-optical amplifier

Figure 3.7 shows the transfer function of the acousto-optical modulator used in the experiment. This function gives the dependence of the applied electric field driving the modulator on the light intensity transferred to the first refracted order of the

modulator. As indicated by the red line, one can expect an almost linear response of the light intensity on the electric field, when the modulator is operated in this regime. Here the light modulation will be not complete and the light intensity $I(t)$ can be described by $I(t)=I_0(1+a\cdot\sin(\omega t))$. I_0 is the average light intensity and ω is the modulation frequency. A good linear response of the ISOMET Model 1206C-778 plus Driver 230 was found for $a \leq 0.2$.

For measuring delayed fluorescence a fast and sensitive detector is required. The frequency response of the detection system should be as fast as possible. Here a photomultiplier tube together with a fast preamplifier was used. In the experiment the laser intensity was modulated sinusoidally and the first and second harmonic, with respect to the applied modulation, of the sample photoluminescence are detected. To correct for any unknown instrumental response, also the first and second harmonic of the laser intensity were recorded.[28] Measurements were performed using the setup described in Figure 3.5. The light intensity was modulated in the frequencies within the range of 10 Hz – 10kHz.

3.2.6 Time-resolved Photoinduced Absorption Experiment[20,21,29]
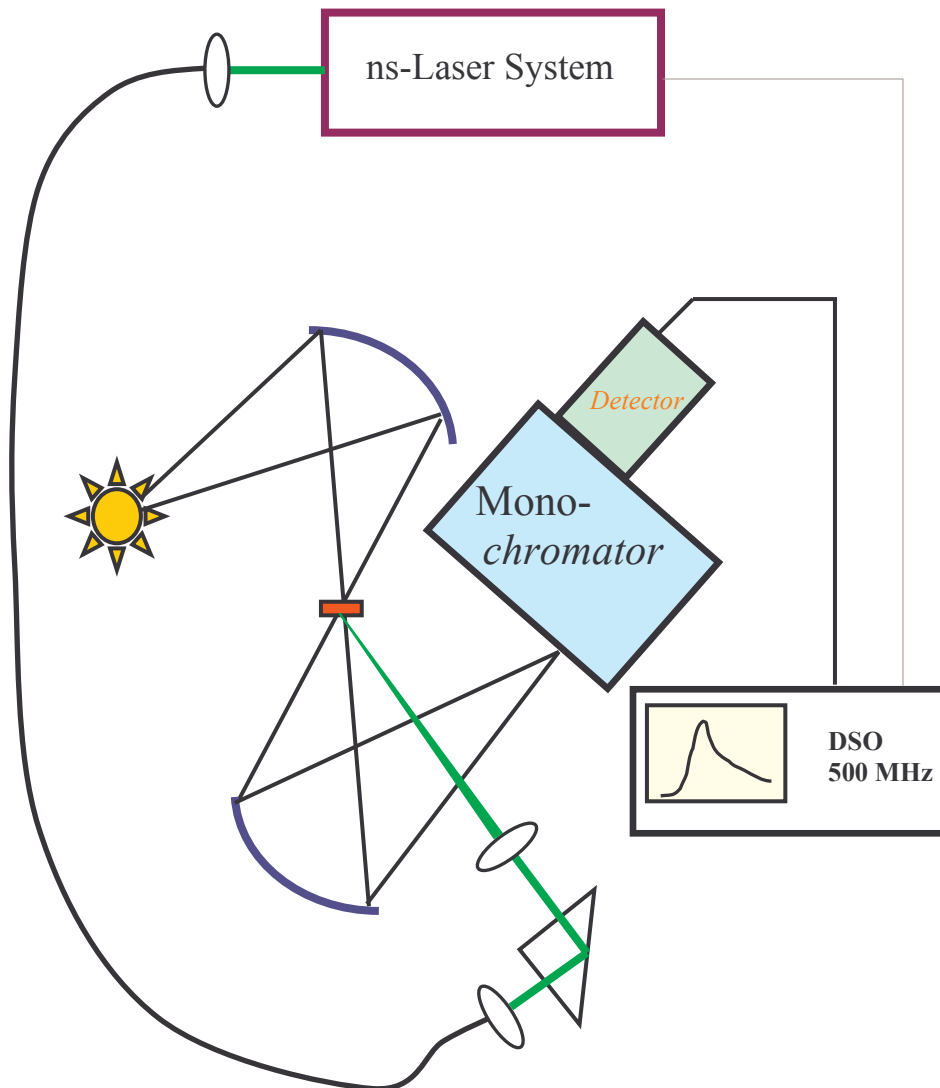
Figure 3.8: Time-resolved photoinduced absorption setup

Coherent Infinity 40-100 Nd-YAG Laser (ns-System)
Lambda Physik Scanmate OPPO
Acton SpetraPro 300i Monochromator
Si-GaAsInSb Two-Color Detector (cooled) Polytec
Tungsten Lamp (Polytec)
Home-built liquid N_2 cryostat
Tektronix Oscilloscope TDS 754C

The experimental setup is shown in Figure 3.8. The ns-pulses are transferred by a 10 m long optical fiber from the pulsed laser system to the photoinduced absorption

setup. A standard fiber coupling system is used to couple the laser pulse into the fiber and to reproduce the beam-profile at the end of the fiber. The propagation of the pulse does not change its width and shape.[30] A prism guides the light pulse towards the sample. An additional lens allows the adjustment of the spot size of the excitation pulse on the sample. White light for probing the transmission of the sample is coming from a tungsten lamp. A spherical mirror creates an image of the lamp on the sample. Another spherical mirror collects the transmitted light and creates an image of the sample on the slit of the monochromator. The detector is connected to a digital storage oscilloscope. The trigger signal for the oscilloscope is delivered by the pulsed laser system. The two-color detector limits the time resolution of the experiment. Between 400 - 1100 nm (Si-detector) the bandwidth of the used detector is ~50 kHz. The GaAsInSb-detector (1100 - 2600 nm) bandwidth is 1 MHz.

Measurements were performed in the following way: The monochromator was set to a certain wavelength. Several hundred transients were averaged to improve the signal to noise ratio. The measurement of the signal was quite difficult. White light probing the transmission created a quasi dc offset of ~ 1V on the detector output. The observed relative changes of transmission ($\Delta T/T$) were in the range of $10^{-3.}$ The transients measured by the oscilloscope had a maximum amplitude of ~ 1 mV, which corresponds to the lowest sensitivity of a standard digital oscilloscope. In the experiment, quite high laser pulse energies had to be used. Usually pulses with ~ 1 mJ had to be applied to observe the transient photoinduced absorption. Due to these high energies, deviations of the sample temperature from the steady-state temperature could not be excluded.

One possibility to improve the experimental arrangement would be the use of two pulsed light-sources. In addition to the ns laser system a flash lamp delivering white light pulses would be advantageous. With such a system, the time-resolution is achieved by simply changing the delay between the two pulses. The measurement would be in the quasi-cw regime and would not require a fast detector and high light intensities.

3.2.7 Reaction yield detected magnetic resonance (RYDMR)[31-34]

Experiments were performed on a Bruker EMX X-band spectrometer. The method for magnetic resonance detection is quite different to the conventional ESR technique. In RYDMR not the external magnetic field but the microwave intensity in the cavity is

periodically modulated. The resonance is detected via changes of the yield of a chemical reaction, or the photoluminescence, photocurrent etc. In Figure 3.9 the arrangement of the home-built microwave intensity modulator is shown.
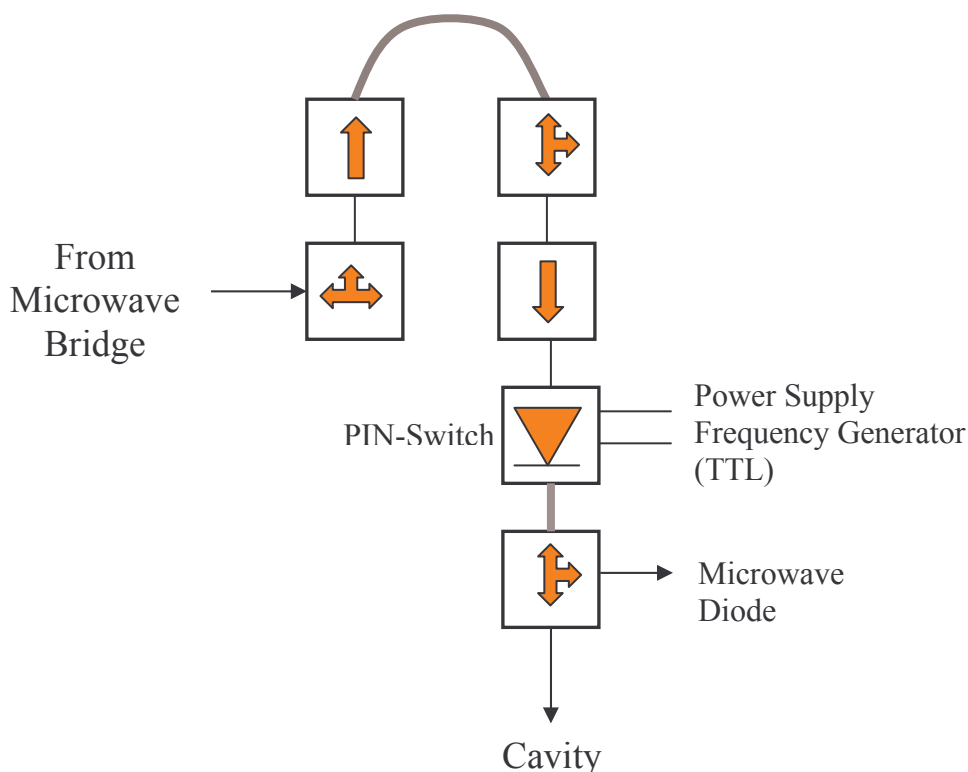

Figure 3.9: Arrangment of microwave components for RYDMR experiement

Microwave isolators and circulators AEROTEK
Microwave PIN-Switch
Microwave detector HP8057

A series of microwave circulator, insulator, semi-rigid waveguides, circulator, insulator, PIN-switch and circulator guide the microwave from the microwave bridge to the cavity. Special care has to be taken to avoid any reflection of the microwave power back into the microwave bridge. For operation, $\pm$ 5 V have to be applied to the PIN-diode. The PIN-diode can be switched from the absorbing to the transmitting mode by applying an additional TTL-signal. The microwave diode connected to the last circulator monitors the microwave power reflected from the cavity. It is used to control the resonance condition of the setup.

Tuning the spectrometer can be done in the following way:

Connect the first and the last circulator at the microwave intensity modulation unit with a semi-rigid wave-guide. Now the microwave reflected from the cavity is guided back into the microwave bridge. In the Tune-Mode of the spectrometer, which is accessible in the standard Bruker Software, the mode of the cavity can be seen. After switching to dual-trace (option in the tune-mode) the resonance tip of the sample cavity can be locked to an external cavity, which is located in the microwave bridge. Now AFC (automatic frequency control) is locked to the mode of the reference-cavity.[35] As a next step, the connection between the first and the last circulator is removed and the microwave diode is connected to the last circulator. This diode measures the microwave power reflected from the cavity. The knob on the front panel of the microwave bridge can be used to change the resonance frequency of the reference cavity. At the same time the frequency of the microwave source is changed. Therefore, using the knob, the system can be tuned to resonance minimizing the reflected microwave power from the cavity.

3.2.8 Photocurrent detected magnetic resonance (PCDMR)[36-38]

In PCDMR small photodiodes are placed in the microwave cavity and changes of the photocurrent induced by microwaves are measured. To protect the samples from degradation due to moisture or oxygen, diodes have to be investigated in an inert atmosphere. This has been done in the following way (see Figure 3.10):

Two thin copper wires of appropriate length were fixed inside a short peace of vacuum tube by epoxy sap. Ends of the wire were attached to the electrodes of the sample by silver paste. After checking the mechanical stability and the electrical quality of the contacts, the sample plus wires were inserted into a standard NMR quartz tube. The short vacuum tube was used to seal the open end of the quartz tube.

Figure 3.10: Encapsulated sample for a PCDMR measurement

The whole procedure was done in an Ar glove-box. Tubes were placed in a rectangular TE_{102} cavity with two windows for optical access inside a magnet of the ESR-spectrometer. Photodiodes were illuminated by light coming from an Ar^+ Laser or a lamp attached to a monochromator.
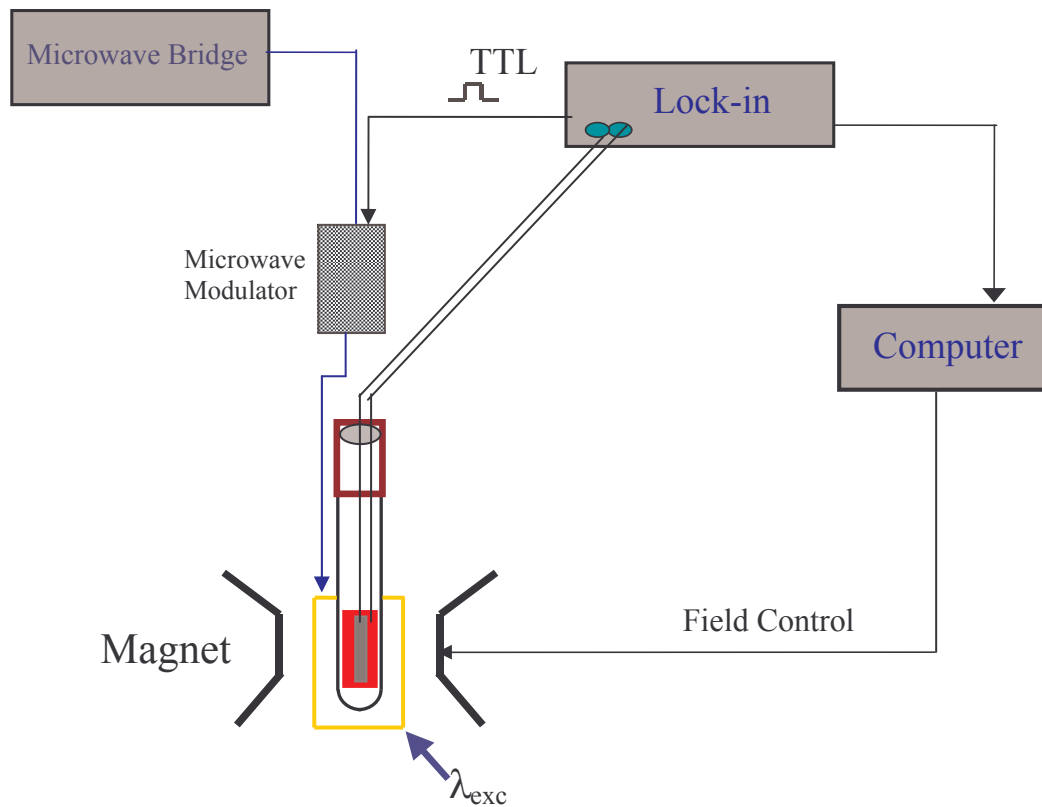
Figure 3.11: Complete experimental setup for a PCDMR experiment

Bruker EMX ESR spectrometer
Home-built microwave power modulator
SRS830 Lock-in Amplifier
HP8351 microwave diode
Coherent Innova 400 Ar^+ Laser
Lamp (CUNOW-Spotlight DC-480 000 R) attached to a monochromator (GM 252)
liquid N_2 quartz cryostat

In the experiment the synchronous changes of the photocurrent, produced by the polymer photodiode, on the square wave modulated microwave power were detected by a lock-in amplifier, while the external magnetic field was gradually changed (Figure 3.11). Samples were exposed to an alternating magnetic field in the cavity. This caused an additional induced current, which was detected by the lock-in amplifier. It did not depend on the external magnetic field and increased with increasing modulation frequency. At high frequencies it was the dominant signal making measurements very difficult.

3.2.9 Photoluminescence detected magnetic resonance (PLDMR)[32,34,36,37]

For PLDMR experiments films were prepared by spin-coating the polymeric solutions on a plastic substrate. Up to ten pieces, each with an approximate size of 1.5 mm x 2 cm, were cut from the substrate and put into an ESR grade quartz tube and sealed in helium atmosphere. In this case, the thermal contact between the sample and the surrounding is maintained by the He-gas in the tube. Thin film samples could also be mounted on a small Teflon holder and placed directly in the cavity.
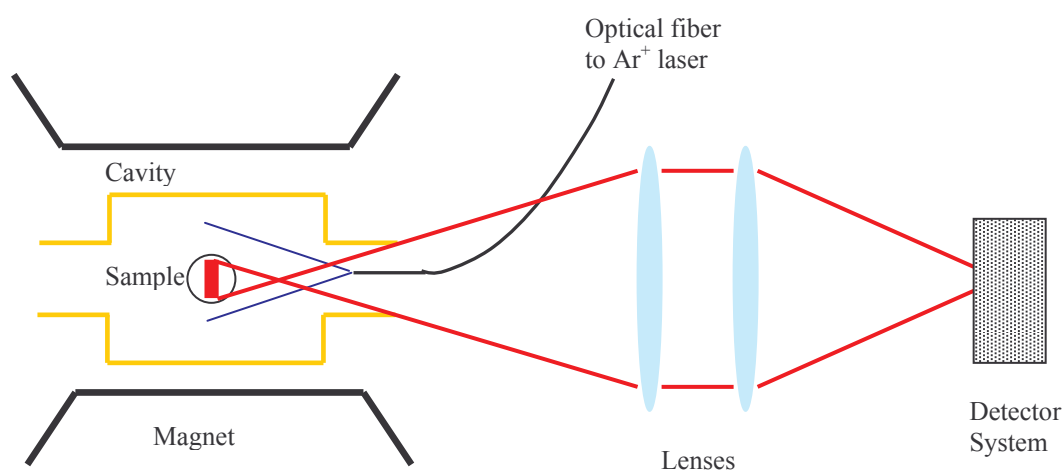
Figure 3.12: Experimental arrangement of optical components for the PLDMR experiment

Bruker EMX ESR spectrometer
Home-built microwave power modulator
SRS830 Lock-in Amplifier
HP8351 microwave diode
Coherent Innova 400 Ar$^+$ Laser
Melles Griot 4103 Si-photodiode
Acton SpetraPro 150i Monochromator
Hammamatsu R630-10 photomultiplier tube
Femto DLPCA-200 Low-noise current preamplifier
Oxford 900 Continuous Flow Cryostat (liquid He)

Another way of forming films was to fill the ESR tube with solution holding the material of interest and than slowly evaporating the solvent. With this procedure films with undefined morphology were formed on the inner wall of the ESR tube. In the PLDMR experiments the same system for microwave intensity switching as in the PCDMR experiments was applied. For the photoexcitation an Ar+ laser was employed. Samples were excited through an optical fiber terminating inside the

optical window of the cavity. A combination of two lenses collected the PL of the samples (Figure 3.12). Long pass filters were used to block stray light from the laser. PL was detected by a silicon diode operated in the photovoltaic mode, or a photomultiplier attached to a small monochromator. The experimental arrangement is often called Voigt configuration i.e. light emitted by the sample is detected in a direction perpendicular to the external magnetic field. A lock-in amplifier was used to detect the synchronous changes of the signal produced by the detector system on the square wave modulated microwave power while gradually sweeping the magnetic field. Special care had been taken to minimize the stray light on the detector. It artificially reduces the relative amplitude of the measurement and introduces additional noise.

References

[1] P. M. Allemand, G. Srdanov, A. Koch, K. Khemani, F. Wudl, Y. Rubin, F. Diederich, M. M. Alvarez, S. J. Anz, and R. L. Whet-ton, J. Am. Chem. Soc. 113, 2780 (1991).

[2] I. D. Parker, Y. Cao, C. Y. Yang, J. of Appl. Phys. 85, 2441 (1999).

[3] L. S. Roman, W. Mammo, L. A. A. Pettersson, M. R. Andersson and O. Inganäs, *Adv. Mater.* 10, 774 (1998).

[3] M. R. Andersson, W. Mammo, T. Olinga, M. Svensson, M. Theander, O. Inganäs, Synth. Met. 101, 11 (1999).

[4] K. E. Aasmundtveit, E. J. Samuelsen, W. Mammo, M. Svensson, M. R. Anderrsson, L. A. A. Pettersson, and O. Inganäs, Macromolecules 33, 5481 (2000).

[5] M. Theander, O. Inganäs, W. Mammo, T. Olinga, M. Svensson, M. R. Andersson, J. Phys. Chem. B 103, 7771 (1999).

[6] C. J. Brabec, C. Winder, M. C. Scharber, and N. S. Sariciftci, J. C. Hummelen, M. Svensson, M. R. Andersson, J. Chem. Phys. 115, 7235 (2001).

[7] M. Berggren, G. Gustafsson, O. Inganäs, M. R. Andersson, O. Wennerström, and T. Hjertberg Appl. Phys. Lett. 65, 1489 (1994).

[8] M. R. Andersson, W. Mammo, T. Olinga, M. Svensson, M. Theander, O. Inganäs, Synth. Met. 101, 11 (1999).

[9] Z. Bao, A. Dodabalapur, and J. Lovinger, Appl. Phys. Lett. 69, 4108 (1996)

[10] H. Sirringhaus, P. J. Brown, R. H. Friend, M. M. Nielson, K. Bechgaard, B. M. W. Langeveld-Voss, A. J. H. Spiering, R. A. J. Janssen, E. W. Meijer, P. Herwig and D. M. de Leeuw, Nature 401, 685 (1999).

[11] A. Dodabalapour, Z. Bao, A. Makhija, J. G. Laquindanum, V. R. Raju, Y. Feng, H. E. Katz, and J. Rgers, Appl. Phys. Lett. 73, 142 (1998)

[12] F. Padinger et al submitted to Adv. Funct. Mat.

[13] A. Cravino, N. S. Sariciftci, J. Mat. Chem. 12, 1931 (2002).

[14] J. C. Jummelen, B. W. Knight, F. Lepec, F. Wudl, J Yao, C. L. Wilkins, J. Org. Chem. 60, 532 (1995)

[15] C.J.Brabec, G. Zerza, N.S.Sariciftci, G.Cerullo, S.DeSilvestri, S.Luzatti, J.C.Hummelen, Chem. Phys. Lett. 340, 232 (2001).

[16] V. Dyakonov, G. Zoriniants, M. Scharber, C. J. Brabec, R. A. J. Janssen, J. C. Hummelen and N. S. Sariciftci, Phys. Rev. B 59, 8019 (1999)

[17] J. De Ceuster, E. Goovaerts, A. Bouwen, J. C. Hummelen, and V. Dyakonov, Phys. Rev. B, 64, 195206 (2001)

[18] G. Zerza, M. C. Scharber, C. J. Brabec, N. S. Sariciftci, R. Gomez, J. L. Segura, N. Martin, V. I. Srdanov, J. Phys. Chem. A 104, 8315 (2000).

[19] N. A. Schultz, M. C. Scharber, C. J. Brabec, N. S. Sariciftci, Phys. Rev. B 64, 245210 (2001).

[20] P. A. Lane, S. V. Frolov, and Z. V. Vardeny, *in Semiconducting Polymers*, (Eds. G. Hadziioannou, P. F. van Hutten) Wiley-VCH, Weinheim p. 189 (2000).

[21]D. W. McBranch and M. B. Sinclar, in *Primary Photoexcitations in Conjugated polymers*, (Ed. N. S. Sariciftci) World Scientific, Singapore (1997).

[22]M. Cardona, in *Modulation Spectroscopy*, Supplement 11, Solid State Physics, Academic Press, New York and London (1969).

[23]C. Botta, S. Luzzati, R. Tubino, D. D. C. Bradley and R. H. Friend, Phys. Rev. B 48, 14809 (1993).

[24]G. Dellepiane, C. Cuniberti, D. Comoretto, G. F. Musso, and G. Figari, A. Piaggi, A. Borghesi, Phys. Rev. B 48 7850 (1993).

[25]Y. Furukawa , Y.-H. Cha, T. Noguchi , T Ohnishi , M. Tasumi, J. of Mol. Struct. 521, 211 (2000).

[26]Y.-H Cha, Y. Furukawa, M. Tasumi, T. Noguchi, T. Ohnishi, Chem. Phys. Lett. 280, 464 (1997).

[27]O. Epshtein, G. Nakhmanovich, Y. Eichen, and E. Ehrenfreund, Phys. Rev. B 63, 125206 (2001).

[28]J. Partee, E. L. Frankevich, B. Uhlhorn, J. Shinar, Y. Ding, and T. J. Barton, Phys. Rev. Lett. 82, 3673 (1999).

[29]W. Demtröder,in *Laser Spectroscopy*, Springer-Verlag, Berlin, Heidelberg (1996).

[30]M. C. Scharber, Diploma Thesis, J.K. University Linz (1998).

[31]U. E. Steiner, T. Ulrich, Chem. Rev. 89, 51 (1989) and references therein.

[32]B. C. Cavenett, Advances in Physics 30, 475 (1981).

[33]E. L. Frankevich, S. I. Kubarev, in *Triplet State ODMR Spectroscopy*, Ed. R. H. Clarke, Wiley Interscience, New York (1982).

[34]A. L. Buchachenko, E. L, Frankevich, *Chemical Generation and Reception of Radio- and Microwaves*, VCH, New York (1994).

[35]See Manual Bruker EMX-Spectrometer (1995).

[36]V. Dyakonov in *Primary Photoexcitations in Conjugated polymers*, (Ed. N. S. Sariciftci) World Scientific, Singapore (1997).

[37]G. Rösler, PhD thesis, Bayreuth (1996).

[38]J. Shinar in *Handbook of organic conductive molecules and polymers*, edited by H. S. Nalwa, (John Wiley & Sons Ltd 1997), vol. 3,a p. 319.

4. Results and Discussion

4.1 Low temperature recombination of long-lived charge carries in conjugated polymers and conjugated polymer electron acceptor mixtures

Light induced electron spin resonance is a very convenient technique to study the recombination of long-lived photoinduced charge carriers.[1-3] Here the method is applied to investigate the recombination kinetics of long-lived photoinduced charges in MDMO-PPV powder, MDMO-PPV/PCBM films and films of polythiophene-anthraquinone (PT-AQ) double cable polymers. Experimental data are analyzed using a model,[1] which has already been successfully applied to describe the recombination kinetics of photoexcited carriers in inorganic amorphous semiconductors. Results suggest a universal recombination mechanism in disordered organic and inorganic materials.

4.1.1 Experimental

MDMO-PPV powder: Samples were excited by the lamp-monochromator system. In the experiments, 0.2 mW microwave power and a magnetic field modulation of 2 G (peak-peak) were applied. Decay kinetic measurements were performed at the magnetic field corresponding to the maximum position of the LESR spectrum.

MDMO-PPV/PCBM film: The concentration of PCBM in the polymer matrix was 10 wt %. Samples were excited by the Ar+ Laser, λ_{exc} = 476 nm. Measurements were performed at 40 K, 2 μW microwave power and a magnetic field modulation of 1 G (peak-peak). Decay kinetic measurements were performed at the magnetic field corresponding to the maximum position of the PCBM$^-$ resonance in the LESR spectrum.

PT-AQ double cable thin films: Samples were excited by the Ar+ Laser, λ_{exc} = 476 nm. Measurements were performed at 20 K, 2 μW microwave power and a magnetic field modulation of 2 G (peak-peak). Decay kinetic measurements were

performed at the magnetic field corresponding to the minimum position of the polymer cation resonance in the LESR spectrum.

The experiments did not allow to determine the number of light induced spins in the samples. Therefore decay curves recorded on the same sample but at different light excitation intensities were normalized to the highest signal observed. By this different measurements can be compared and analyzed.[3]

4.1.2 Results and Discussion

4.1.2.1 LESR on MDMO-PPV powder

In Figure 4.1 the (L)ESR spectra of pristine MDMO-PPV powder are shown. It is quite common to find an ESR signal in conjugated polymers without any photoexcitation. These spins have been attributed to chemical impurities and deeply trapped polarons.[4,5] The LESR spectrum is obtained by subtracting the spectrum of the dark spin from the light induced spectrum.
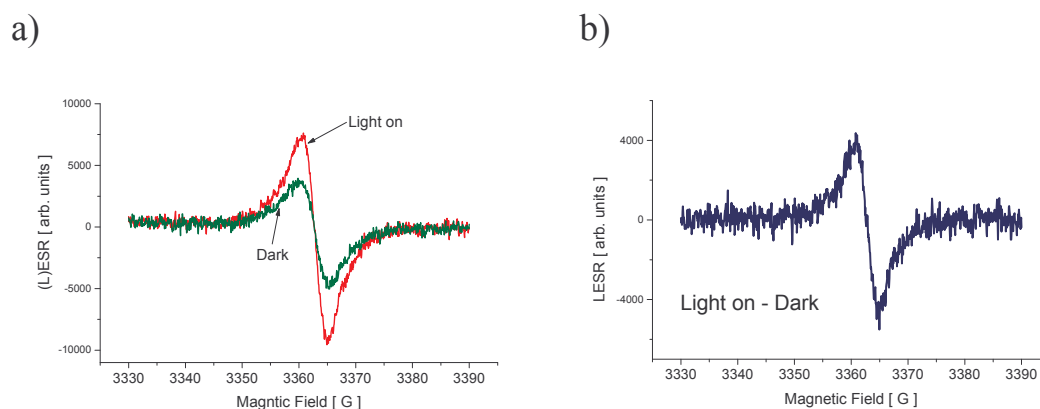
a)   b)

Figure 4.1: a) Dark (green) and light induced (red) electron spin resonance spectrum of MDMO-PPV powder, T = 60 K, λ_{exc} = 550 nm, light intensity 14 mW/cm², b) Spectrum of light induced spins obtained by subtracting the dark spectrum from the light induced spectrum shown in Figure 4.1 a).

It is interesting to note that higher energy light excitation was found to produce charge carriers more efficiently in the LESR experiment.[4] A typical measurement of the decay kinetic of light induced charges is shown in Figure 4.2 a). After recording the dark spin density for a few minutes the light is switched on. The ESR signal increases and starts to saturate after some time (depending on the light excitation intensity).

When the light excitation is switched off, the decay of light induced species can be observed.

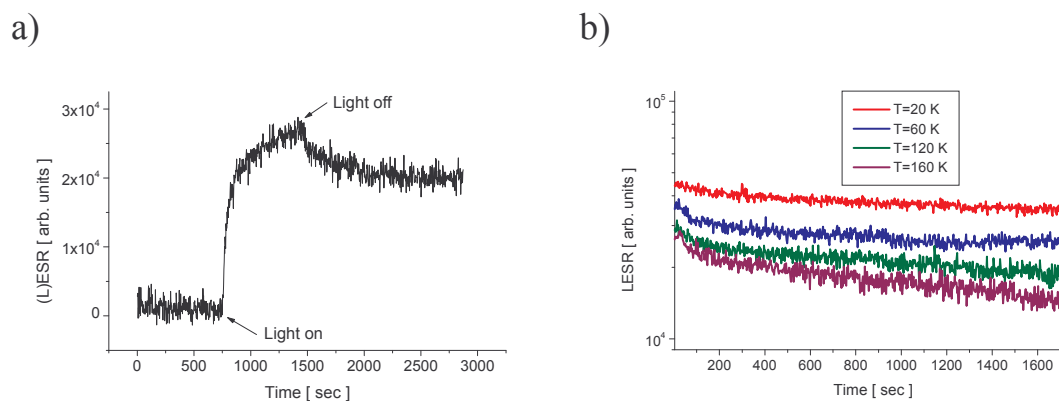a)   b)

Figure 4.2: a) Typical measurement of the decay kinetics of light-induced spins in MDMO-PPV. b) Decay kinetics recorded at different temperatures 20 K (red), 60 K (blue), 120 K (green), 160 K (violet). For all measurements the sample was excited by 14 mW/cm^2, 375 nm.

In Figure 4.2 b) decay curves of long-lived spins recorded at different temperatures are compared. While the decay curves at 20 K and 60 K are almost parallel, the decay at higher temperatures appears to be faster, due to activated recombination mechanisms.

In Figure 4.3 two decay curves of photoexcited species in MDMO-PPV are plotted. The measurements were performed at 20 K. Samples were excited by 9 mW/cm^2, 375 nm (a) and 14 mW, 550 nm (b).

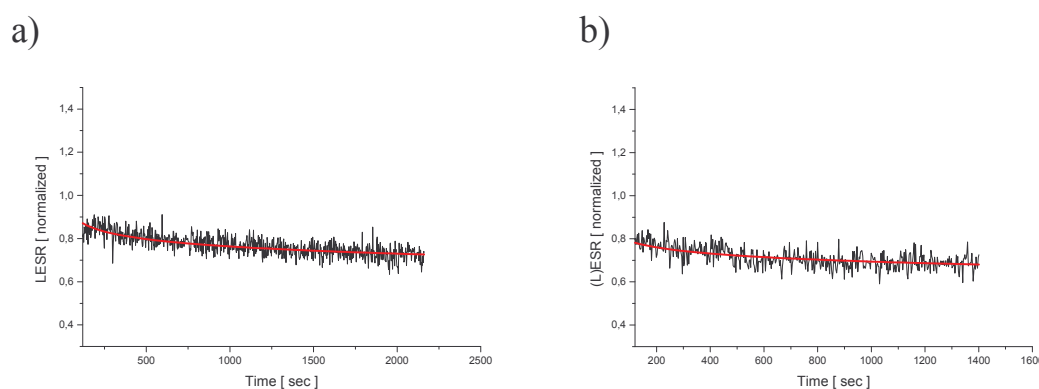a)   b)

Figure 4.3: a) Decay curve recorded at 20K, light excitation 9 mW/cm^2, 375 nm. b) Decay curve recorded at 20K, light excitation 14 mW/cm^2, 550 nm.

Red lines in Figure 4.3 are fits based on equation 2.4. t_1 was chosen to be 120 sec. Values for n_1/n_0 at $t=t_1$ were read from the graphs. Both curves can be reproduced

reasonably good choosing $\tau_0 = 10$ μs and $n_0 a^3 = 10^{-5}$. Assuming a localization radius of $a \approx 3$ nm, which corresponds to the typical effective conjugation length (5 PPV repeating-units), a spin density of $5 \cdot 10^{15}$ cm^3 can be calculated. This spin density is very low and explains the difficulties to measure LESR on thin (~100 nm) films of MDMO-PPV.

4.1.2.2 LESR on MDMO-PPV-PCBM thin film[3]

Adding small amounts of the fullerene PCBM to MDMO-PPV the LESR signal is drastically enhanced.[6] Figure 4.4 shows the LESR signal of MDMO-PPV-PCBM measured at 40 K. The resonance is a superposition of two individual resonances that have been attributed to a positive polaron (low magnetic fields) and the radical anion of PCBM (high magnetic fields).[6]

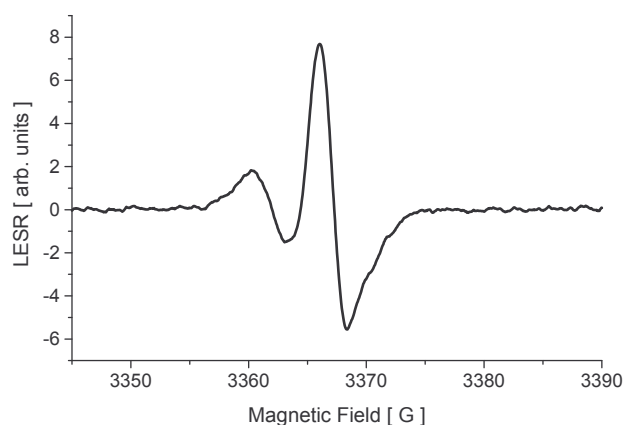Figure 4.4: Light induced electron spin resonance spectrum of MDMO-PPV/PCBM (10 % wt) at 40 K
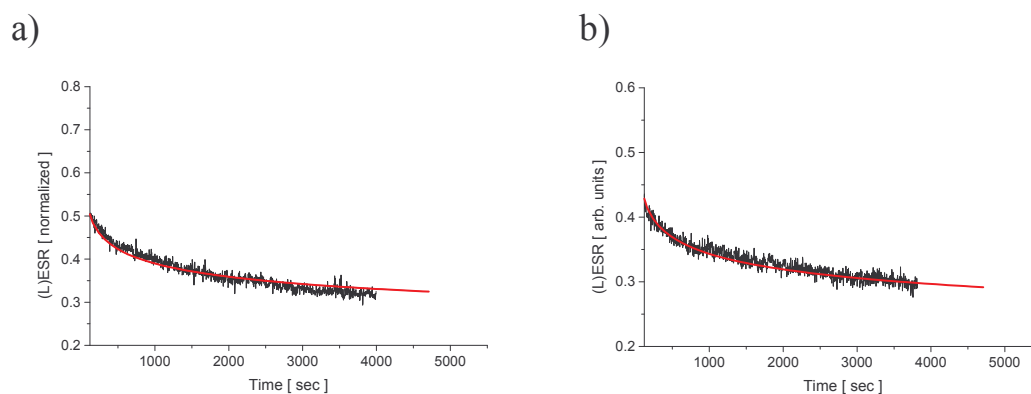
a)

b)

Figure 4.5: Charge carrier decay measured at 40 K, static magnetic field 3366 G, light excitation intensity a) 10 mW/cm^2 and b) 100 μW/cm^2

The recombination kinetics of both signals exhibited very long-living components at low temperatures. Two decay curves acquired for 10 mW/cm^2 and 100 µW/cm^2 light excitation intensity are shown in Figure 4.5 a) and b). Decay curves were recorded at a magnetic field corresponding to the maximum of the PCBM anion resonance (3366 G). Red lines in Figure 4.5 are fits based on equation 2.4. Values for n_1/n_0 at t_0 were taken directly from the graphs. Both curves can be fitted with $\tau_0 = 6 \cdot 10^{-5}$ s and $n_0 a^3 = 7 \cdot 10^{-4}$. Assuming a localization radius of a ~ 1 nm (diameter of the fullerene) a spin density of ~ 10^{18} cm^{-3} results from the measurement. This value corresponds to a saturation spin concentration of approximately 1 electron on 100 fullerene molecules.

4.1.2.3 LESR on a PT-AQ double cable

All compounds showed a dark electron spin resonance signal, which might result from chemical impurities. In the light induced ESR experiments for all PT-AQs two superimposed signals were found (Figure 4.8, 4.10, 4.12, 4.13 a)). The low field signal is attributed to the AQ$^-$ anion[7] (g = 2.0042) and high field signal is assigned to the positive polaron on the polymer chain (g = 2.0024). The deviation of the g-value of the anthraquinon radical from the free electron g-value is fairly large. This is very unusual for an organic molecule and may be related to a non-zero orbit angular moment in the molecule. Studying the decay kinetics in the system, again very long-living decay components were found for all maxima and the minimum in the LESR spectrum. Due to the overlap of anion and the cation resonance at low fields an analysis of the decay kinetics was not possible. Therefore the study was focused on the minimum of the LESR spectrum at high fields (3367 G). When possible, decay curves were recorded for different light excitation intensities and normalized to the highest amplitude observed in the experiment. In the investigated system the concentration of electron accepting units was very high compared to the system discussed above.

a) PT-AQ (100 %)

Figure 4.6 shows the light on, light off and the dark ESR spectrum of PT-AQ (100%). Compared to the other PT-AQ materials a very strong dark signal was observed. Decay curves were recorded at two different excitation intensities. In Figure 4.7 a) the

sample was excited by 50 mW/cm^2 and in Figure 4.7 b) the excitation intensity was 0.5 mW/cm^2. The red lines are best fits to the experimental data obtained in the same way as described above. Both curves can be fitted with the same set of parameters. Only the value n_1/n_0, the normalized spin concentration at t = 120 sec had to be adjusted. From the fits values for τ_0 and n_0a^3 are found to be 10^{-6} s and $1.5 \cdot 10^{-4}$.
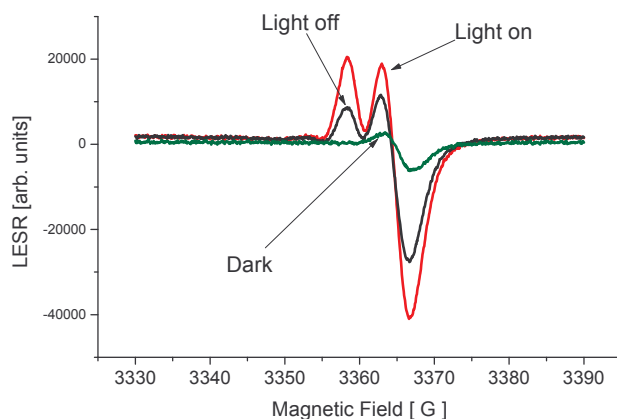

Figure 4.6: Light on, Light off and dark ESR spectra of PT-AQ(100%).

a)

b)

Figure 4.7: Charge carrier decay measured at 20 K, static magnetic field 3367 G, light excitation intensity a) 50 mW/cm^2 and b) 0.5 mW/cm^2.

b) PT-AQ (75 %)

Figure 4.8 shows the light on, light off and the dark ESR spectrum of PT-AQ (75%). Decay curves were recorded applying light intensities of 50 mW/cm^2 (Figure 4.9 a)) and 0.5 mW/cm^2 (Figure 4.9 b)). The red lines are best fits to the experimental data obtained in the same way as described above. Both curves can be fitted with the same set of parameters. Assuming that τ_0 is 10^{-6} s, n_0a^3 is found to be $1.4 \cdot 10^{-4}$.

Figure: 4.8: Light on, Light off and dark ESR spectra of PT-AQ(75%).

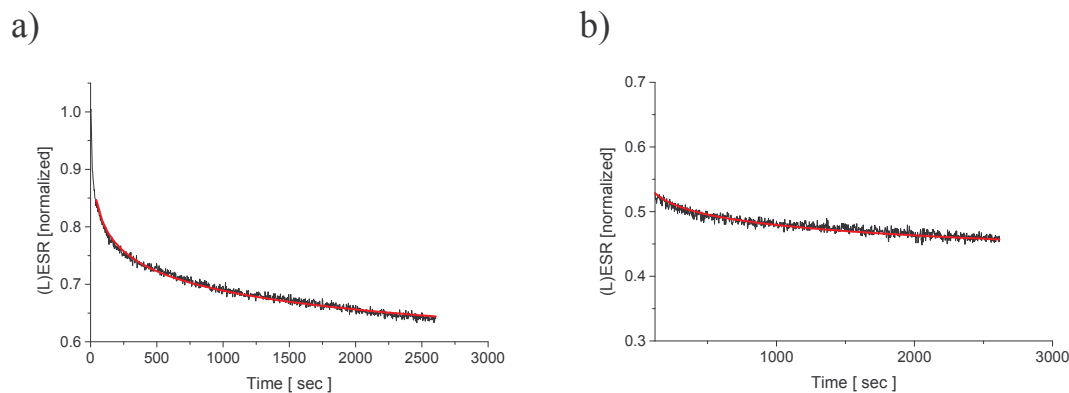a)   b)

Figure 4.9: Carrier decay measured at 20 K, static magnetic field 3367 G, light excitation intensity a) 50 mW/cm^2 and b) 0.5 mW/cm^2 .

c) PT-AQ (50 %)

Figure 4.10 shows the light on, light off and the dark ESR spectrum of PT-AQ (50%).

Figure 4.10: Light on, Light off and dark ESR spectra of PT-AQ(50%).

Decay measurements were performed for two light excitation intensities, namely 50 mW/cm^2 and 5 mW/cm^2 (Figure 4.11a), b)). Assuming that τ_0 is 1 μs the fits give $1.2 \cdot 10^{-4}$ for $n_0 a^3$.

a)   b)
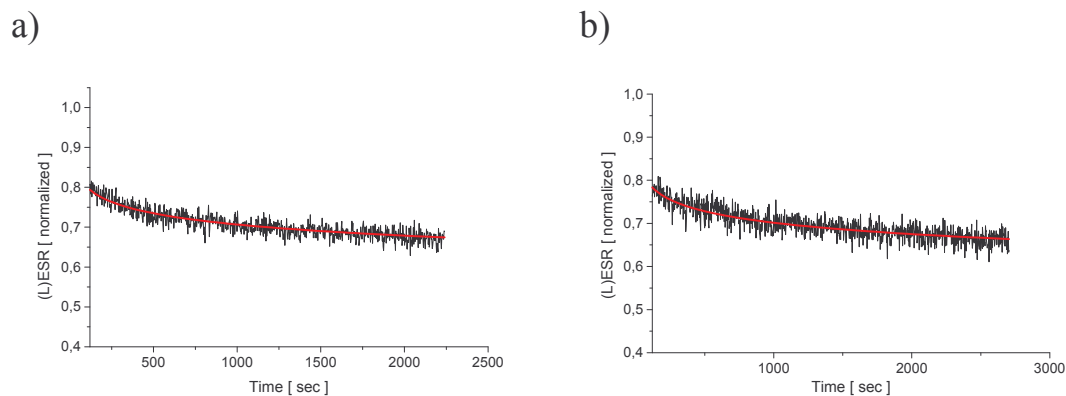
Figure 4.11: Charge carrier decay measured at 20 K, static magnetic field 3367 G, light excitation intensity a) 50 mW/cm^2 and b) 5 mW/cm^2.

d) PT-AQ (25%)

Figure 4.12a shows the light on, light off and the dark ESR spectrum of PT-AQ (25%). Compared to the other PT-AQ compounds the smallest signal amplitude was observed. The decay curve could only be measured at high excitation intensities (50 mW/cm^2). Assuming 1 μs for τ_0, the fit gives $9 \cdot 10^{-5}$ for $n_0 a^3$ (Figure 4.12 b)).

a)   b)
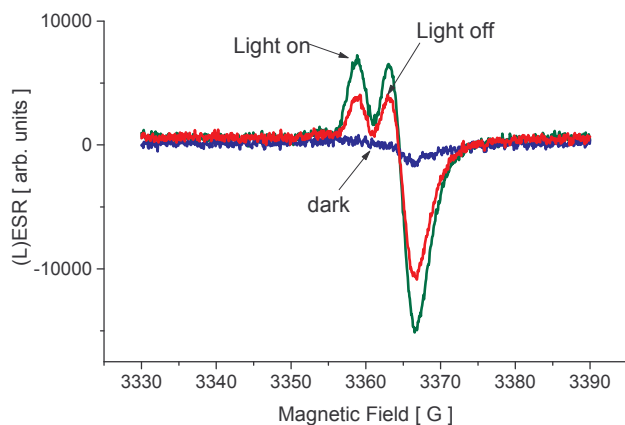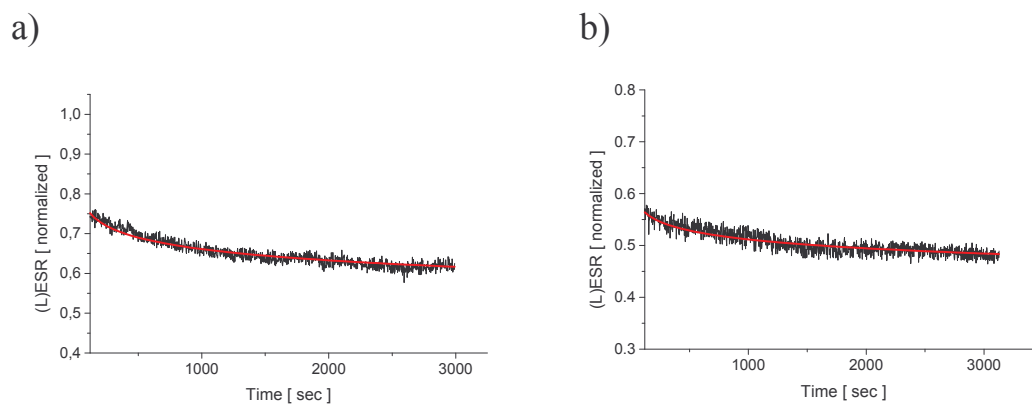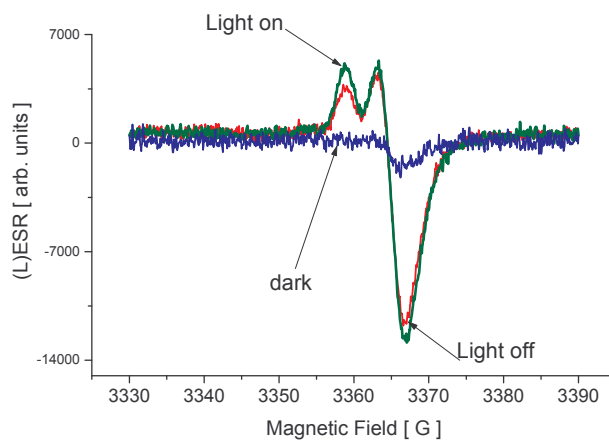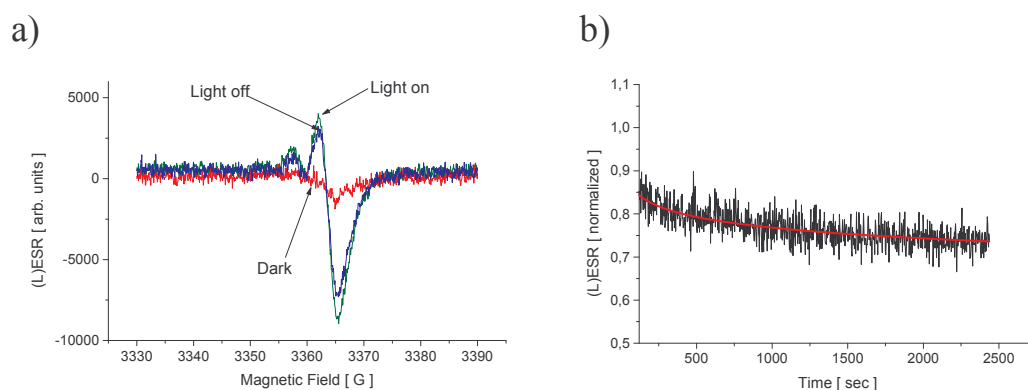

Figure 4.12: a) Light on, Light off and dark ESR spectra of PT-AQ(25 %). b) Charge carrier decay measured at 20 K, static magnetic field 3367 G, light excitation intensity 50 mW/cm^2

All decay curves presented above can be well fit with the model presented in chapter 2.1 without the use of any scaling parameter. Also the values obtained for the spin density are very reasonable. However, the τ_0 appears to be rather large compared to values of a-Si:H (10^{-8} s).[2] These much larger values for τ_0 have been ascribed to

polaronic effects in conjugated polymers. Due to the formation of polarons the energy barrier for tunneling is probably higher than in inorganic semiconductors.

It is very remarkable that all decay curves of PT-AQ can be fitted assuming the same value for τ_0. Due to the different composition of PT-AQ double cable polymers, one may expect that the effective localization radius a_0 is becoming smaller when the acceptor concentration is increased (the effective conjugation length of the polymer should be reduced). A simple model can be used to estimate the spin concentration in the samples. Assuming that the number of light induced spins is proportional to the acceptor concentration and that the effective localization radius linearly depends on the acceptor concentration the product $n_0 a^3$ can be expressed by

$$a^3 n_0 = \left(a_0 - \Delta a_0 \cdot x\right)^3 \left(n \cdot x\right) \qquad (4.1)$$

where x is the acceptor concentration, n is the maximum spin density and Δa_0 determines the change of the localization radius. In Figure 4.13 the values $a^3 n_0$ obtained from the decay fits are plotted versus the acceptor concentration. The red line represents the best-fit using equation 4.1. For the fit, a_0 was set to 0.7 nm, which corresponds to the length of the AQ molecule and a value of $1.2 \cdot 10^{18}$ spin/cm^3 is found for n.
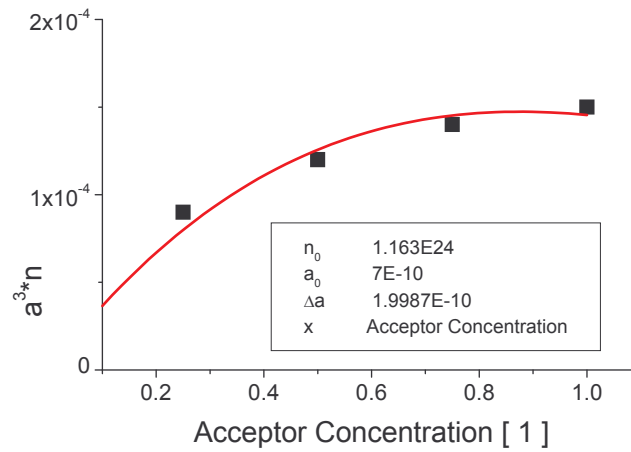
Figure 4.13: $a^3 n_0$ plotted versus the acceptor concentration. The red line represents the best fit using equation 4.1.

4.1.3 Summary

Low temperature recombination kinetics of photoinduced charge carriers in samples with different electron acceptor concentrations were studied. The observed decay curves can be described by a theoretical model, which was first applied to recombination processes of long-lived charges in inorganic amorphous semiconductors. The model excludes thermal reexcitation and focuses on a tunneling recombination process of photoexcited carriers, which did not recombine at short times. Results suggest that the electronic structure of localized states is similar in organic and inorganic amorphous semiconductors and that the concept of recombination by tunneling is very generally applicable.

4.2 Time-resolved photoinduced absorption

Time-resolved photoinduced absorption measurements were carried out to study the recombination of photoinduced charges in a conjugated polymer fullerene composite film. The charge carrier decay was found to be thermally activated and an activation energy could be estimated from the experiments.

4.2.1 Experimental

Experiments were performed on MDMO-PPV/UCM2 films. The relative concentration of the components in the film was 4:1 in (wt %). Samples were excited by 3 ns pulses coming from a Nd-YAG Laser, 532 nm, 4 mJ/cm^2 and the change in transmission was probed at 2200 nm. Measurements were carried out at 100 K, 200 K and 300 K.

4.2.2 Results and Discussion

In Figure 4.14 time-dependent changes of the relative PIA are plotted for different temperatures. Figure 4.14 a) shows transients recorded short times after the excitation pulse, while Figure 4.14 b) shows a longer sequence of the photoinduced absorption decay. Form Figure 4.14 a) it can be seen that the short decay component is temperature dependent i.e. the decay is faster for higher temperature. Decay curves shown in Figure 4.14 a) suggest that the decay kinetics can be analyzed by $-\Delta T/T = const.*(time)^b$ (see Table 4.1). From the exponent b one can deduce a characteristic decay time (time in which the signal has decayed to 1/10 of the total amplitude). An example is shown in Figure 4.15 a). In Figure 4.15 b) the rate constants of the decays ((Figure 4.14 a)) are plotted versus the inverse temperature. Assuming that the recombination of photoinduced carriers is thermally activated, an activation energy (ΔE) of ~15 meV can be estimated from a linear fit.

a)   b)
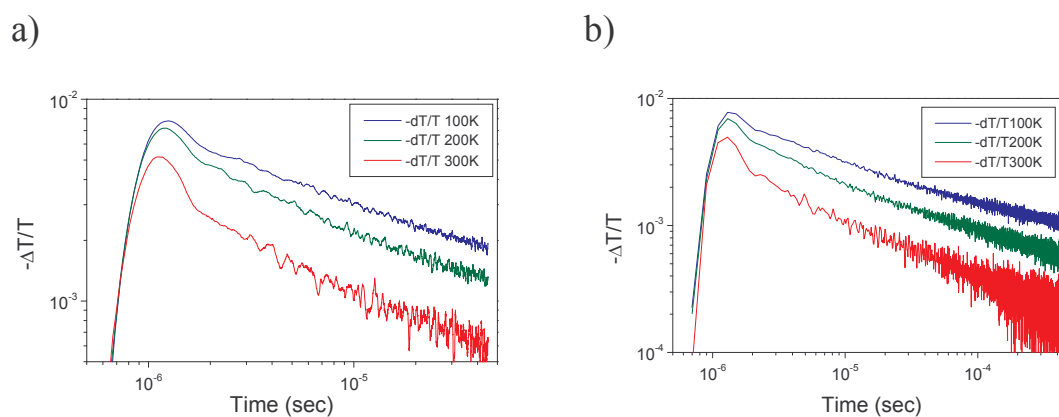
Figure 4.14: Transient photoinduced absorption recorded in different time windows – a) up to 45 μs, b) up to 450 μs and at different temperatures 100 K (blue), 200 K (green), 300 K (red).

In a very similar way, an activation energy can be deduced from transients shown in Figure 4.14 b). For the decay at t > 20 μs, an Arrhenius plot gives ΔE ~ 40 meV. These energies are very similar to activation energies observed in other conjugated polymer fullerene mixtures by other techniques like light induced ESR or electrical studies on photovoltaic cells.[8,9]

Table 4.1: b values for transient PIA in Figure 4.14

T [K]	b (45μs)	b (450μs)
100	-0.36	-0.26
200	-0.41	-0.33
300	-0.46	-0.44

a)   b)

Figure 4.15: a) Transient photoinduced absorption measured at 100 K – the red line shows the linear fit. b) Inverse characteristic decay time is plotted versus the inverse temperature – the red line is the linear fit to extract an activation energy.

According to the experimental results the charge separated state and the ground state of a conjugated polymer (segment) fullerene arrangemen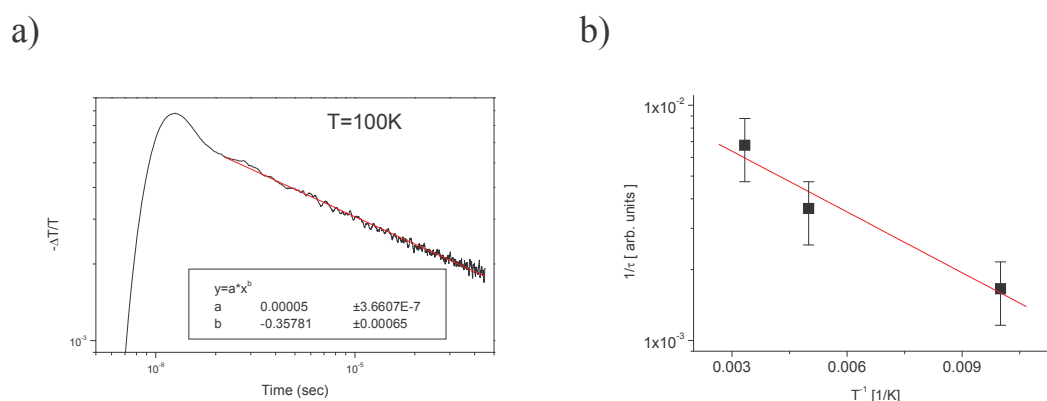t are separated by an energy barrier (Figure 4.16). The nature of this barrier is still unknown. The additional energy required to go from the charge-separated state to the ground-state can be provided by phonons (thermally activated process). Another possibility to reach the ground state is tunneling through the barrier. At low temperatures ($k_B T \ll \Delta E$) this is the dominant recombination pathway.
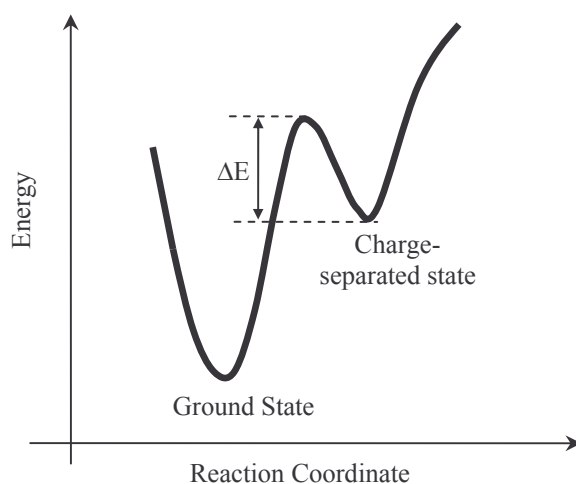
Figure 4.16: Schematic energy diagram representing the charge separated and the ground state in conjugated polymer/fullerene mixtures

4.2.3 Summary

In time-resolved photoinduced absorption measurements thermally activated recombination of photoinduced charges was observed. Measurements were used to estimate values for theses activation energies (ΔE). ΔE is found to be around 30 meV in the MDMO-PPV/UCM2 mixture. Similar energies were found in other conjugated polymer fullerene mixtures. These fairly high activation energies (comparable to $k_B T$ at room temperature) may explain the meta-stability of the charge-separated state in these systems.

4.3 Photoinduced Absorption at low temperatures and high frequencies

Photoinduced absorption (PIA) experiments performed at various modulation frequencies can be used to distinguish different photoexcitations. In this study thin MDMO-PPV/PCBM films were investigated. The PIA spectrum of these films shows exclusively charged excitations of the conjugated polymer (polaron). Measurements were used to assign different regions of the spectrum to different polaronic species according to theoretical calculations.[10,11]

4.3.1 Experimental

Experiments were performed on MDMO-PPV/PCBM films. The relative concentration of the components in the film was 1:3 in (wt %). Samples were excited by an Ar^+ Laser, 476 nm, 10 mW/cm^2. Measurements were carried out at T =16 K.

4.3.2 Results and Discussion

In Figure 4.17 a) the PIA spectra (in phase and out of phase), acquired at a modulation frequency of 330 Hz are shown. Both components have similar amplitude and show a very similar spectral dependence. In both spectra, peaks and shoulders have similar shapes and positions.
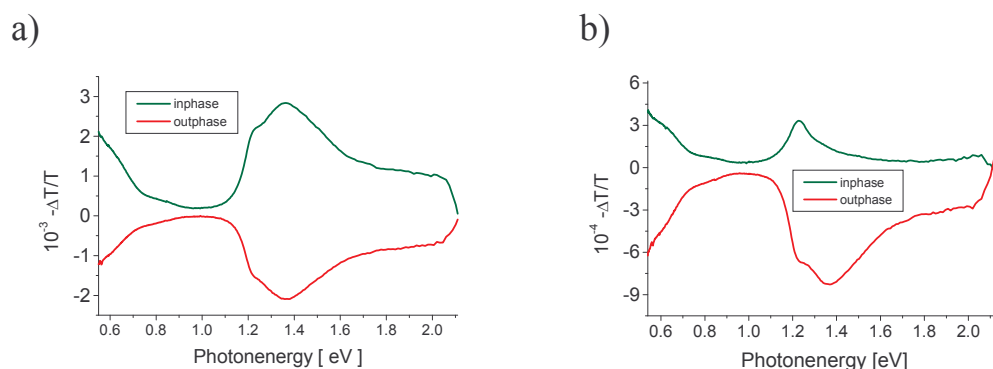
a)

b)

Figure 4.17: a) Photoinduced absorption spectra of MDMO-PPV/PCBM acquired at a) 330 Hz and b) 2970 Hz. In both spectra in-phase (green) and out-of-phase components are plotted.

Increasing the modulation frequency the in-phase component of the photoinduced absorption spectrum is changing significantly, while the shape of the out-of-phase part remains the same (Figure 4.17b). Instead of a broad PIA between 1.1 eV and 2.1 eV one fairly symmetric peak with smaller amplitude is found in the in-phase component. The maximum is positioned at 1.25 eV. The feature at low energies (0.55 eV – 0.9 eV) does not change position and shape. Only its intensity is reduced compared to the low frequency spectrum. In Figure 4.18 a) the in-phase spectra of Figure 4.17 a), b) are plotted together for better comparison.

a)
b)
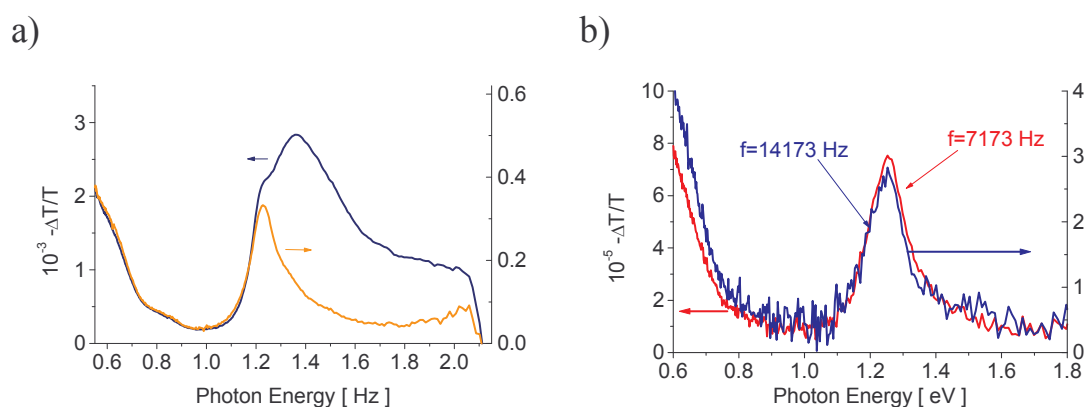
Figure 4.18: a) In-phase component of the photoinduced absorption spectra shown in Figure 4.17 a), b). b) Comparison of the in-phase photoinduced absorption spectra of MDMO-PPV/PCBM acquired at 7173 Hz (blue) and 14173 Hz (red).

Increasing the modulation frequency further, the in phase component does not change position and shape only the amplitude is reduced (Figure 4.18 b)).

a)
b)
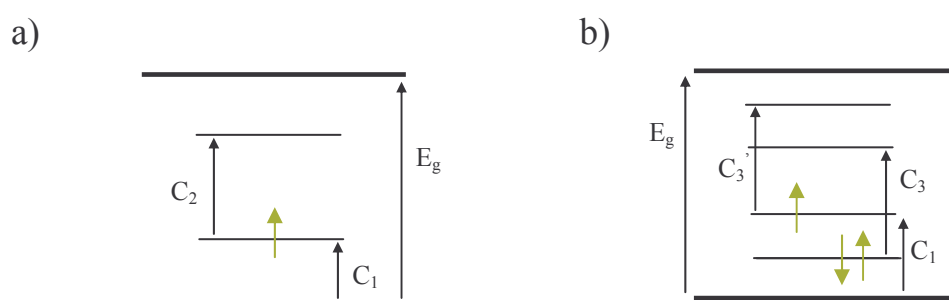
Figure 4.19: a) Allowed optical transitions in a localized polaron and b) delocalized (on two conjugated segments) polaron. Energetic positions of different levels are only schematic

According to theoretical calculations[10] the optical absorption spectrum of a positive polaron extended on one conjugated segment (intrachain polaron) should consist of two strong absorption bands (Figure 4.19 a)). The energy E_g and the position of the

levels P_1 and P_2 depend on the effective conjugation length of the chain segment the positive polaron is located on. It is well known that due to randomly introduced defects and morphological effects a distribution of effective conjugation lengths exist in a solid state conjugated polymer film. Therefore broad absorption features are expected for the transitions C_1 and C_2.

Recently the influence of interchain interactions on the optical response of a singly charged polaron has been addressed in a theoretical study. In the calculations co-facially aggregated dimers of two five-unit PPV oligomers separated by four angstrom have been considered.[10] Results show that the positive polaron is delocalized over both chains and that four polaron levels are present in the bandgap (interchain polarons). Again, the distribution of the lengths of conjugated segments will introduce a broadening of the optical transitions. In addition the coupling of more than two chains will result in additional states and optical transitions. The optically allowed transitions within a delocalized polaron are shown in Figure 4.19 b). Calculations show that transitions C_3 and $C_3{'}$ are expected at higher energies compared to the transition C_2 of the localized polaron. In the experiment a combination of "on one chain " and "on more than one chain" distributed polarons may be observed.

The experimental results described above may be explained in the following way:

At low modulation frequencies the PIA-spectrum contains features of localized and delocalized polarons. Increasing the modulation frequency, long-living components of the spectra are suppressed and only species with a lifetime $\sim$ 1/(modulation frequency) can be observed in the spectrum.
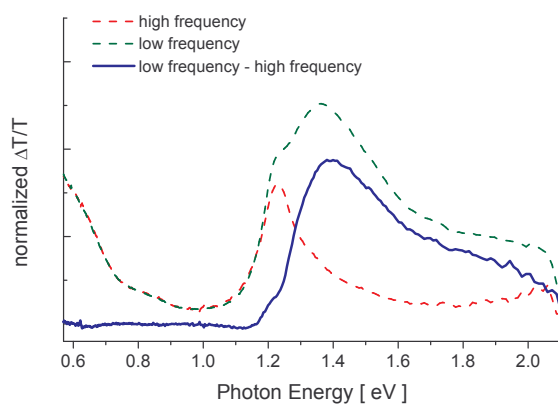
Figure 4.20: Normalized (at 0.57 eV) PIA spectra recorded at high (red) and low (green) frequencies and the difference between the high and the low frequency spectra (blue).

The PIA-spectrum at a high modulation frequency shows only two dominant features. According to the theoretical work described above, two absorptions are expected for intrachain polarons. Therefore one may conclude that the part of the spectrum present in the spectrum acquired at 330 Hz but missing at 2970 Hz is related to delocalized polarons (Figure 4.20). Calculations also show that absorption features of both polarons appear at similar energies.[1] Therefore one can expect an overlap of both spectra in certain energy ranges. If so, an estimation of the lifetime by a measurement of the frequency dependence of the PIA signal is difficult. The presented experiment offers a possibility to separate different photoexcitations present in a PIA spectrum. To work with sufficient signal amplitudes measurements it is favorable to work at low temperatures.

4.3.3 Summary

In the PIA spectrum of a MDMO-PPV/PCBM film two different photoexcitations were identified by comparing low and high frequency measurements. Theoretical calculations suggest that the observed species are intrachain and interchain polarons. According to the measurements, the lifetimes of intrachain polarons are shorter compared to interchain polarons.

4.4 Triplet–Triplet annihilation (TTA) in conjugated polymers[12]

Delayed photoluminescence produced by TTA is a well-known process in organic crystals.[13] The importance of this process in conjugated polymers has not been explored extensively up to now. Following the procedure suggested by E. Frankevich[12] (see Chapter 2.3) the delayed photoluminescence in MDMO-PPV was investigated. From this measurement a value for the triplet exciton lifetime can be deduced. Another estimation of this lifetime can be obtained by the frequency dependence of the triplet-triplet absorption in the photoinduced absorption measurement.

4.4.1 Experimental

Delayed photoluminescence and PIA experiments were performed under very similar experimental conditions; T = 19 K and an average laser intensity of ~ 5 mW, 476 nm. The experimental procedure is described in Chapter 3.2.5.2.

4.4.2 Results and Discussion

In Figure 4.21 the corrected ratio of the second and the first harmonic of the photoluminescence of MDMO-PPV is plotted. The red line represents the best fit to the experimental data using equation 2.12. From the fit a triplet lifetime of 100 μs can be calculated. This value is very similar to the values reported by Partee et al.[12] In Figure 4.22 a) typical photoinduced absorption spectrum of a thin film of MDMO-PPV is shown (T = 19K). Only one excited state absorption feature at 1.35 eV is observed, which has been attributed to a triplet-triplet absorption transition.[14] The frequency dependences of the triplet-triplet absorption are shown in Figure 4.23. The laser intensity was modulated sinusoidally (Figure 4.23 a)). The red line is the best fit using equation 2.6. For comparison the frequency dependence was also measured with a mechanical chopper (SR540 Chopper wheel with 30 slits).

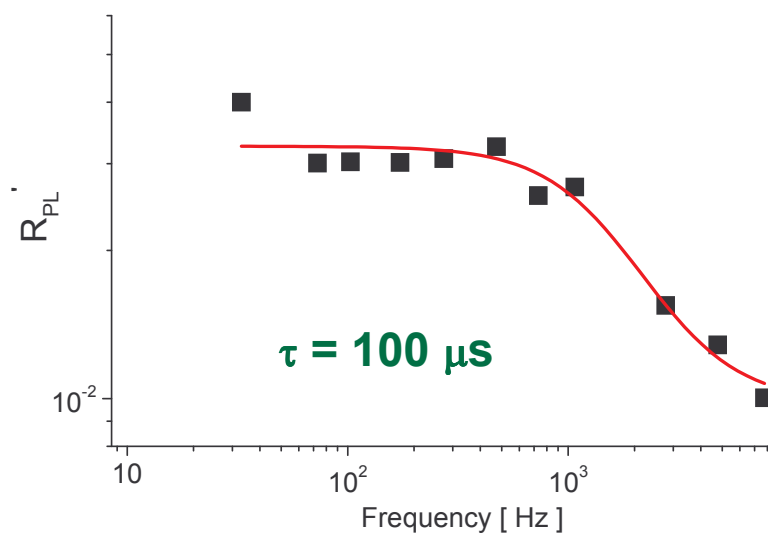Figure 4.21: Delayed photoluminescence (see equation 2.12) of MDMO-PPV detected at 630 nm.
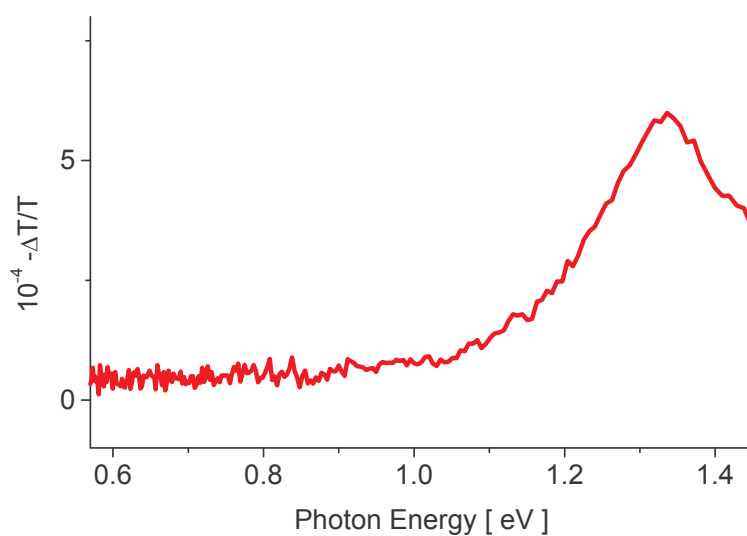

Figure 4.22: PIA spectrum of MDMO-PPV; The laser intensity modulation frequency was 171 Hz.

In Figure 4.23 b) the total amplitude is plotted versus the frequency. The fit (red line) is not very good compared to 4.23 a). This may be related to the complicated excitation intensity profile, which is neither sinusoidal nor rectangular.

The lifetimes estimated from both fits are very similar namely 370 μs for sinusoidal modulation and 350 μs for mechanical modulation. Increasing the sample temperature to 100K the PIA spectrum amplitude was reduced, however the shape of the spectrum did not change. Estimating the triplet lifetime by measuring the frequency dependence, a reduction of the lifetime from ~ 350 μs to ~190 μs was found at T=100K. A decrease of the triplet state lifetime was also observed when the excitation was increased.

a)

b)
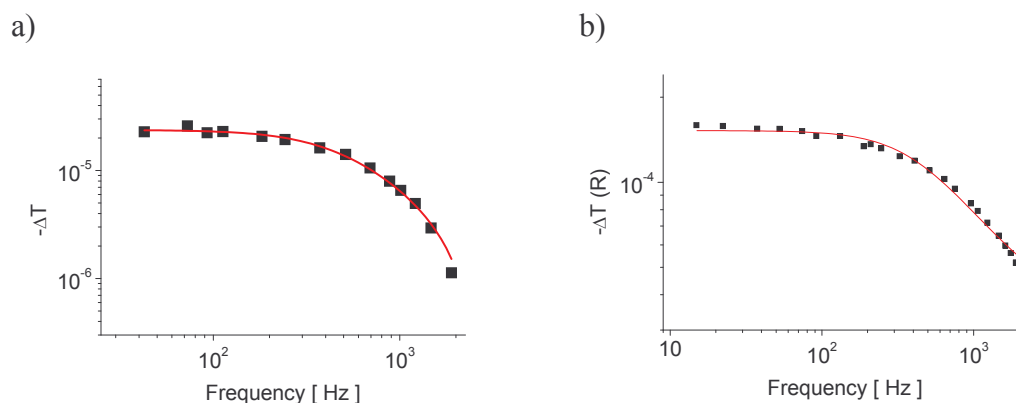
Figure 4.23: Frequency dependence of the PIA observed in MDMO-PPV at 1.35 eV measured with a) a sinusoidal b) a quasi-rectangular modulation of the laser excitation intensity.

The observed frequency dependence of the second harmonic of the photoluminescence of MDMO-PPV suggests that TTA is active in this material. However, it should be noted that other second order processes competing with a first order process (see equation 2.7) like e.g. radiative recombination of nongeminate charges could contribute to the second harmonic of the photoluminescence. The presence of a second order process is also supported by the observation that the triplet-triplet absorption depends sub-linearly on the excitation intensity[14] and that the triplet lifetime is decreasing with increasing light excitation intensity. This means triplets recombine via a monomolecular but also higher order processes.

The origin of the different triplet lifetimes extracted from delayed photoluminescence and photoinduced absorption experiments is still under discussion. One possible explanation is as follows: While the experiment probing the triplet-triplet absorption is sensitive to all triplets the delayed photoluminescence measurements considers only species, which have the ability to contribute to the second order process. Triplets not participating in the second order process may be trapped at defect sites and have a longer lifetime. Therefore one may expect a longer triplet lifetime measured in the

photoinduced absorption experiment. A consequence of this explanation would be the existence of trapped and mobile triplets in MDMO-PPV.

4.4.3 Summary

Frequency resolved photoluminescence measurements on MDMO-PPV demonstrate the presence of a second order recombination process, which has been identified before in other polymers as triplet-triplet annihilation.[12] The triplet lifetime extracted from this measurement is three times shorter than the triplet lifetime estimated by photoinduced absorption. This may be explained by mobile and trapped triplets generated in MDMO-PPV at low temperatures.

4.5 Magnetic resonance studies on a substituted polythiophene with two different solid state morphologies

In general, conjugated polymers form thin, amorphous, solid-state films when spin coated from solution. Film properties are strongly influenced by different possibilities of monomer units' coupling (regio-regularity) and the degree of morphological disorder originating from the chemical structure as well as the film preparation procedure. These aspects together with the chemical synthesis of the polymer determine the number of intrinsic defects. Another important structural parameter influencing the electronic and optical properties is the stacking of polymer segments, which directly determines the intermolecular interaction. It has been shown that even in solutions of soluble methoxy-ethylhexyloxy-substituted poly(*para*-phenylenevinylene)s (*i.e.* MEH-PPV) aggregates are formed that decrease the photoluminescence yield.[15] The nature of these aggregates is still under discussion. Early studies of photoinduced absorption on films of poly(*p*-phenylene vinylene) (PPV) and MEH-PPV suggested the formation of inter-chain charge pairs with high yield.[16,17] Also the formation of excimers (excited state dimers) has been proposed.[18,19] For the investigation of the interplay between the molecular arrangement on the one hand and optical properties on the other hand polythiophenes (PT) are very interesting. After attaching a side-group to the thiophene ring, polymerization can lead to different couplings between monomer units (head to tail (HT), head to head (HH) or tail to tail (TT)). HH couplings result in a sterically driven twist of adjacent thiophenes that break the conjugation, while the favourable conformation of HT coupled (3-substituted) thiophene rings is planar, leading to longer effective conjugation.[20] Regioregularity denotes the percentage of stereoregular HT attachments of side chains to the 3-position of the thiophene rings.[20] It plays an important role for the morphology and therefore for the optical and electrical properties of thin solid-state films of substituted polythiophenes.[20-28] Regioregular PT tends to form self-organized oriented crystalline lamella structures while films of regiorandom PT are usually amorphous.[25-28] Comparing optical absorption spectra of films of poly((3-hexyl)thiophene)s with different degrees of regioregularity, a significant red-shift of the absorption onset is found for the more regular compound.[22,23] Also outstanding electrical properties have been reported for

regioregular P3HT.[25-27] Recently the existence of 2D excitations in regioregular poly(3-alkythiophene) has been suggested.[26,29]

In this work magnetic resonance experiments were performed on thin films of PEOPT, which depending on the preparation procedure can be more amorphous or more crystalline. This gives the very rare possibility to study the influence of the morphology on the photoexcitation pattern of a conjugated polymer without being obscured by differences in the chemical structure when using different materials with different morphologies. The influence of the film crystallinity on photoexcitations is in the center of this study and is investigated by comparing PLDMR and PCDMR results from both phases.

4.5.1 Experimental

For PLDMR experiments polymer films were spin-coated from 1.5 wt % PEOPT chloroform solution on a plastic substrate. This procedure results in an orange film. Films of the blue phase were prepared by exposing orange films to chloroform vapor for several seconds immediately after spin coating. This procedure leads to films of comparable thickness for both phases. Photocells for the PCDMR measurements were prepared as described before. The photoactive layer was spin-coated from a chloroform solution (1.5 wt % PEOPT) and conversion to the blue phase was performed by exposure to chloroform vapor. The PCDMR experiments presented here were performed between ambient temperature and 135 K, PLDMR experiments in the range of 7 K – 120 K.

4.5.2 Results

a) Photoluminescence experiments

In Figure 4.24 the absorption and the photoluminescence spectra of the two different phases of PEOPT are shown. The main absorption and photoluminescence features of the blue phase are shifted by about 100 nm towards longer wavelength with respect to the orange phase.
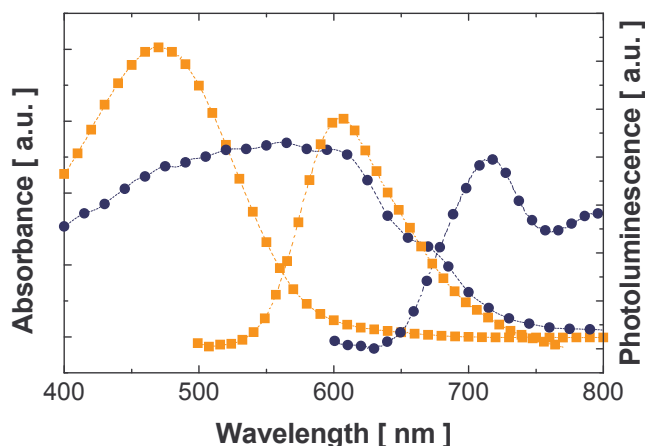
Figure 4.24: Optical absorption and photoluminescence spectra of a solid state film of the orange (squares) and the blue phase (circles); film thickness ~ 100 nm, T = 298 K

In Figure 4.25 a strong narrow PL-enhancing resonance measured at 10 K of orange and blue thin films are compared. The relative changes of the photoluminescence (dPL/PL) are plotted as a function of the external magnetic field. A narrow asymmetric resonance at g = 2.0023 (peak position) of similar amplitude (dPL/PL) is observed for the orange and the blue phase.
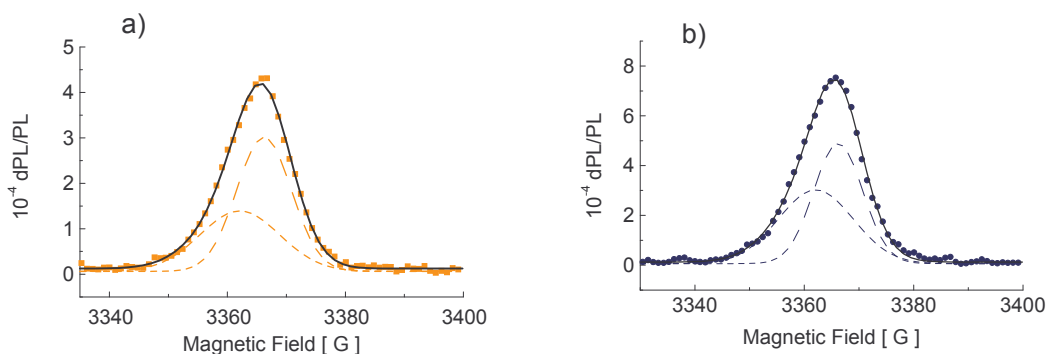
Figure 4.25: PLDMR spectra of an orange (squares) and a blue (circles) polymer film; the solid lines represent the best fit of the spectrum with one Lorentzian and one Gaussian lines (dashed), λ_{exc} = 476 nm, light excitation intensity 50 mW/cm^2, microwave power modulation frequency 371.3 Hz, T = 10 K.

For both phases the resonance can be synthesized by a sum of a broad ($\Delta B_{1/2}$ = 14 G) and a narrow ($\Delta B_{1/2}$ = 8.7 G) Gaussian-shaped resonance at g = 2.0042 and 2.0018 respectively.[30] However, a similar good decomposition can be obtained by the sum of a broad Lorentzian-shaped ($\Delta B_{1/2}$ = 13 G) and a narrow Gaussian-shaped ($\Delta B_{1/2}$ = 8.7

G) resonance. Asymmetric PLDMR signals at g ≈ 2.00 have already been reported for other polythiophenes.[31] A superposition of two lines[31,32] resulting from different trapping sites[31] has been suggested to cause this asymmetry. By investigating the influence of the temperature on the narrow resonances, different dependences are found for the two phases (Figure 4.26). While below 20 K the signals show only a weak temperature dependence, the intensities of resonances show a much stronger dependence at higher temperature. At 120 K the signal of the blue phase is only weakly detectable while the PLDMR spectrum of the orange phase can clearly be observed.
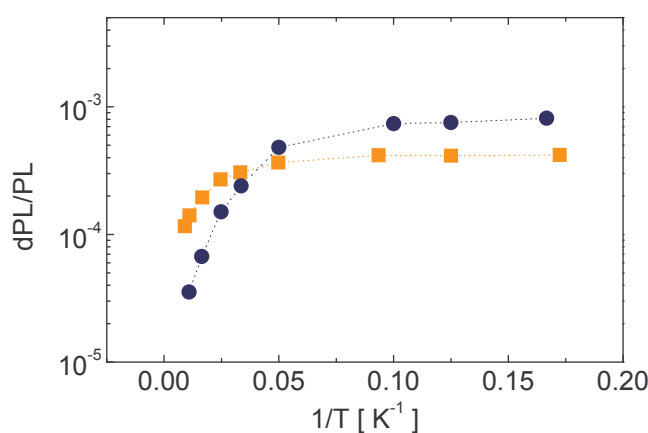
Figure 4.26: Temperature dependence of the PLDMR signal (amplitude), orange phase (squares), blue phase (circles), λ_{exc} = 476 nm, 50 mW/cm^2, microwave power modulation frequency 371.3 Hz

In Figure 4.27 PLDMR spectra of the orange and the blue phase are compared again, but now in a wide magnetic field range around g ≈ 2.00 and g ≈ 4.00.
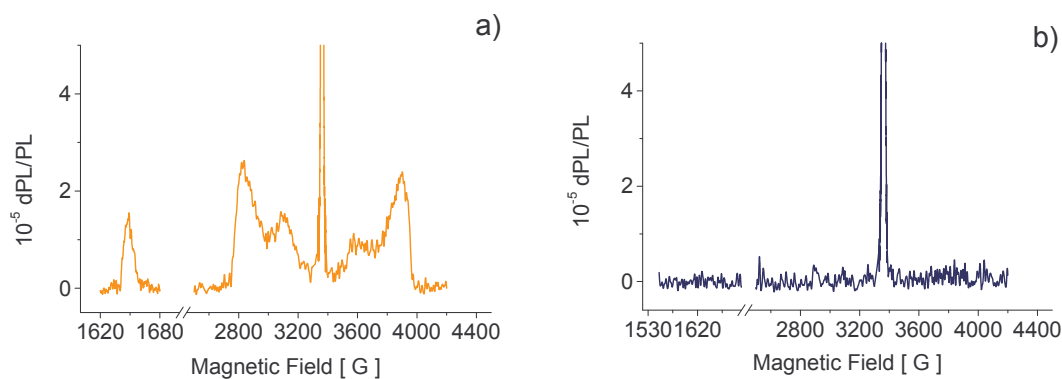
Figure 4.27 PLDMR spectra of an orange a) and a blue b) polymer film acquired over a wide magnetic field range; λ_{exc} = 476 nm, light excitation intensity 50 mW/cm^2, microwave power modulation frequency 371.3 Hz, T = 10 K.

For the orange phase a full field and a half field resonance can be observed that are ascribed to triplet patterns, while the blue phase shows no triplet signal in the performed experiments.

b) Photocurrent experiments

The current-voltage (I-V) characteristics of the prepared photocells for 80 mW/cm^2 white light illumination are shown in Figure 4.28 a). The cells show a short circuit current of ~8.3 μA/cm^2 and typically have an open circuit voltage, V_{oc}, of about 1 V – 1.3 V with the higher V_{oc} observed for the orange phase. The energy conversion efficiencies of the two photodiodes are < 10^{-2} % at 80 mW/cm^2 white light illumination.

In Figure 4.28 b) the PCDMR spectra of orange and blue phase diodes are compared. A reduction of the short circuit photocurrent i_{sc} at magnetic resonance is observed for both phases. The relative change di_{sc}/i_{sc} of the short circuit photocurrent is plotted as a function of the external magnetic field. The orange phase shows a much stronger PCDMR signal than the blue phase. The observed lines are again asymmetric. The g-value corresponding to the maximum of the signal in Figure 4.28 b) is 2.0025. For both phases the resonance can be synthesized by a sum of a wide ($\Delta B_{1/2} = 7.2$ G) and a narrow ($\Delta B_{1/2} = 4.6$ G) Gaussian-shaped resonance at g = 2.004 and 2.0024 respectively. A linear dependence of both i_{sc} (not shown) and δi_{sc} at resonance (Figure 4.29 a)) on the pumping light intensity is observed. The temperature dependence of the PCDMR (Figure 4.29 b)) of the two phases is found to be different. -di_{sc}/i_{sc} of the orange phase is constantly increasing at temperatures higher than 130 K reaching a broad maximum around 250 K and decreasing at higher temperatures. In contrast, the relative resonant changes of i_{sc} in the blue phase decrease at higher temperatures. The lines in Figure 4.29 b) are fits using the polaron pair model.[33]

a)

b)
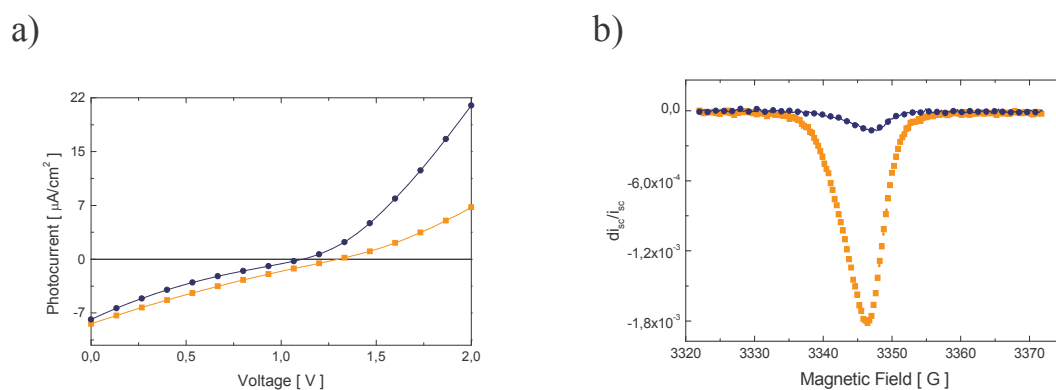
Figure 4.28: a) IV-characteristic of the investigated diodes measured under 80 mW/cm^2 white light illumination, orange phase (squares), blue phase (circles). b) PCDMR spectra of photodiodes based on orange (squares) and blue (circles) phase films, λ_{exc} = 500 nm, light excitation intensity 10 mW/cm^2, microwave power modulation frequency 146.65 Hz, T = 298 K.

a)

b)
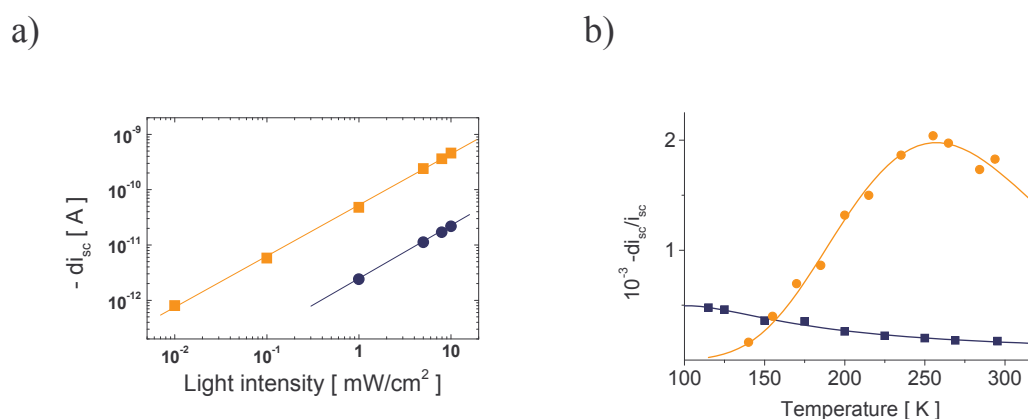
Figure 4.29: a) Dependence of the PCDMR signals (amplitude) on the light intensity, T = 298 K, microwave power modulation frequency 146.65 Hz. b) Dependence of the PCDMR signals (amplitude) on temperature, orange phase (squares), blue phase (circles), λ_{exc} = 500 nm, light excitation intensity 10 mW/cm^2, microwave power modulation frequency 146.65 Hz.

4.5.3 Discussion

Similar to other *para*-substituted phenyl-PT a shift of the absorption maximum to the red is observed when an orange PEOPT film is exposed to solvent vapor[34,35]. This treatment is irreversible which indicates that the blue phase is energetically more stable. For POPT, a polymer very similar to PEOPT, the red shift was found to be accompanied by an increase of film crystallinity.[35] Following their x-ray studies Aasmundtveit et al.[34] suggest that all *para*-substituted poly(phenylthiophene)s can be transferred from a metastable, poorly crystalline state to a state of higher order by

thermal or solvent vapor treatment. For spin-cast POPT films x-ray diffraction measurements showed that the crystalline fraction is doubled after chloroform vapor treatment.[35] The new morphology in the ordered state leads to a stronger interchain interaction (π-stacking). Due to this tight packing of the macromolecules an increase in effective conjugation length is observed which causes the red-shift in the optical absorption.[18] Spectral photocurrent measurements demonstrated that the additional optical absorption of the blue phase PEOPT can be used to create free charge carriers.[36] The short circuit photocurrents for both morphologies are approximately the same under white light illumination in not optimized devices (Figure 4.28 a)). Due to the enhanced spectral absorption in the visible range and the expected higher hole mobility of the blue phase,[26] higher photocurrents could be expected for the blue phase. However, as demonstrated in Ref. 36 higher charge carrier mobilities in the blue phase compared to the orange phase can also cause stronger bimolecular recombination reducing the overall photocurrent. As shown in Figure 4.25 and Figure 4.28 b) in both phases asymmetric resonances in PLDMR and PCDMR are observed. These asymmetric line shapes suggest a superposition of multiple lines.[31,32] It has been proposed[31] that two distinct interchain polaron pair trapping sites are present in alkyl substituted polythiophenes. The lower magnetic field component was attributed to a trapping site adjacent to negatively charged ions while polaron pairs trapped at the sulphur heteroatom contribute to the higher field component.[31]

There are two different regimes in the temperature dependence of the PLDMR signals. Below 20 K the signal decreases slowly with increasing temperature while above 50 K the signals decrease more rapidly. It is interesting to note that the transition between the different regimes takes place in a temperature range where the TSL (Thermally Stimulated Luminescence) signals of the orange and blue phase have their maxima.[37]

The changes of the PCDMR spectra with temperature can be described by a qualitative model derived by Frankevich et al.[33,38] As described before (see Chapter 2.4.1 - equation (2.16)) the formula derived in Ref. 33 can also be used to describe the temperature dependence observed in the PCDMR experiment. From the fits shown in Figure 4.28 b) values for E_1 and E_2 for both phases can be extracted. For the orange form E_1 and E_2 are found to be 0.1 eV and 0.2 eV (K=0.028, A=0.0031, B=703). These values are very similar to values published for other conjugated polymers.[33]

Values for the blue phase are significantly smaller. The fit gives $E_1 = E_2 = 0.03$ eV (K=0.0003, A=0.008, B=2.635) indicating that the formation of free charge carriers from polaron pairs is more likely in the blue phase due to the lower activation energies. This smaller activation barrier in the blue phase could be caused by the more tightly packed morphology and the formation of interchain pairs causing a larger initial separation of the polarons forming the pair. The stronger interaction between neighboring chains might support the formation of free charge carriers.

The origin of the triplet PLDMR signal in conjugated polymers is usually ascribed to magnetic resonance enhanced recombination of triplet excitons.[36] The distribution of molecules in the film gives rise to the observed broad triplet spectrum.[40] By analyzing these pattern different authors concluded that triplet excitons in conjugated polymers are very localized.[41] Their approximate extension is one benzene or thiophene ring.[41] The observed shape of the triplet pattern in the PLDMR spectrum of the orange phase cannot be explained by a simple powder pattern resulting from randomly arranged molecules. As numerical calculations of E. Lifshitz et al. demonstrated, the triplet pattern of the orange phase may originate from molecules aligned parallel to the substrate.[42]

Recently Österbacka et al. investigated differently substituted polythiophenes.[29] In thin films having a more amorphous morphology (regiorandom polymers) they observed triplet excitons in photoinduced absorption and magnetic resonance experiments. However, the more ordered films (regioregular polymer) showed no triplet exciton signal although a photoinduced absorption spectrum with several features was found. They attribute the observed PA bands in the regioregular polythiophenes to interchain species. Excitations delocalize in the highly ordered lamella structure on different chains and strongly localized triplet excitons are no longer favorable excitations.[26,43] PA studies on PEOPT give similar spectra.[36] The orange phase shows one feature, which is attributed to the triplet exciton. In the blue phase a PA spectrum with several features was observed but none could be ascribed to triplets. Very recently the so-called spin-dependent exciton formation cross section (σ_S/σ_T), which is the number of photoexcited singlet excitons divided by the number of photoexcited triplet excitons, was determined for a series of oligomers and polymers, including regioregular and regiorandom P3HT.[44,45] In the experiment a smaller value for (σ_S/σ_T) is found for the regiorandom polymer compared to the

regioregular polymer. Also a relation between the conjugation length and (σ_S/σ_T) has been found. The authors suggested a linear relation between (σ_T/σ_S) and 1/(conjugation length).[45] One may therefore conclude that due to different conjugation lengths the spin-dependent exciton formation cross section of the orange form of PEOPT is smaller than for the blue form. Therefore the probability of triplet exciton formation could be smaller in the blue phase compared to the orange one, explaining the missing triplet PLDMR.

There are different other possibilities why the PEOPT blue phase shows no triplet signal in the presented experiments. 1) The triplet state has a very different (much shorter) lifetime compared to the orange phase. This would result in a steady state triplet exciton concentration, which could be below the detection limit of the performed experiment. 2) Triplet states do not interact with the species causing the photoluminescence. They are localized at trapping sites and cannot contribute to photoluminescence. This would mean that in the more ordered blue form triplet excitons are effectively trapped.

Following the results presented in this contribution, PEOPT can show photo-excitations like a regiorandom (orange phase) but also like a regioregular (blue phase) polythiophene. A simple modification of the sample preparation procedure can cause very different photoexcitations.

4.5.4 Summary

The photo-physics of a phenyl-substituted polythiophene have been studied using PLDMR and PCDMR. Depending on the processing conditions, this material forms different solid-state morphologies. The results presented in this work illustrate the influence of the morphology on the properties of the photoexcited carriers. The radical pair (polaron pair) resonance is identified in the orange (amorphous) as well as in the blue (more crystalline) phase. However, especially in the PCDMR experiments, the orange phase shows a much stronger temperature dependence compared to the blue phase demonstrating the influence of the morphology on the radical pair formation/recombination. Furthermore the orange phase shows a typical triplet powder pattern in the PLDMR experiment originating from randomly oriented triplet

excitons, while a triplet signal cannot be observed in the blue phase. This could be related to different triplet exciton formation cross-sections in the orange and the blue phase due to different effective conjugation lengths[45] or to the fact that in the crystalline phase interchain excitations are the dominant photoexcitations as has been suggested before.[29]   Finally, the results presented in this work also demonstrate the importance of sample preparation. The chosen solvent and different film preparation methods can make it very difficult to compare results obtained in different laboratories.

4.6 PLDMR on MDMO-PPV – The influence of the solvent used for film preparation

It is well known that the solvent used for film preparation can have very strong influence on the optical and electrical properties of a thin conjugated polymer film.[25,46,47] From this point of few MDMO-PPV in a very interesting polymer. Using toluene and chlorobenzene as solvents for MDMO-PPV significantly higher hole mobilities were observed in field effect transistor when spin-coating the polymer from chlorobenzene solution compared FETs prepared from toluene solutions.[48] Also the efficiency of the plastic solar cell (MDMO-PPV/PCBM) could be more than doubled changing the solvent from toluene to chlorobenzene.[49] Similar to the polymer PEOPT discussed before, one may expect to see changes in the PLDMR spectrum of MDMO-PPV if films prepared from toluene and chlorobenzene would have different morphologies.

4.6.1 Experimental

Thin films were spin-coated on a plastic substrate from 3 mg/ml toluene and chlorobenzene solutions. PLDMR experiments were carried out at 10 K. Samples were excited by an Ar+ laser, 50mW/cm^2, 476 nm.

4.6.2 Results and discussion

In Figure 4.30 the half field and the full-field PLDMR signals of the chlorobenzene and the toluene sample are plotted. For half field measurements 200 mW microwave power and for full field measurements 100 mW microwave power were applied. Both samples showed similar signal amplitudes. The spectral shape as well as the position of the spectra did not change when changing the solvent.
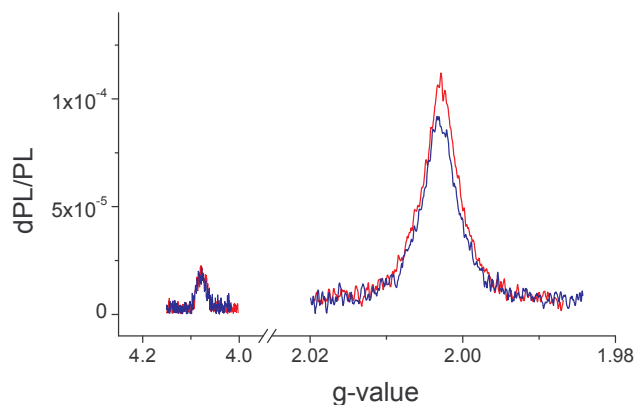
Figure 4.30: PLDMR spectrum of MDMO-PPV films prepared from chlorobenzene (red line) and toluene (blue line) solutions. Half field spectra (g~4) were recorded with 200 mW microwave power, full field spectra (g ~ 2) were recorded with 100 mW microwave power.

Also the possibility of a full-field triplet powder pattern was checked. For both samples the full-field triplet powder pattern signal was below the detection limit of the experiment and not observed.

The performed experiments demonstrate that magnetic resonance active photoinduced species are the same and appear in similar quantities in thin films prepared from chlorobenzene and toluene. From FET mobility measurements one may expect a better-ordered microstructure of the film prepared from chlorobenzene (higher hole mobility). However, this is not supported by the presented PLDMR experiments.

The influence of the solvent on the PLDMR was also investigated for MDMO-PPV films with small amounts of PCBM. Also in these experiments only minor differences between samples prepared from chlorobenzene and toluene could be observed.

4.6.3 Summary

PLDMR was applied to films of MDMO-PPV prepared from different organic solvents. Although solvent effects were found for this polymer in electrical measurements no effect on the PLDMR spectrum was observed.

4.7 The influence of PCBM on the PLDMR and PCDMR spectra of MDMO-PPV

MDMO-PPV (poly(2-methoxy-5-(3',7'-dimethyloctyloxy)-1,4-phenylenevinylene) and PCBM [6,6]-phenyl C_{61}butyric acid methyl ester are the prototype materials for the plastic solar cell.[49] Magnetic resonance techniques were applied to study photoexcitations and the charge recombination process in the pristine polymer and in conjugated polymer-fullerene mixtures with different fullerene concentrations. Experiments show that at low PCBM concentrations polymer cation – fullerene anion pairs are created upon photoexcitation while at high fullerene concentration dominantly free charge carriers are created.

In mixtures of these two components the photoinduced charge transfer was found to occur within 45 fs.[50] Light induced ESR studies identified two light-induced features, namely positive polarons at g = 2.0025 and the PCBM anion at g = 1.9995.[6] Using MDMO-PPV and PCBM, efficient photovoltaic devices (plastic solar cell) can be prepared. Shaheen et al. demonstrated an energy conversion efficiency of 2.5 % under AM1.5 illumination for this system.[49] To improve the understanding of charge generation and recombination processes in these mixture a systematic experimental analysis of the effect of mixing of PCBM into MDMO-PPV by photoluminescence detected magnetic resonance (PLDMR) as well as in photocurrent detected magnetic resonance (PCMDR) supported by optical excited state spectroscopy was performed.

4.7.1 Experimental

PCDMR experiments were carried out at room temperature. Photodiodes were excited by spectrally dispersed light λ = 476 nm, 10 mW/cm^2 coming from a Xenon arc lamp. PLDMR experiments were carried out at 10 K except were noted otherwise. Samples were excited by an Ar+ laser, 50 mW/cm^2, 476 nm. For the wavelength dependence of the PLDMR signal a PMT attached to a monochromator was used as detector. In all magnetic resonance experiments presented here 200 mW microwave power was applied.

4.7.2 Results

In Figure 4.31 typical current-voltage characteristics of the investigated photodiodes are shown. Samples were illuminated by white light (60 mW/cm^2). Adding fullerenes
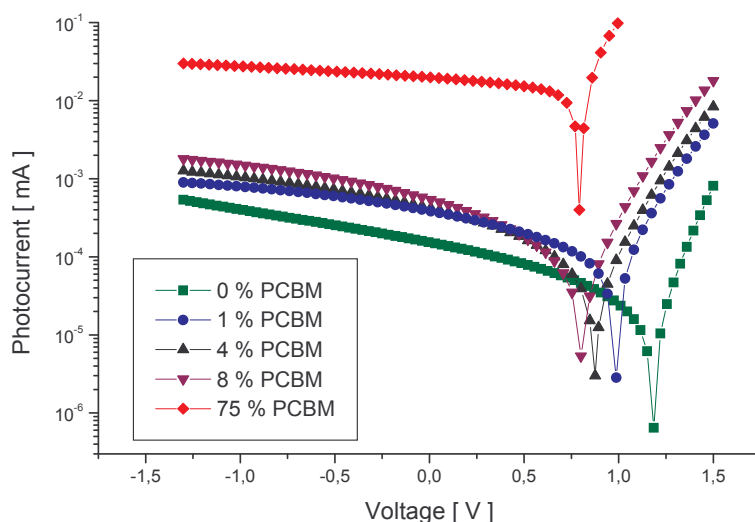

Figure 4.31: Current-voltage curves of diodes with different concentration of PCBM recorded under white light 60 mW/cm^2 illumination

Adding fullerenes to the conjugated polymer, the open circuit voltage (V_{oc}) of the diodes is reduced and saturates at approximately 750 mV. Y. Yang et al. observed something similar for MEH-PPV – C_{60} diodes.[51] The origin of V_{oc} and the shift of V_{oc} upon addition of PCBM is still subject to debate.[51,52] In Figure 4.32 PCDMR spectra of diodes with different fullerene content are plotted. A reduction of the short circuit photocurrent (i_{sc}) at magnetic resonance conditions is clearly observed. For the pure polymer diode without fullerenes the signal is found to be largest. The PCDMR resonance has Lorentzian line-shape and a g-value of 2.0028, $\Delta B_{1/2} = 7.3$ G with an amplitude di_{sc}/i_{sc} of $-3.4 \cdot 10^{-4}$. Adding small amounts of fullerenes the maximum of the PCDMR resonance is weakened systematically, slightly shifted to smaller g-values and a new shoulder at lower g-values is observed. For 1 % of PCBM a signal amplitude di_{sc}/i_{sc} of $-2.8 \cdot 10^{-4}$ was found. Adding more fullerenes the resonance weakened further, however the line shape did not change significantly at a concentration of 4 % PCBM. For 4 % of PCBM a signal amplitude di_{sc}/i_{sc} of $-1.7 \cdot 10^{-4}$

was found. For the diode with 8 % PCBM content the PCDMR signal was already very small (di_{sc}/i_{sc} =-7·10^{-5}) and the weak resonance did not allow determining the exact position and line shape of the spectrum.

Figure 4.32: Photocurrent detected magnetic resonance spectra of MDMO-PPV photodiodes holding different concentrations of PCBM. Measurements were performed at room temperature and 200 mW modulated microwave power. Diodes were illuminated by 10 mW/cm^2 @ 476 nm.

For the fullerene concentrations used in the plastic solar cell (75 % PCBM) the influence of microwave modulation on the photocurrent is below the detection limit of our experiment (~1·10^{-5}). PCDMR results for g ~ 2 are summarized in Figure 4.33. The amplitude of the relative change of the photocurrent (di_{sc}/i_{sc}) and the amplitude of the photocurrent change di_{sc} are plotted versus the fullerene concentration.
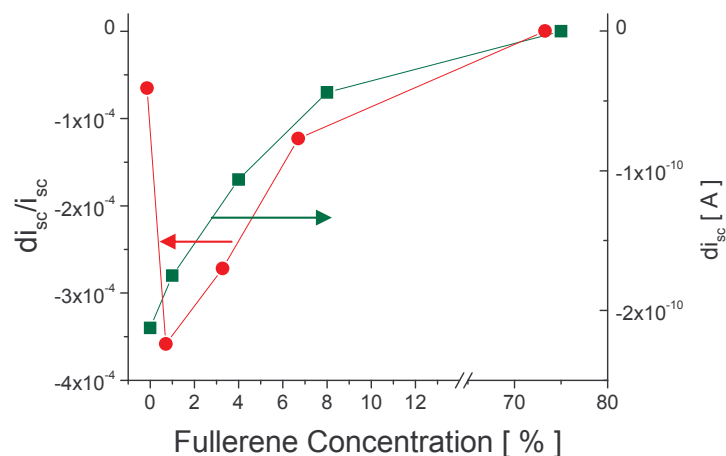
Figure 4.33: Change of the photocurrent dPC (circles) and the relative photocurrent dPC/PC (squares) plotted versus the fullerene concentration

In all PCMDR experiments also the possibility of triplet type excitations was checked with signals at half field ($\Delta m_s = 2$) but no signal could be observed for all reported concentrations of fullerenes. In Figure 4.34 PLDMR spectra of thin films of MDMO-PPV mixed with various concentrations of PCBM are compared. The pure polymer shows a PL enhancing magnetic resonance signal with Lorentzian line shape (solid line in Figure 4.34) at g = 2.0028, $\Delta B_{1/2}$ = 11.6 G with an amplitude dPL/PL of $1.6 \cdot 10^{-4}$. This resonance is comparable in intensity to that observed in typical PPV's and other conjugated polymers. By adding 1% of PCBM, the resonance increases by a factor of 8 (dPL/PL = $1.2 \cdot 10^{-3}$), the g-value of the maximum shifts to a lower value and an additional shoulder is observed. At higher fullerene concentration the resonance increases further, reaches an amplitude of $\sim 3.25 \cdot 10^{-3}$ at 5 % PCBM content and remains approximately constant up to 10 % PCBM (Figure 4.35). The strong quenching of PL by PCBM does not allow a further increase of the fullerene concentration in our experiments. In the inset of Figure 4.35 the first derivative of the PLDMR spectrum of the sample holding 1 % of PCBM is shown. It clearly indicates the presence of two features in the magnetic resonance spectrum. Independent of the PCBM concentration the spectral dependence of all PLDMR features resembles the photoluminescence of MDMO-PPV (Figure 4.36).
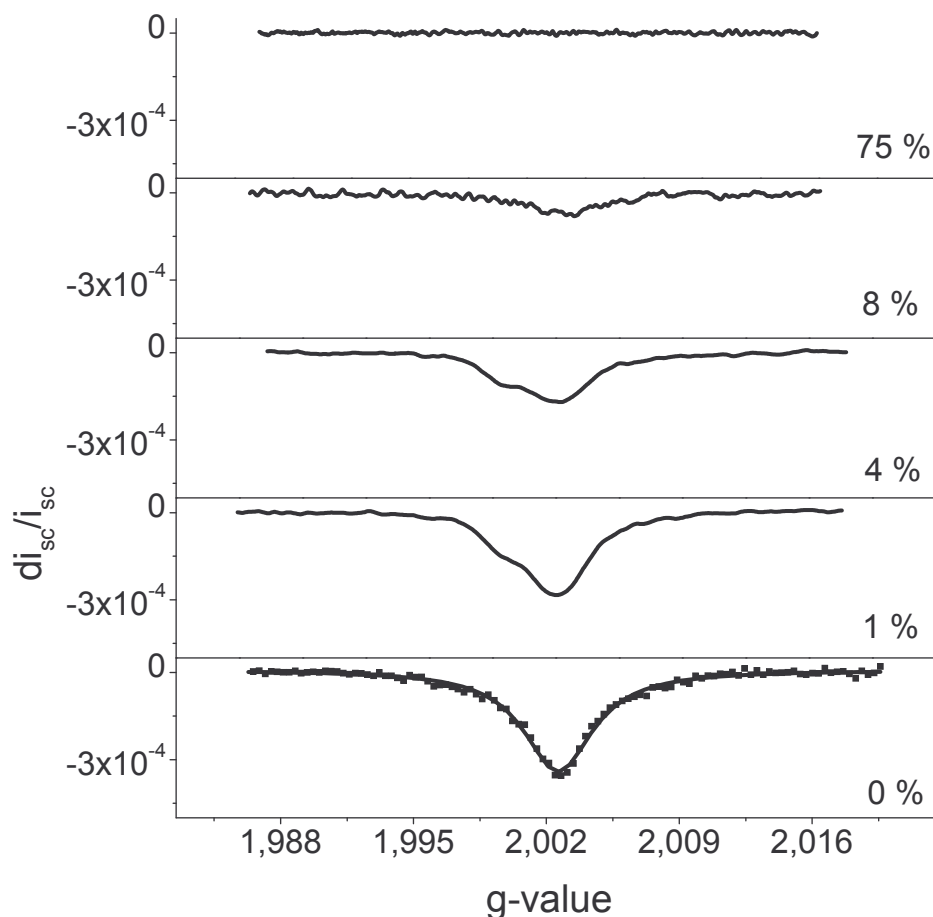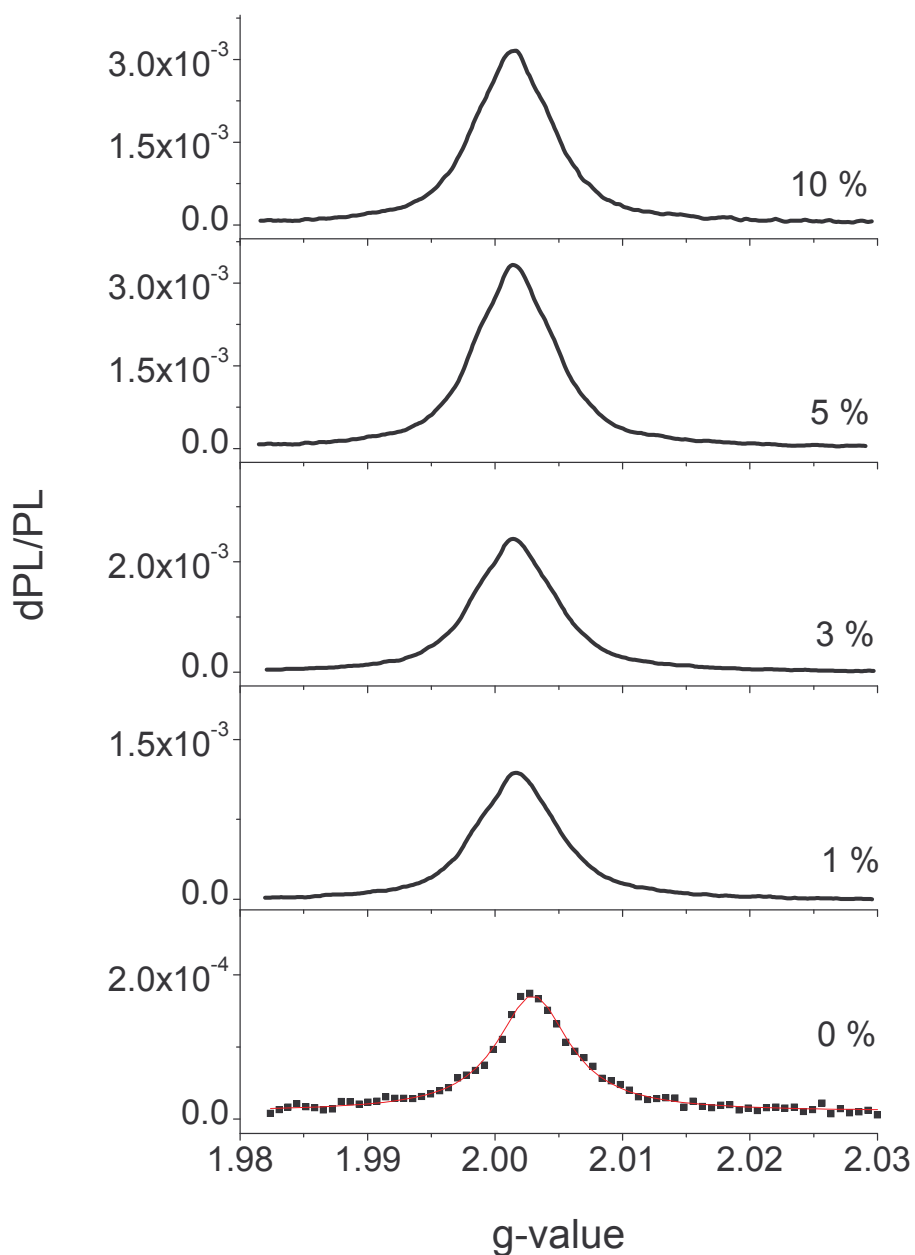
Figure 4.34 Photoluminescence detected magnetic resonance spectra of MDMO-PPV with different concentrations of PCBM. Measurements were performed at T = 10 K and 200 mW modulated microwave power. Samples were excited by 50 mW/cm^2 at 476 nm.

This suggests that magnetic resonance does not act on the species producing PL (singlet excitons cannot be manipulated by ESR transitions) but on species, which indirectly influence the singlet exciton density.
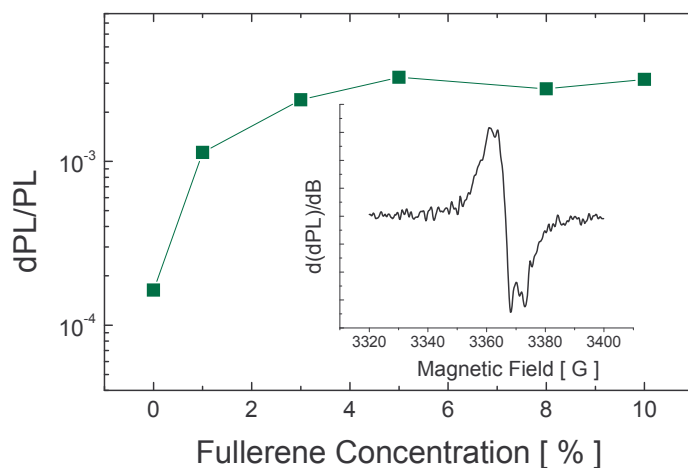
Figure 4.35: Maximum amplitude of all spectra shown in Figure 4.34 plotted versus the PCBM concentration. The inset show the first derivative of the sample MDMO-PPV plus 1% PCBM.

a)   b)
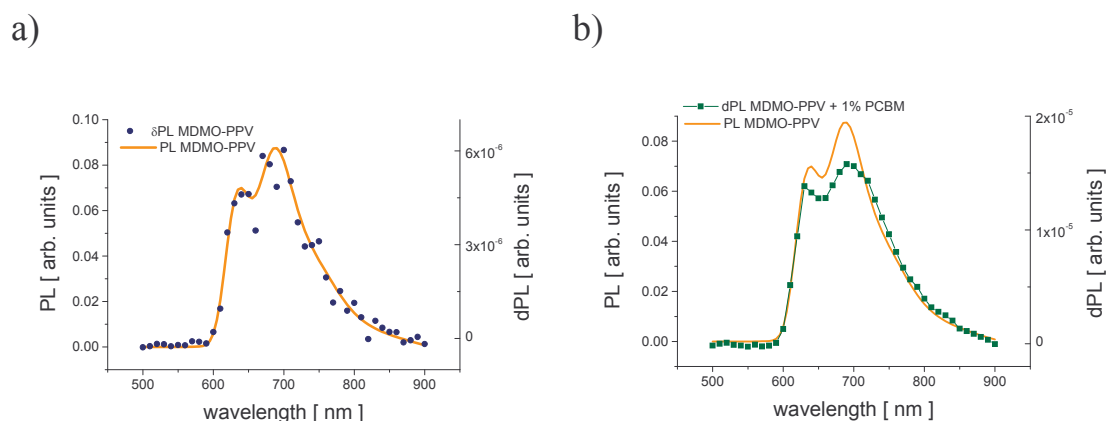
Figure 4.36: a) Photoluminescence detected magnetic resonance spectra of MDMO-PPV and b) MDMO-PPV with 1% PCBM. Measurements were performed at T = 20 K and 200 mW modulated microwave power.

Small amounts of fullerene also increase the resonance at half field ($\Delta m = 2$) g ~ 4.0 in the PLDMR spectrum (Figure 4.37). At 1 % PCBM doping also a weak full field triplet powder pattern could be observed (Figure 4.37). At higher fullerene concentrations the half field resonance decreases significantly and can no longer be distinguished from the noise level at the higher PCBM load. In Figure 4.38 the photoinduced absorption spectra of MDMO-PPV and MDMO-PPV with 1% PCBM are compared. Both films have the same optical density at 476 nm and were investigated under the same experimental conditions. Pure MDMO-PPV shows one photoinduced absorption located at around 1.35 eV, which has been attributed to a triplet-triplet absorption.[14] Adding 1% of PCBM to the polymer, the PIA signal at

1.35 eV increases. In addition a weak absorption at 0.6 eV is observed, indicating the presence of polarons.[14]
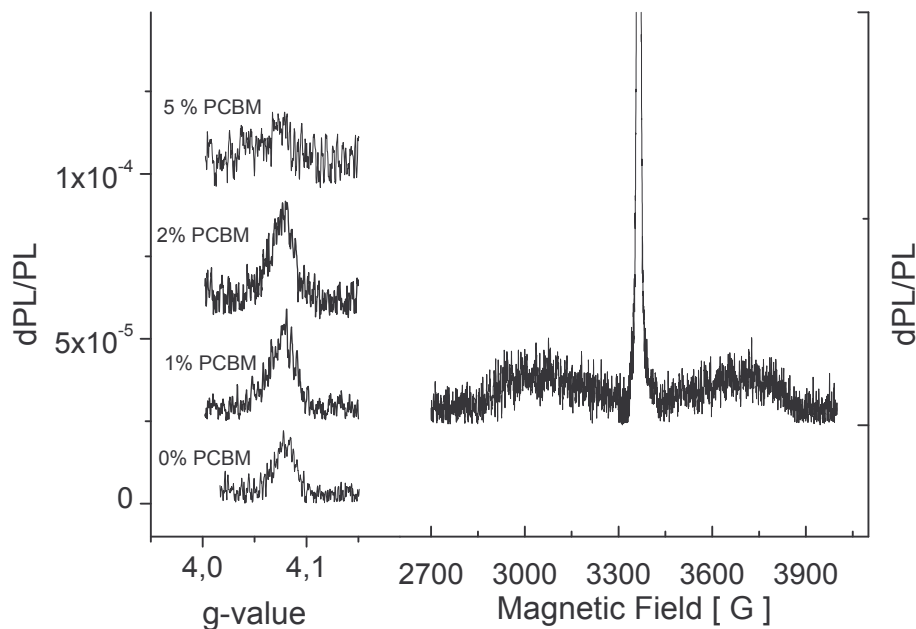
Figure 4.37: Comparison of the half-field PLDMR spectra for various concentrations of PCBM in the MDMO-PPV film (left hand side). On the right hand side full-field triplet powder pattern and the polaron resonance of the sample MDMO-PPV plus 1% PCBM is shown. Measurements were performed at T = 10 K. Samples were excited by 50 mW/cm^2 at 476 nm.
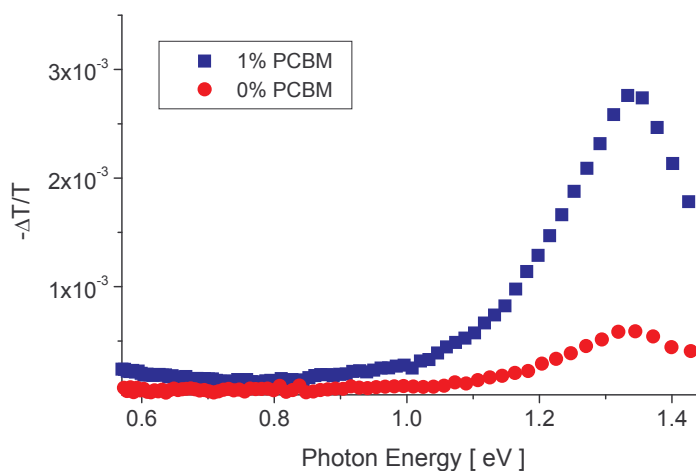
Figure 4.38: Comparison of PIA-spectra recorded for a thin film of MDMO-PPV and a film with the same optical density in the visible range of MDMO-PPV plus 1 % PCBM. Both spectra were measured at T = 19 K. Samples were excited by 5 mW/cm^2 at 476 nm.

4.7.3 Discussion

a) Photocurrent detected magnetic resonance

The observation of a reduction of the photocurrent in conjugated polymer diodes is usually explained by microwave-enhanced recombination of polaron pairs.[37] In the pure MDMO-PPV diode positive and negative polarons are created by charge transfer to a neighboring chain or chain segment or by dissociation of singlet excitons. In the PCDMR experiment, a single line with Lorentzian-like line-shape at a g-value of g = 2.0028 is observed. This suggests that the g-values of the positive and the negative polarons are similar. This is in contrast to observations in electrochemically induced polarons in derivatives of polythiophenes.[53] From light induced ESR experiments, the g-value of the positive polaron in these PPV derivatives is known to be around 2.0025.[6] Assuming a slightly higher g-value for negative polarons, which are weakly exchange coupled to the positive counterparts, the observed common g-value can be rationalized by merging of the resonance into one at the arithmetic average of the two g-values.[54]

The PCDMR spectrum changes by adding PCBM in several ways. The resonance intensity decreases indicating that the free charge carrier generation via pairs, which can be influenced by magnetic resonance, is getting less important. At the same time the position of the resonance and the line-shape is changing. The spectra for 1% PCBM and 4 % PCBM can be reconstructed by one Lorentzian line at g = 2.0025 and a Gaussian line at g = 2.0003. The g-value of the positive polaron on MDMO-PPV is around g = 2.0025 and the g-value of PCBM anion is around g = 1.9995.[6] This suggests that the main contribution to this observed resonance comes from positive polarons on the polymer and negative charges on the fullerene. That is also displaying a polaron pair as defined above but now in two different species consisting of the donor cation radical (positive polaron on the chain) and the acceptor anion radical. Increasing the fullenene content further the fraction of charges created from intermediate pairs is becoming smaller and smaller and no influence of microwaves on the photocurrent is observed for the highly loaded polymer mixtures as used in the plastic solar cell (75 % PCBM). From these results one may conclude that the photo-generation of free charges is influenced in the pure conjugated polymer by the dissociation of polaron pairs, which are formed upon photo-excitation. Adding small amounts of fullerenes, photoinduced electron transfer produces pairs of polymer[+] -

fullerene⁻ radicals, which contribute to the photocurrent by dissociation into free charge carriers. At high fullerene concentrations, photo-excitation produces dominantly free charge carriers, which results in the high incident photon to electron conversion of this system up to 70% quantum efficiency.[49]

b) Photoluminescence detected magnetic resonance

The PLDMR spectrum of a thin film of MDMO-PPV shows one g ≈ 2 PL-enhancing feature. The resonance has a Lorentzian line shape and is positioned at g = 2.0028 and has also been ascribed to microwave enhanced recombination of polaron pairs.[17,39,56,57] Adding a small amount of fullerene to the polymer increases the PL-enhancing resonance. The position of the signal maximum is shifted to smaller g-values and a line-shape similar to the PCDMR (compare Figure 4.31) experiment is observed. The PLDMR spectrum of the film holding 1% of PCBM can be reconstructed by a Lorentzian line and a Gaussian line centered at g = 2.0025 and g = 1.9995 respectively. The appearance of a component at g < 2 indicates that the PCBM⁻ radical contributes to the observed spectrum since this unusually low g-value for the fullerene radical has been identified earlier.[58] By adding more fullerenes dPL and PL are gradually diminished due to the strong luminescence quenching which makes signal analysis unreliable.

P. Lane et al. observed a similar increase of the PLDMR signal in various conjugated polymer C_{60} mixtures.[42] In addition, they were able to use very high C_{60} concentrations and they found that the signal was decreasing again at high C_{60} loads. Because they observed no changes in the resonance line shape, they concluded that in the systems they investigated, the increase of the PLDMR at low fullerene concentrations does not result from photoinduced electron transfer, but explained the increase of the PLDMR intensity by fullerene induced structural changes of the polymer. Only at high C_{60} loads charge transfer reduced the PLDMR intensity.

In the study presented here, an increase of half field PLDMR is found upon light fullerene doping in agreement with earlier studies.[42] The position and shape of the half field signal does not change from the pure polymer to doped samples. In addition, the sample with 1 % PCBM shows a very weak full-field triplet powder pattern, which could not be observed in the pure polymer or at higher PCBM concentrations. In Ref. 42 the increase of the triplet resonance was ascribed to fullerene induced

structural changes. In this work, a different process yielding a higher triplet exciton population on the conjugated polymer is proposed. Considering the energy level diagram of the investigated materials, a back-transfer of the electron on the PCBM to the polymer directly followed by the formation of a triplet exciton seems to be energetically possible. HOMO and LUMO levels of MDMO-PPV and the LUMO level of PCBM were determined by electrochemistry to be –5.3 eV, -3 eV and –4 eV respectively versus vacuum.[59] The energy difference between the ground state and the first triplet excited state, S_0-T_1, of MDMO-PPV is not known, but this quantity has been measured for poly(2-methoxy-5-(2´-ethyl-hexyloxy)-*p*-phenylenevinylene) (MEH-PPV), a polymer very similar to MDMO-PPV to be 1.27 eV.[60] Using these numbers, one can estimate the energetic positions of the T_1-level of the polymer and the LUMO-level of the fullerene to be quite similar. Therefore the formation of triplet excitons on the polymer via an electron back-transfer from fullerene could be possible and this process could also explain the increase of the half-field PLDMR.

With increasing PCBM concentration the half-field resonance decreases in intensity and cannot be observed for the sample with 10 % PCBM. The reduction of the triplet resonance has been attributed to the quenching of triplet excitons by charges.[42] Another indication for the increase of the triplet exciton concentration is found in the photoinduced absorption experiments. Although there is a contribution of the polaron-PIA in samples doped with small amounts of fullerene, the net increase of the PIA-feature at 1.35 eV (triplet-triplet absorption) indicates a net increase of the triplet yield on the polymer by addition of small amount of fullerene. This also supports our proposal that additional triplets could be produced by recombination of MDMO-PPV[+] and PCBM[-] as described above. At high fullerene concentration neither triplets nor photoluminescence are observed in the PIA spectrum as photoinduced absorption detected magnetic resonance spectra have demonstrated.[61]

4.7.4 Summary

The photophysics of fullerene-doped conjugated polymers were studied by PCDMR and PLDMR. Introduction of PCBM into the polymer matrix quenches PL and increases PC. PCDMR shows a negative signal that decreases in magnitude upon

addition of fullerene. This is attributed to a change of the free charge carrier generation process. While dissociation of polaron-pairs is important in pure MDMO-PPV, photoinduced electron transfer is the dominating process in the presence of PCBM. At high fullerene concentrations free charge carriers are formed without an intermediate pair. PLDMR magnetic resonance is positive in sign and small fullerene doping enhances its intensity. An increase of triplet excitons on the polymer via recombination of the charge-separated state between polymer and the fullerene is proposed for this enhancement. The resonance spectra (both PLDMR and PCDMR) show a shoulder at lower g-values when small amounts of PCBM are present, which demonstrates that the products of the charge transfer (MDMO-PPV$^+$ and PCBM$^-$) are manipulated by the microwave radiation. This indicates an intermolecular radical pair formation between the polymer and the fullerene, at these small fullerene concentrations. At higher fullerene concentrations free charge carriers are formed with no luminescence detectable. Furthermore, photocurrent detected resonance effects are fully quenched at high fullerene concentrations.

4.8 Photocurrent detected magnetic resonance (PCDMR) on conjugated polymer diodes

Photoexcitation in conjugated polymers can create pairs, consisting of one positive and one negative charge (polaron pair), with high yield.[62,63] These pairs are bound by Coulomb interaction and additional energy is required to dissociate the pair into free charge carriers. PCDMR can be used to estimate these energies and to study the dissociation/recombination processes of polaron pairs. Experimental data are analyzed using a model suggested by E. Frankevich.[33,38]

4.8.1 Experimental

The active layers of the investigated polymer diodes were MDMO-PPV films prepared from toluene and chlorobenzene solutions, P3HT films and PEOPT films with different morphological order. Current-voltage curves were acquired under 60 mW/cm^2 white light illumination at room temperature. PCDMR measurements were performed between room temperature and approximately 100 K. A microwave power of 200 mW was applied in all experiments. Samples were excited by monochromatic light 10 mW/cm^2, 500 nm.

4.8.2 Results and Discussion

For every sample one plot shows the temperature dependence of the short circuit photocurrent and as an inset the room temperature current voltage curve. In all measurements a reduction of the short-circuit photocurrent amplitude was found under magnetic resonance. The absolute value of the maximum change of di_{sc}/i_{sc} (PCDMR signal) due to resonance is plotted versus the temperature in a second figure. The solid line in this graph represents a fit obtained using equation 2.16. From this fit the values E_1 and E_2 can be extracted.

a) MDMO-PPV (cast from chlorobenzene)

In Figure 4.39 the current-voltage curve and the temperature dependence of the short circuit photocurrent (i_{sc}) are plotted. Figure 4.40 shows the temperature dependence of the PCDMR signal. The fit gives $E_1 = 0.1$ eV and $E_2 = 0.12$ eV for the activation energies to created free charge carriers from a polaron pair.
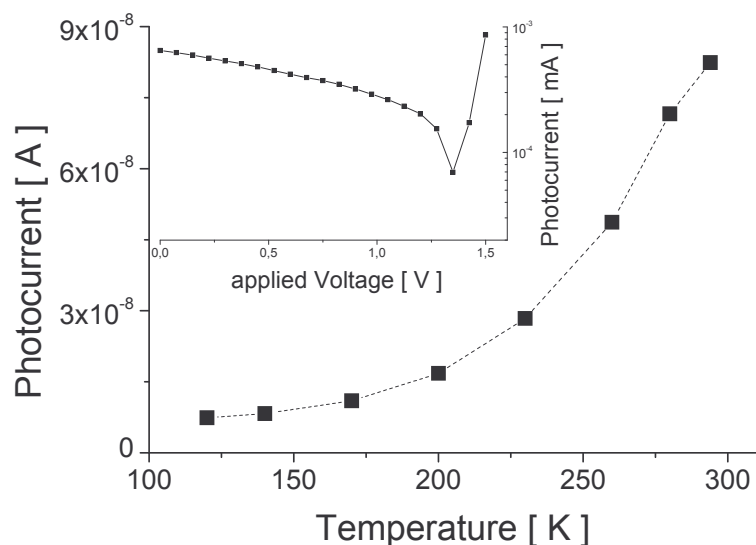

Figure 4.39: Temperature dependence of the short circuit photocurrent and the current voltage-curve of an MDMO-PPV diode prepared from chlorobenzene solution.

Figure 4.40: Maximum amplitude of the PCDMR signal measured on an MDMO-PPV diode prepared form chlorobenzene solution plotted versus temperature. The solid line shows a fit of the experimental data with equation 2.16.

b) MDMO-PPV (from Toluene)

In Figure 4.41 the current-voltage curve and the temperature dependence of the short circuit photocurrent (i_{sc}) are plotted. Figure 4.42 shows the temperature dependence of the PCDMR signal. The fit gives $E_1 = 0.07$ eV and $E_2 = 0.16$ eV for the activation energies to created free charge carriers from a polaron pair.
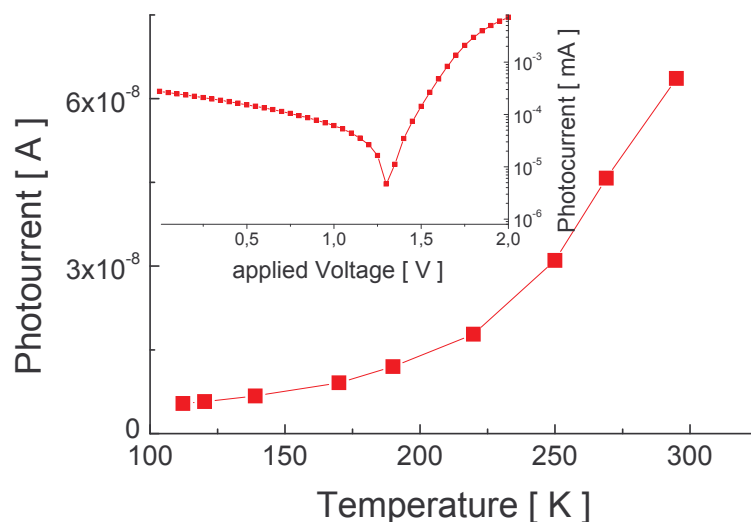
Figure 4.41: Temperature dependence of the short circuit photocurrent and the current voltage-curve of an MDMO-PPV diode prepared from toluene solution.
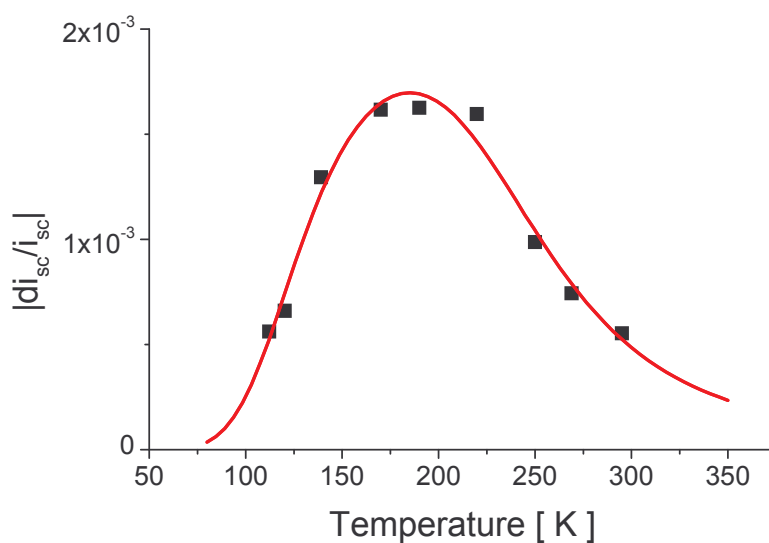
Figure 4.42: Maximum amplitude of the PCDMR signal measured on an MDMO-PPV diode prepared form toluene solution plotted versus temperature. The solid line shows a fit of the experimental data with equation 2.16.

c) Regio-regular P3HT

In Figure 4.43 the current-voltage curve and the temperature dependence of the short circuit photocurrent (i_{sc}) are plotted. Figure 4.44 shows the temperature dependence of the PCDMR signal. The fit gives 0.016 eV and 0.165 eV for the activation energies E_1 and E_2 respectively.
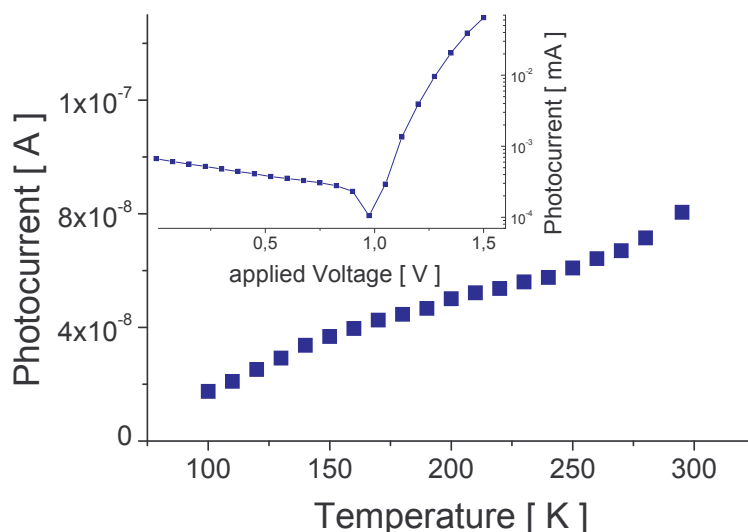
Figure 4.43: Temperature dependence of the short circuit photocurrent and the current voltage-curve of a P3HT diode.
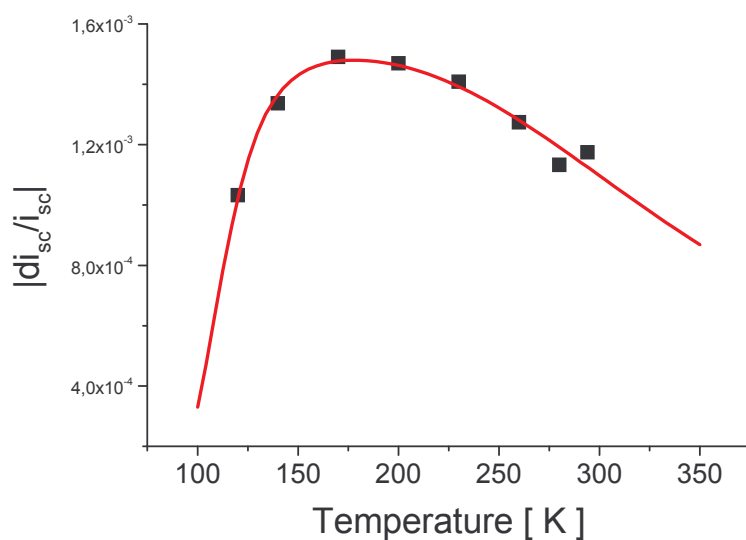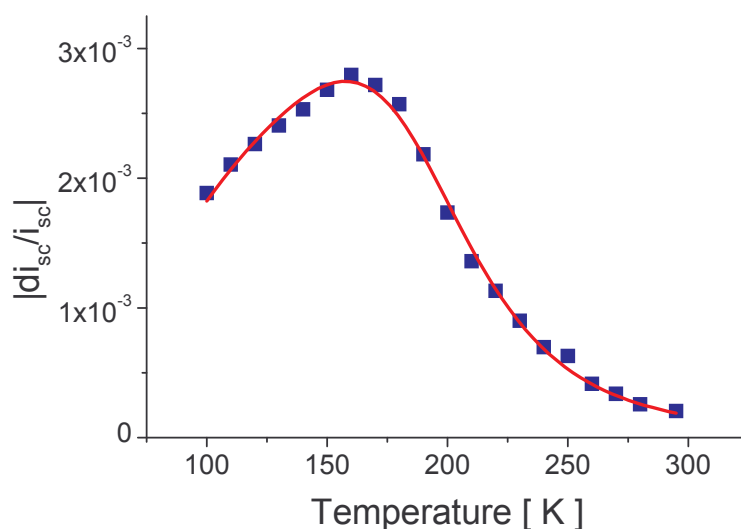

Figure 4.44: Maximum amplitude of the PCDMR signal measured on an MDMO-PPV diode prepared form toluene solution plotted versus temperature. The solid line shows a fit of the experimental data with equation 2.16.

d) PEOPT (orange and blue phase)

In Figure 4.45 the current-voltage curve and the temperature dependence of the short circuit photocurrent (i_{sc}) of an orange phase diode are plotted. Figure 4.29 b) shows the temperature dependence of the absolute value PCDMR amplitude. The fit gives $E_1 = 0.1$ eV and $E_2 = 0.19$ eV .
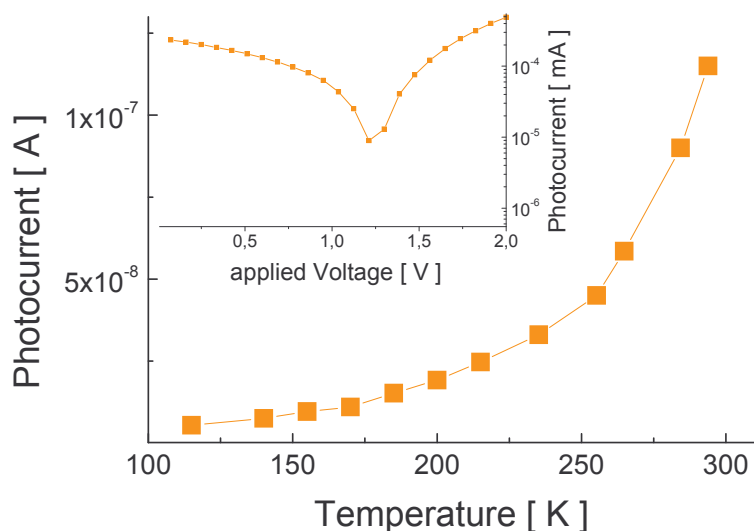
Figure 4.45: Temperature dependence of the short circuit photocurrent and the current voltage-curve of a PEOPT diode (orange phase)

Figure 4.46: Temperature dependence of the short circuit photocurrent and the current voltage-curve of a PEOPT diode (blue phase)

In Figure 4.46 the current-voltage curve and the temperature dependence of the short circuit photocurrent (i_{sc}) of a blue phase diode are plotted. Figure 4.29 b) shows the temperature dependence of the PCDMR signal. The fit gives $E_1 = 0.035$ eV and $E_2 = 0.035$ eV for the activation energies to created free charge carriers from a polaron pair.
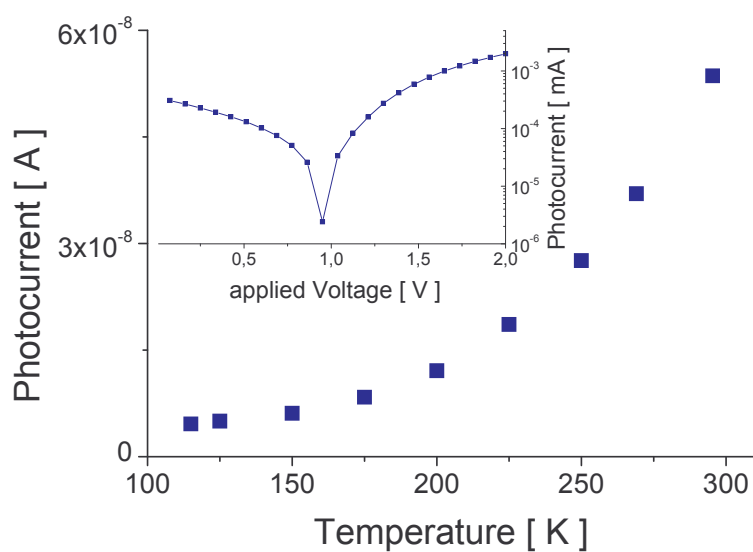
In table 4.2 all activation energies obtained for different materials are collected. Similar values have been found in magnetic field effect experiments on other conjugated polymers. Results presented here demonstrate that the polaron pair model can be applied to photocurrent detected magnetic resonance experiments. All values for E_1 and E_2 are comparable or larger than k_BT at room temperature.

Table 4.2 Values for E_1 and E_2 obtained in experiments discussed above.

	E_1 [meV]	E_2 [meV]
MMDMO-PPV (chlorobenzene)	100	120
MDMO-PPV (toluene)	70	160
P3HT	16	165
PEOPT (orange phase)	100	190
PEOPT (blue phase)	35	35

Therefore the probability for free charge carrier generation should be small at ambient temperatures. The effect of the morphology on the PCDMR has already been discussed in chapter 4.5 in the case of PEOPT. However, it is interesting to note that the influence of the solvent on the PCDMR of MDMO-PPV diodes is again small (see also chapter 4.6). This suggests that the improved electrical properties of the MDMO-PPV film prepared from chlorobenzene might come from a better interface between the polymer and the electrode and the changes in the bulk morphology are negligible.

4.8.3 Summary

The temperature dependence of the PCDMR resonance signal was studied on different conjugated polymer photodiodes. Experimental results are interpreted in terms of the polaron pair model. The activation energies required to dissociate photoexcited polaron pairs are found to be comparable or larger than k_BT at room

temperature. Therefore free charge carrier generation via thermal dissociation of polaron pairs should be an inefficient process. For the polymer PEOPT a strong influence of the morphology on the activation energies was observed. For the more ordered phase significantly smaller values were observed compared to the disordered phase. Almost no influence on the PCDMR was found for MDMO-PPV diodes prepared from different solvents.

References

[1]B. Yan, N. Schultz, A. L. Efros, P. C. Taylor, Phys. Rev. Lett. 84, 4180 (2000).

[2]N. Schultz, B. Yan, L. Efros, and P. C. Taylor, J. Non-Cryst. Solids 266-269, 372 (2000).

[3]N. A. Schultz, M. C. Scharber, C. J. Brabec, and N. S. Sariciftci, Phys. Rev. B 64, 245210 (2001).

[4] S. Kuroda , K. Marumoto, H. Ito, N.C. Greenham, R.H. Friend, Y. Shimoi,

S. Abe, Chem. Phys. Lett. 325, 183 (2000).

[5]S. Kuroda, T. Ohnishi, T. Noguchi, Phys. Rev. Lett. 72, 286 (1994).

[6]V. Dyakonov, G. Zoriniants, M. Scharber, C.J. Brabec, R.A.J. Janssen, J.C. Hummelen, N.S. Sariciftci, Phys. Rev. B59, 8019 (1999).

[7]M. Vuolle, R. Mäkelä, J. Chem. Soc. Faraday Trans. 1, 1987, 83, 51.

[8]L. Smilowitz, N. S. Sariciftci, R. Wu, C. Gettinger, A. J. Heeger, and F. Wudl, Phys. Rev. B 47, 13835 (1993)

[9]V. Dyakonov, D. Godovsky, J. Parisi, C. J. Brabec, N. S. Sariciftci, J. C. Hummelen, J. De Ceuster, E. Goovaerts, Synth. Met. 121, 1529 (2001).

[10]D. Beljonne, J. Cornil, H. Sirringhaus, P. J. Brown, M. Shkunov, R. H. Friend and J. L. Bredas, Adv. Funct. Mat. 11, 1 (2001).

[11]J. Cornil, D. Beljonne, J. P. Calbert, and J. L. Bredas, Adv. Mat. 13, 1053 (2001).

[12]J. Partee, E. L. Frankevich, B. Uhlhorn, J. Shinar, Y. Ding, and T. J. Barton, Phys. Rev. Lett. 82, 3673 (1999).

[13]*Electronic Processes in Organic Crystals*, Eds. M. Pope, C. E. Swenberg Oxford University Press, New York (1998).

[14]G. Zerza, M. C. Scharber, C. J. Brabec, N. S. Sariciftci, R. Gomez, J. L. Segura, N. Martin, V. I. Srdanov, J. Phys. Chem. A 104, 8315 (2000).

[15]T. Nguyen, V. Doan, B. J. Schwartz, J. Chem. Phys. **110**, 4068 (1999).

[16]M. Yan, L. J. Rothberg, F. Papadimitrakopoulos, M. E. Galvin, T. M. Miller, Phys. Rev. Lett. **72**, 1104 (1994).

[17]M. Yan, L. J. Rothberg, E. W. Kwock, T. M. Miller, Phys. Rev. Lett. **75**, 1992 (1995).

[18]B. Xu, S. Holdcroft, Macromolecules **26**, 4457 (1993).

[19]R.Jakubiak, C. J. Collison, W. C. Wan, L. J. Rothberg, B. R. Hsieh, J. Phys. Chem. A **103**, 2394 (1999).

[20]D. McCullough, Ad. Mater. 10, 93 (1998).

[21]H. Mao, B. Xu, and S. Holdcroft, Macromolecules 26, 1163 (1993).

[22]B. Xu, and S. Holdcroft, Macromolecules 26, 4457 (1993).

[23]T. Chen, X. Wu, and R. D. Rieke, J. Am. Chem. Soc. 117, 233 (1995).

[24]T. J. Prosa, M. J. Winokur, and R. D. McCullough, Macromolecules 29, 3654 (1996).

[25]Z. Bao, A. Dodabalapur, and J. Lovinger, Appl. Phys. Lett. 69, 4108 (1996).

[26]H. Sirringhaus, P. J. Brown, R. H. Friend, M. M. Nielson, K. Bechgaard, B. M. W. Langeveld-Voss, A. J. H. Spiering, R. A. J. Janssen, E. W. Meijer, P. Herwig and D. M. de Leeuw, Nature 401, 685 (1999).

[27]A. Dodabalapour, Z. Bao, A. Makhija, J. G. Laquindanum, V. R. Raju, Y. Feng, H. E. Katz , and J. Rgers, Appl. Phys. Lett. 73, 142 (1998).

[28]G. Horowitz, Adv. Mater. 10, 365 (1998).

[29]R. Österbacka, C.P. An, X.M. Jiang, Z.V. Vardeny, Science **287**, 839 (2000).

[30]L. S. Swansson, J. Shinar, and K. Yoshino, Phys. Rev. Lett. 65, 1140 (1990).

[31]J. Shinar in *Handbook of organic conductive molecules and polymers*, edited by H. S. Nalwa, (John Wiley & Sons Ltd 1997), vol. 3, p. 319.

[32]A. Maier, A. Grupp, M. Mehring, Solid State Com. **99**, 623 (1996).

[33]E. L. Frankevich, A. A. Lymarev, I. A. Sokolik, Chem. Phys. 162, 1 (1992).

[34]K. E. Aasmundtveit, E. J. Samuelsen, W. Mammo, M. Svensson, M. R. Anderrsson, L. A. A. Pettersson, and O. Inganäs, Macromolecules 2000, 33, 5481

[35]H. J. Fell, E. J. Samuelsen, M. R. Anderrson, J. Als-Nielsen, G. Grübel, J. Mardalen, Synth. Met. **73**, 279 (1995).

[36]C. J. Brabec, C. Winder, M. C. Scharber, and N. S. Sariciftci, J. C. Hummelen, M. Svensson, M. R. Andersson, J. Chem. Phys. 115, 7235 (2001).

[37]to be published.

[38]E. L. Frankevich, A. A. Lymarev, I. Sokolik, F. E. Karasz, S. Blumstengel, R. H. Baughman, H. H. Hörhold, Phys. Rev. B **46**, 9320 (1992).

[39]E. J. W. List, C.-H. Kim, A. K. Naik, U. Scherf, G. Leising, W. Graupner, and J. Shinar, Phys. Rev. B 64, 155204 (2001).

[40]J. A. Weil, J. R. Bolton, J. E. Wertz, Electron Paramagnetic Resonance (J. Wiley & Sons, INC., New York, 1994) p. 160.

[41]L. S. Swanson, P. A. Lane, J. Shinar, F. Wudl, Phys. Rev. B 44, 10617 (1991).

[42]E. Lifshitz, A. Kaplan, E. Ehrenfreund, D. Meissner, Chem. Phys. Lett. 300 626 (1999).

[43]O. J. Korovyanko, R. Österbacka, X. M. Jiang, and V. Z. Vardeny, Phys. Rev. B 64, 235122 (2001).

[44]M. Wohlgenannt, K. Tandom, S. Mazumdar, S. Ramasesha, Z. V. Vardeny, Nature (London) 409, 494 (2001).

[45]M. Wohlgenannt, X. M. Jiang, Z. V. Vardeny, R. A. J. Janssen, Phys. Rev. Lett. 88, 197401 (2002).

[46]Y. Shi, J. Liu, and Y. Yang J. Appl. Phys. 87, 4254 (2000).

[47]C. Y. Yang, F. Hide, M. A. Diaz-Garcia, A. J. Heeger and Y. Cao, Polymer 39, 2299 (1998).

[48]W. Geens private communication.

[49]S.E. Shaheen, C.J. Brabec, N.S. Sariciftci, F. Padinger, T. Fromherz, J.C. Hummelen, Appl. Phys. Lett. 78, 841 (2001).

[50]C. J. Brabec, G. Zerza, N. S. Sariciftci, G. Cerullo, S. DeSilvestri, S. Luzatti, J. C. Hummelen, Chem. Phys. Lett. 340, 232 (2001).

[51]J. Liu, Y. Shi, and Y. Yang, Adv. Funct. Mat.11, 424 (2001).

[52]C. J. Brabec, A. Cravino, D. Meissner, N. S. Sariciftci, T. Fromherz, M. Minse, L. Sanchez, J. C. Hummelen, Advan. Funct. Mat. 11, 374 (2001).

[53]A. Cravino, H. Neugebauer, S. Luzzati, M. Catellani, A. Petr, L. Dunsch, and N. S. Sariciftci, J. Phys. Chem. B 106, 3583 (2002).

[54]P. W. Anderson, J. Phys. Soc. Jpn. 9, 316 (1954).

[55]V. Dyakonov, R. Rösler, M. Schwoerer, E. L. Frankevich, Phys. Rev. B 56, 3852 (1997)

[56]V. Dyakonov,G. Rosler, M. Schwoerer, S. Blumstengel, K. Luders, J. Appl. Phys. 79 1556 (1996).

[57]V. Dyakonov, E. L. Frankevich, Chem. Phys. **227**, 203 (1998).

[58]P. M. Allemand, G. Srdanov, A. Koch, K. Khemani, F. Wudl, Y. Rubin, F. Diederich, M. M. Alvarez, S. J. Anz, and R. L. Whet-ton, J. Am. Chem. Soc. 113, 2780 (1991).

[59]D. Mühlbacher, thesis, Univ. of Linz.

[60]A.P. Monkman, H.D. Burrows, M. da G. Miguel, I. Hamlett, S. Navaratnam, Chem. Phys. Lett. 307, 303 (1999).

[61]X. Wei, Z. V. Vardeny, N. S. Sariciftci, and A. J. Heeger, Phys. Rev. B 53, 2187 (1996).

[62]J. G. Müller, U. Lemmer, and J. Feldmann, U. Scherf, Phys. Rev. Lett. 88, 147401 (2002).

[63]E. Conwell '*in Primary Photoexcitations in Conjugated Polymers*' (Ed. N. S. Sariciftci) p. 99 (World Scientific, Singapore, 1997).

5. Summary and Conclusion

In the presented work different photoinduced processes in conjugated polymer and conjugated polymer fullerene mixtures were investigated.

The very slow recombination of light induced charge carriers in these systems has been identified as tunneling process. Decay kinetics studied on different systems, pure conjugated polymer, conjugated polymer with different concentrations of electron acceptors can be explained by a model which has first been applied to inorganic amorphous semiconductors. The model describes the recombination of localized charges for temperatures where no thermal re-excitation occurs. The idea of recombination by tunneling is supported by the observation of thermally activated recombination in conjugated polymer fullerene mixtures. In photoinduced absorption experiments activation energies of ~ 30 meV were found. Therefore at low temperatures, $k_BT \ll 30$ meV, tunneling through energy barriers trapping charges may be the only possibility to approach recombination partners. The observation of one and the same recombination process in amorphous inorganic semiconductors and conjugated polymers is very astonishing. It demonstrates a similar electronic structure of both material classes near the band edges, where long-living charges are localized at low temperatures. One may speculate that the observed recombination process is active in all disordered systems.

In optically and photocurrent detected magnetic resonance experiments the role of the conjugated polymer film morphology and the presence of electron acceptor molecules were studied.

The morphology was found to be a dominating factor for the nature of photoexcitations in the model compound PEOPT. In films with a less ordered microstructure the triplet exciton was identified as dominate photoexcitation in PLDMR experiments. In the more ordered film no triplet excitation was detected. This is in good agreement to resent experimental and theoretical studies suggesting different probabilities for triplet exciton formation in different conjugated polymers. The probability for triplet formation divided by the probability for singlet exciton formation (σ_T/σ_S) was suggested to be inverse proportional to the conjugation length. A strong red shift of the optical absorption and photoluminescence is observed for the

more ordered phase films of PEOPT compared to the less ordered ones. Therefore one may expect a longer conjugation length for the material with a smaller band gap, which would explain lower triplet exciton formation probability in more ordered PEOPT films. This observation can be very important for conjugated polymer light emitting diodes. According to simple spin statistics recombination of free charge carriers should lead to ¾ triplet excitons and ¼ singlet excitons limiting the maximum quantum efficiency to 25 %. However, if (σ_T/σ_S) depends on the active materials used in PLEDs one may hope to overcome the limit of 25 %.

For PEOPT the arguments about PLEDs might be misleading because a higher photoluminescence efficiency is found for the disordered polymer film compared to the ordered one. Therefore also a higher electroluminescence should be expected for the less ordered PEOPT LED. A narrow resonance at g ~ 2.00 was found in both PEOPT phases. This demonstrates the presence of polaron pairs. However, the temperature dependence of the PCDMR as well as the PLDMR amplitude was observed to be different. PCDMR experiments showed that the activation energies for free charge carrier generation from polaron pairs are significantly smaller in films with the more ordered microstructure. Activation energies for forming free charge carriers from polaron pairs were found to be comparable or even larger then k_BT at room temperature for all investigated conjugated polymers. This implies that the probability of thermal dissociation of polaron pairs into free charges is low. In contrast to PEOPT PLDMR and PCDMR experiments on MDMO-PPV films prepared form toluene and chlorobenzene solutions did not give evidence for different film morphologies.

Adding small amounts of PCBM to MDMO-PPV an additional resonance, which is attributed to MDMO-PPV$^+$/PCBM$^-$ pairs is observed in PLDMR and PCDMR experiments. Magnetic resonance transitions within these pairs have the same influence on the photoluminescence and the photocurrent than magnetic resonance transitions in pristine polaron pairs. The presence of MDMO-PPV$^+$/PCBM$^-$ pairs demonstrates that the free charge carriers are at least partially generated via intermediate states. At high PCBM concentrations the PCDMR signal is quenched. Free charges are now dominantly formed without intermediate pairs. This might be one of the reasons besides the very efficient charge transfer for the very high incident photon to electron conversion efficiency in conjugated polymer fullerene photovoltaic

devices. An increase of the triplet PLDMR signal was observed for MDMO-PPV films holding small amounts of PCBM. According to the energy levels of MDMO-PPV$^+$ and PCBM$^-$ an additional formation of triplet excitons on MDMO-PPV chains by direct recombination of MDMO-PPV$^+$ and PCBM$^-$ seems to be possible. At higher fullerene concentrations the triplet PLDMR decreases due to quenching of excitons by charges.

In summary in the work presented here the recombination process of long-lived charges was identified, the influence of the film morphology on the nature of photoexcitation was demonstrated and the influence of fullerene on the charge generation process in conjugated polymers was investigated.

Eidesstattliche Erklärung

Ich erkläre an Eides statt, dass ich die vorliegende Dissertation selbstständig und ohne fremde Hilfe verfasst, andere als die angegebenen Quellen und Hilfsmittel nicht benutzt bzw. die wörtlich oder sinngemäß entnommenen Stellen als solche kenntlich gemacht habe.

Linz, Oktober 2002   Dipl.Ing. Markus Scharber

Die vorliegende Dissertation entstand zwischen Dezember 1998 und November 2002 am Forschungsinstitut für Organische Solarzellen der Technisch-Naturwissenschaftlichen Fakultät der Universität Linz unter Betreuung von o.Univ.- Prof. Dr. N. S. Sariciftci.

Curriculum Vitae

7th of November 1971	Born in Salzburg, Austria
October 1991 - December 1998	Studies in Physics at the Johannes Kepler University Linz, Austria
September 1995 - July 1996	Napier University Edinburgh, Scotland 1st class Bachelor of Science Honors Degree
November 1997 - November 1998	Diploma thesis at the Johannes Kepler University Linz, Austria, in Physical Chemistry
December 1998 – November 2002	PhD Studies in physics at the Johannes Kepler University Linz, Austria, in Physical Chemistry

Conferences, Summerschools and Seminars

Science and technology of electro-active organic materials
(Inst. f. Festkörperphysik TU Graz), Obdach (Ö) (8.10.-11.10.97)

International Conference on Science and Technology of Synthetic Metals, Montpellier (F) (12.7. -
18.7.1998)

Poster presentations

Time-Resolved Electron Spin Resonance Studies on Photoinduced Electron Transfer in Donor-
Acceptor Assemblies
M. C. Scharber, C. J. Brabec, V. Dyakonov and N. S. Sariciftci

Light Induced ESR Studies in Conjugated Polymer-Fullerene Composites
G. Zoriniants, V. Dyakonov, M. C. Scharber, C.J. Brabec,
R.A.J. Jannsen, J.C. Hummelen and N. S. Sariciftci

Photoexcitations in Carbazoly Substituted Polydiacetylene (PDA) Fullerene Composites
C. Brabec, M. Scharber, H. Johannson, D. Comoretto,
G. Dellepiane, I. Moggio, A. Cravino, J. C. Hummelen,
N. S. Sariciftci

European Summerschool on Quantum Solar Energy Conversion, Hirschegg (Ö) (16.8. - 22.8.98)

Nanoforum Linz (Ö) (13.05. - 14.05.99)

Oral presentation

Molekulare Heterostrukturen & Fullerene , Wege zur molekularen Elektronik
M. C. Scharber

Summerschool "Advanced Methods in Electron Paramagnetic Resonance Spectroscopy, Caorle,
Venice, (I) (12.9. - 19.9.1999)

Oral and poster presentation

Magnetic field effect on the photocurrent and photocurrent detected magnetic resonance on MDMO-
PPV and MDMO-PPV - fullerene diodes
M. C. Scharber, C. J. Brabec, F. Padinger, N. S. Sariciftci

MRS Fall Meeting, Boston (MA) (USA) (29.11. - 03.12.99)

Poster presentation

Quenching of the magnetic field effect on the photocurrent and photocurrent detected magnetic
resonance inconjugated polymer - fullerene diodes
M. C. Scharber, C. J. Brabec, F. Padinger, N. S. Sariciftci

Investigation of Photoexcited Triplet States in Various Substituted Fullerenes with and without
Optically Active Sidegroups

M. C. Scharber, C. J. Brabec, G. Zerza, M. Maggini, M. Prato,
J. Segura, N. Martin, J. C. Hummelen, N. S. Sariciftci

Photoinduced charge transfer between TCAQ derivatives and conjugated polymers
G. Zerza, M. C. Scharber, N. S. Sariciftci, J.L. Segura, R. Gomez, N. Martin

The Influence of Ordering on the Photoinduced Charge Transfer in Composites pf Phenyl-type
Substituted Polythiophenes with Methanofullerenes
C. J. Brabec, C. Winder, M. C. Scharber, N. S. Sariciftci,
M. R. Anderson, O. Inganäs, J. C. Hummelen

Optical Probes 2000, Salt Lake City (UT) (USA) (15.02. - 19.02.00)

Poster presentation

Quenching of the magnetic field effect on the photocurrent and photocurrent detected magnetic
resonance on conjugated polymer - fullerene diodes
M. C. Scharber, C. J. Brabec, F. Padinger, N. S. Sariciftci

197th Meeting of The Electrochemical Society,Toronto (Ont) (CAN) (14.05. - 18.05.00)

Oral presentation

Magnetic Resonance Studies on Photoexcited Fullerenes and Conjugated Polymer/Fullerene
Composites
M. C. Scharber, C. J. Brabec, N. A. Schultz, N. S. Sariciftci

**International Conference on Sciene and Technology of Synthetic Metals, Bad Gastein (Ö) (15.7. -
21.7.2000)**

Poster presentation

Magnetic Resonance Studies on Conjugated Polymer Fullerene Mixtures
        M. C. Scharber, N. A. Schultz, C. J. Brabec, N. S. Sariciftci

University of British Columbia, Vancouver (BC) (CAN)
Seminar: Department of Chemistry (3.11.2000)

Oral presentation

Conjugated polymer fullerene mixtures – a route to plastic solar cells
        M. C. Scharber, C. J. Brabec, N. S. Sariciftci

MRS – Spring Meeting, San Francisco (15. 04. - 21. 04. 2001)

Poster presentation

Influence of the morphology on the photoexcitation in a phenyl-substituted polythiophene
M. C. Scharber, N. A. Schultz, C. J. Brabec, M. Svensson, M. R. Andersson, N. S. Sariciftci

Oral presentation

Low temperature recombination kinetics of persistent photoexcited charge carriers in conjugated polymer/fullerene composite films
N. A. Schultz, M. C. Scharber, C. Brabec, N.S. Sariciftci

**International School of Physics „Enrico Fermi" Villa Monastero,
Varenna (I) (31.07. - 10.08.2001)**

Organic Nanostructures Science and Application

IFHF-Dresden Seminar – Group L. Dunsch (7.12.2001)

Oral presentation

LESR-Untersuchungen von Ladungsträgerrekombinations-prozessen in konjugierten Polymer – Fulleren Mischungen

M. C. Scharber, N. A. Schultz, C. J. Brabec, N. S. Sariciftci

Tagung der Deutsche Physikalische Gesellschaft, Regensburg (D) (11.03. - 15.03.2002)

Oral presentation

Ultrafast spectroscopy of excitons and polaron pairs in conjugated polymer solar cells
J. G. Müller,U. Lemmer, J. Feldmann, U. Scherf, M. Scharber,
C. Brabec, and S. Sariciftci

European Optical Society – Organic Optoelectronics, Technology and Devices, Topical Meeting, Engelberg (CH) (25.03. - 26.03.2002)

Oral presentation

Controlling the spectral response of organic photodiodes
J. G. Müller, R. Koeppe, U. Lemmer, J. Feldmann,U. Scherf, M. Scharber, C. Brabec, S. Sariciftci

CLE/QELS (Conference on Laser and Electro-optics/Quantum Electronics&Laser Science Conference) Los Angeles (CA) (USA) (19.05. - 24.05.2002)

Oral presentation

Ultrafast spectroscopy of excitons and polaron pairs in organic photodetectors
J. G. Müller, U. Lemmer, J. Feldmann, M. Scharber, S. Sariciftci, U. Scherf

Publication List

Photoinduced charge carriers in conjugated polymer-fullerene composites studied with light-induced electron-spin resonance
V. Dyakonov, G. Zoriniants, M. C. Scharber, C. J. Brabec, R. A. J. Janssen, J. C. Hummelen, N. S. Sariciftci
Phys. Rev. B, **59**, 12, 8019 (1999)

Photoinduced charge transfer between tetracyano-anthraquino-dimethane derivatives and conjugated polymers for photovoltaics
G. Zerza, M. C. Scharber, C. J. Brabec and N. S. Sariciftci, R. Gómez, J. L. Segura and N. Martín V. I. Srdanov
J. Phys. Chem. **104,** 35, 8315 (2000)

Influence of disorder on the Photoinduced excitations in phenyl substituted polythiophenes
C. J. Brabec, C. Winder, M. C. Scharber and N. S. Sariciftci, J. C. Hummelen, M. R. Andersson
J. Chem. Phys. **115**, 15, 7235 (2001)

Low temperature recombination kinetics of persistent photoexcited charge carriers in conjugated polymer/fullerene composite films
N. Schultz, M. C. Scharber, C. Brabec, J. C. Hummelen, N.S. Sariciftci
Phys. Rev. B **64**, 245210 (2001)

Morphology dependent photoexcitation mechanism in substituted polythiophenes studied by magnetic resonance
M. C. Scharber, N. A. Schultz, C. J. Brabec, M. Svenssson, M. R. Andersson, N. S. Sariciftci
Submitted to Phys. Rev. B

Optical- and Photocurrent Detected Magnetic Resonance Studies on Conjugated Polymer/ Fullerene Composites
M. C. Scharber, N. A. Schultz, N. S. Sariciftci, C. J. Brabec
Submitted to Phys. Rev. B

A soluble PEDOT derivative for Polymeric Solar Cells: Photophysics and Devices
C. Winder, M. A. Loi, A. Cravino, M. C. Scharber, C.J. Brabec, H. Neugebauer, N. S. Sariciftci, I. Perepichka and J. Roncali
Submitted to J. of Materials

Conference Proceedings

Dielectric and electrooptic studies of a novel ferroelectric liquid crystal mixture
J. Gruber, M. C. Scharber, J. Hajto, A. Vajda, K. Fodor-Csorba, I. Janossy
Proceedings-of-the-SPIE, The-International-Society-for-Optical-Engineering. **3318**;
1998; p.78-81.

Photoexcitations in carbazolyl substituted polydiacetylene (PDA) fullerene
composites
C. J. Brabec, M. C. Scharber, H. Johansson, D. Comoretto, G. Dellepiane, I. Moggio,
A. Cravino, J. C. Hummelen, N. S. Sariciftci
Synth. Met. vol.**101**, no.1-3; May 1999; p.298-9.

Time resolved photoinduced electron spin resonance studies on conjugated polymer
fullerene mixtures in solution
M. C. Scharber, C. J. Brabec, V. Dyakonov, N. S. Sariciftci
Synthetic-Metals. vol.**101**, no.1-3; May 1999; p.356-7.

Light-induced ESR studies in conjugated polymer-fullerene composites
G. Zoriniants, V. Dyakonov, M. C. Scharber, C. J. Brabec, R. A. J. Janssen,
J. C. Hummelen, N. S. Sariciftci
Synth. Met. vol.**102**, no.1-3; June 1999; p.1241-2.

Quenching of the magnetic field effect on the photocurrent and photocurrent detected
magnetic resonance inconjugated polymer - fullerene diodes
M. C. Scharber, C. J. Brabec, F. Padinger, N. S. Sariciftci
Mat. Res. Symp. Proc. Vol. 598, BB 3.29.1-5 (2000)

Photoinduced charge transfer between TCAQ derivatives and conjugated polymers
G. Zerza, M. C. Scharber, N. S. Sariciftci, J. L. Segura, R. Gomez, N. Martin
Mat. Res. Symp. Proc. Vol. 598 (2000), BB 3.28.1-6

The Influence of Ordering on the Photoinduced Charge Transfer in Composites of
Phenyl-type Substituted Polythiophenes with Methanofullerenes
C. J. Brabec, C. Winder, M. C. Scharber, N. S. Sariciftci, M. R. Anderson,
O. Inganäs, J.C. Hummelen
Mat. Res. Symp. Proc. Vol. 598, BB 3.24.1-6 (2000)

Magnetic Resonance Studies on Photoexcited Fullerenes and Conjugated

Polymer/Fullerene Composites

M. C. Scharber, C. J. Brabec, N. A. Schultz, N. S. Sariciftci
Fullerenes Vol. 8: Electrochemistry and Photochemistry, Editors: S. Fukuzumi, F.

D'Souza, and D. M. Guldi, 336 pgs, ISBN 1-56677-275-3

Magnetic Resonance Studies on Conjugated Polymer Fullerene Mixtures

M. C. Scharber, N. A. Schultz, C. J. Brabec, N. S. Sariciftci
(ICSM 2000) Synth. Met. **121** (2001), 1567-1568

Photoinduced electron transfer in solid C_{60} donor/acceptor complexes
D. V. Konarev, G. Zerza, M. C. Scharber, N. S. Sariciftci, R. N. Lyubovskaya
Synth. Met. **121** (2001) 1127-1128

A novel processable low band-gap polymer: spectroscopic and photovoltaic properties
of pedotheiitn
A Cravino, M. Loi, M. Scharber, C. Winder, H. Neugebauer, S. Sariciftci,
H. Meng, Y. Chen, F. Wudl
Proccedings ICEPOM-4 Lviv, Ukraine (2002)

Ultrafast spectroscopy on polaron pairs in polymer solar cells
J. G. Müller, M. Scharber, U. Lemmer, J. Feldmann, U. Scherf, N. S. Sariciftci
(ICSM 2002) submitted to Synthetic Metals

Temperature-dependence of the electrically detected magnetic resonance (EDMR) in
conjugated polymer photodiodes
M. C. Scharber, N. S. Sariciftci
(ICSM 2002) submitted to Synthetic Metals

Spectroscopic properties of PEDOTEHIITN, a novel soluble low band-gap
conjugated polymer
A. Cravino, M. A. Loi, M. C. Scharber, C. Winder, H. Neugebauer, P. Denk, H.
Meng, Y. Chen, F. Wudl, and N. S. Sariciftci
(ICSM 2002) submitted to Synthetic Metals

A soluble pEDOT derivative for bulk heterojunction solar cells
C. Winder, M. Loi, A. Cravino, C. Brabec, M. Scharber, H. Neugebauer, N.S.
Sariciftci, I. Perepichka, J. Roncali
(ICSM 2002) submitted to Synthetic Metals